Title	Studies on UV Curable Resins with Reworkable Property
Author(s)	Matsukawa, Daisaku
Editor(s)	
Citation	
Issue Date	2011-02
URL	http://hdl.handle.net/10466/14190
Rights	

Studies on UV Curable Resins with Reworkable Property

Daisaku Matsukawa

February 2011

Doctoral Thesis at Osaka Prefecture University

Contents

Chapter 1 General Introduction

1-1. Progress in thermosets with reworkable property

Production and application of plastics and petroleum-based polymeric materials increased during the last decades. Thus, polymer waste is a serious problem in modern society. In recent years, great efforts have been launched in the field of recycling of plastics. Although several attempts, e. g., hydrolysis of conventional polymeric materials using sub- and supercritical water, have been made, more effective and safe process is still desired.[1-5]

Thermosets are widely used in various applications, e. g., coatings, printing inks, and adhesives.[6-8] In general, multi-functional (meth)acrylate monomers and oligomers are mainly used in such applications because the crosslinked materials show excellent physical and/or thermal properties which are based on their highly crosslinked three-dimensional network structures. Recently, much attention has been paid to recovery or recycling of polymeric materials due to environmental regulations and interests in environmentally friendly materials.[9-11] However, it is difficult to remove the cured resins from substrates because of their intractability. In order to remove these materials from substrates, scratching or chemical treatments with strong acid or base must be conducted. Thus, the cured materials are difficult or impossible to be thoroughly removed without damaging underlying substrates.

Recently, some thermosets which are thermally or chemically degradable under a given condition have been developed. [12-33] These materials have labile or degradable covalent bonds in the network structures and are called ‘reworkable’ materials. Studies on reworkable systems have increased gradually. Scheme 1-1 shows the concept of reworkable thermosets. Recent developments of reworkable thermosets and their applications appeared in some reviews.[9-11]

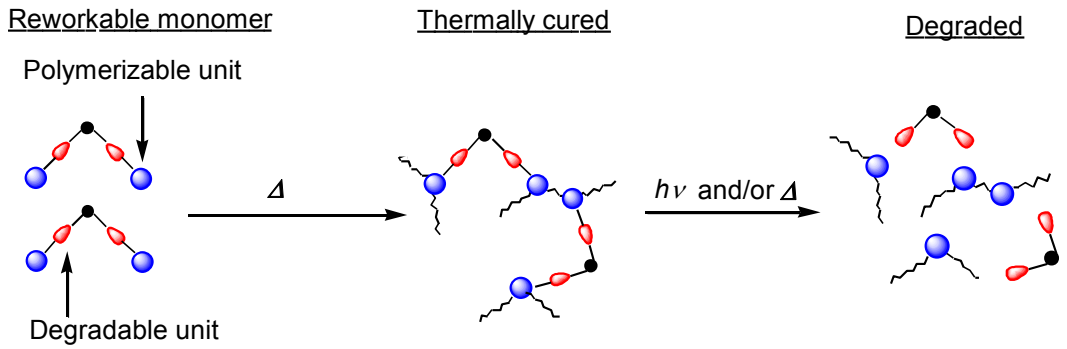

Scheme 1-1. Concept of thermosets with reworkable property.

1-2. Types of thermosets with reworkable property

1-2-1. Reworkable resin having disulfide linkages

The first study on reworkable thermosets was reported by Tesoro and Sastri in 1990.[12,13] This system is shown in Scheme 1-2. Epoxy monomer **1** was cured with a disulfide-containing aromatic diamine **2** to yield three dimensional networks. At stoichiometric ratios of **1** to **2**, cure kinetics, gelation behavior, crosslink density, and glass transition temperature of the cured resin having disulfide linkages were essentially comparable with the resin without disulfide linkages in the structure. The resulting networks containing disulfide linkages could be cleaved feasibly by treatment with triphenylphosphine to generate thiols. In this system, the degradation reaction occurred completely at lower crosslink density of the networks. Since it was difficult for the reducing agent to penetrate into the tightly crosslinked network, the complete solubilization was not observed in this system.

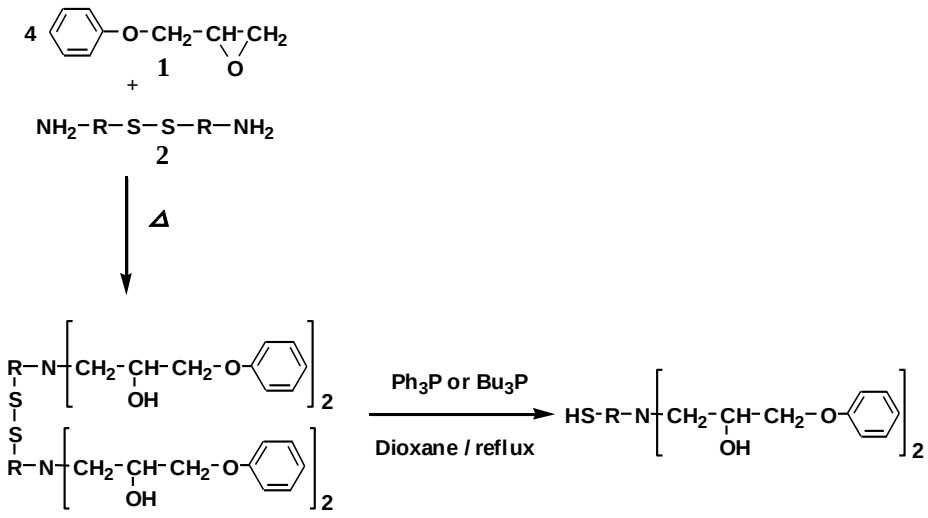

Scheme 1-2. Curing and degradation of epoxide - disulfide system.

1-2-2. Reworkable resin having ester linkages

Diepoxides having primary, secondary, or tertiary ester linkages were studied by Ober et al. [14,15] The networks of the cured resins **3** and **4** which have tertiary ester linkages were broken down at lower temperature than those with primary or secondary ester linkages. The thermally labile tertiary ester linkages of the networks were cleaved at elevated temperatures (~220 ^{o}C) to form carboxylic acid and alkene derivatives as degradation products (see Scheme 1-3). Some of the carboxylic acid groups reacted further to form anhydrides during heating. The thermosets cured from these epoxides have the advantage of being thermally decomposable at relatively modest temperatures without introduction of solvent or catalyst into the system. The cured thermosets with tertiary esters retained the same mechanical behavior as of conventional thermosets at room temperature, while having reduced mechanical properties at elevated temperatures, thereby offering the possibility of easier thermoset removal.

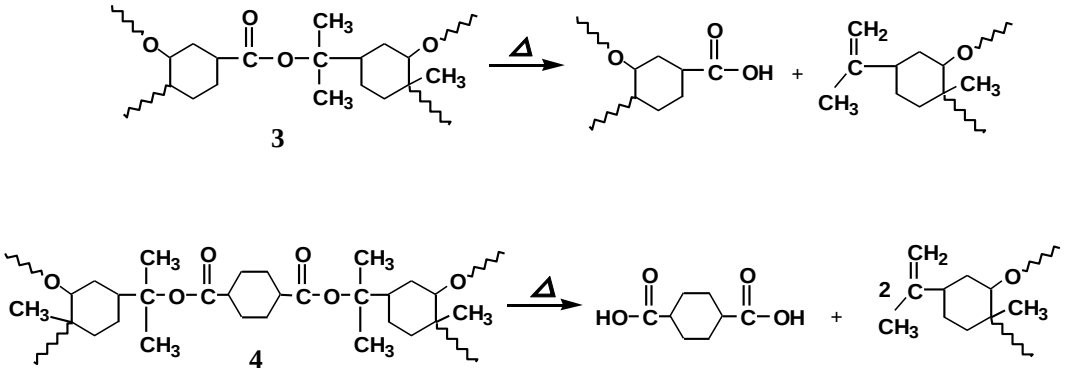

Scheme 1-3. Degradation mechanism of networks having tertiary ester linkages.

Endo and co-workers reported reusable polymers obtained from bicyclic ortho ester **5** and spiro ortho ester **6**.[16-18] These systems are shown in Scheme 1-4. These polymers successfully converted into the corresponding monomers by the treatment with a cationic catalyst in diluted conditions. These systems based on cationic equilibrium polymerization were also applied to chemical recycling system.[18] The linear polymer with bicyclic ortho ester groups **7** demonstrated reversible crosslinking – decrosslinking behavior. Although they showed one basic concept exploring new fields of polymer recycling, they observed the incomplete decrosslinking of the crosslinked polymer in the case of high crosslinking density.

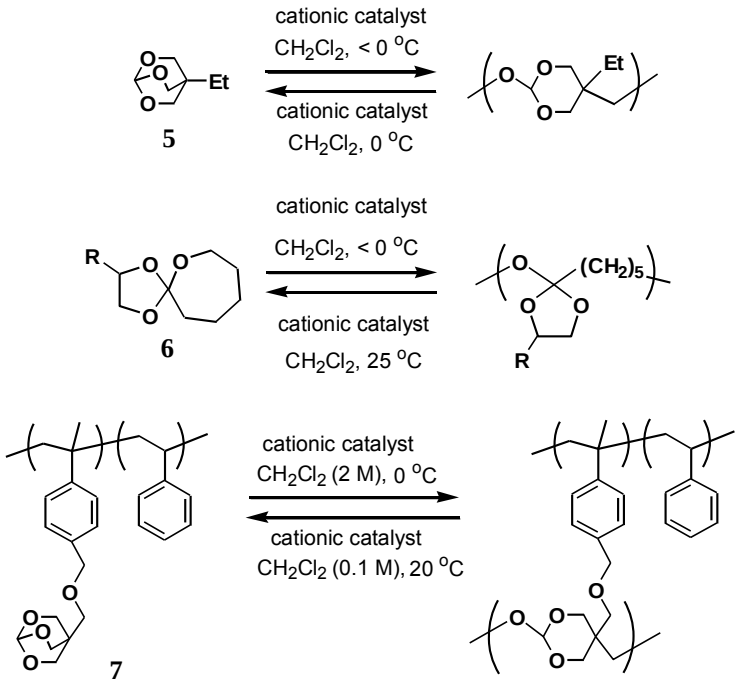

Scheme 1-4. Polymerization and depolymerization of ortho esters.

1-2-3. Reworkable resin using Diels – Alder reaction

Reworkable systems which use Diels-Alder (DA) and retro-Diels-Alder (rDA) reaction were also reported by Yoshie et al.[19] The advantages of the usage of DA and rDA reactions are both no requirement of additives such as catalyst and no generation of by-products in the system. A macromonomer **8** was copolymerized with maleimide **9** by DA reaction at 60 °C (Scheme 1-5). The resulting networks decomposed completely by rDA reaction at 145 °C to reproduce **8** and **9**. The cycles of DA and rDA reactions did not induce the loss of elasticity of the DA products or reduction of the molecular weight of the rDA products. Although the recyclability of the reworkable system was confirmed up to eight times, the system required relatively high temperatures to form and degrade the network.

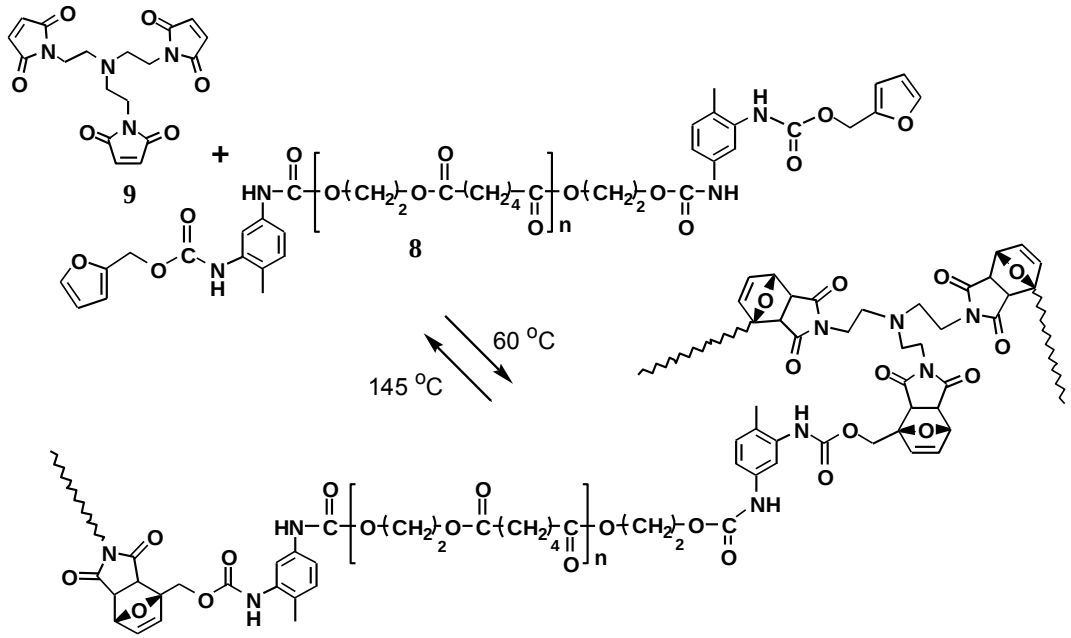

Scheme 1-5. Reworkable resin based on DA and rDA reactions.

1-2-4. Reworkable resin having acetal linkages

Epoxy resins having ketal, acetal, or formal groups were studied by Buchwalter and Kosber.[20] Scheme 1-6 shows the crosslinking and decrosslinking of diepoxide **10** having acetal linkage. It is known that acetal linkage is stable under neutral or basic conditions and decomposes readily under acidic conditions. Thus, the cured resins containing acetal groups could be dissolved in acid-containing organic solvents due to the hydrolysis of acetal linkages. However, the dissolution rate of the acetal diepoxide networks was highly dependent on temperature. Little or no dissolution occurred at room temperature.

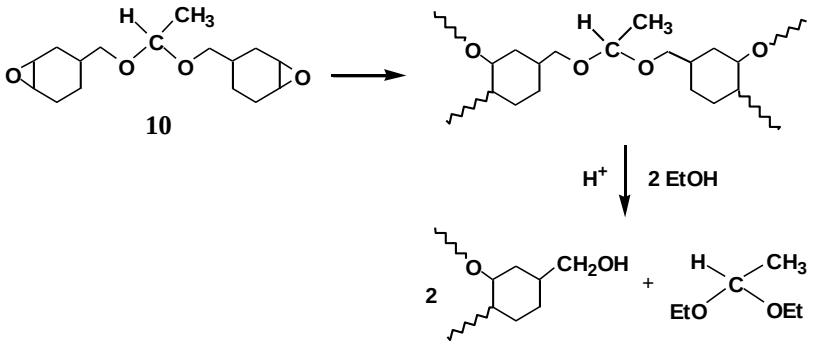

Scheme 1-6. Crosslinking and decrosslinking of diepoxide containing acetal linkage.

1-2-5. Reworkable resin having hemiacetal ester linkages

Many analogous protection techniques of active functional groups have been examined in synthetic organic chemistry. Especially, the carboxyl groups can be easily converted into esters or amides as protected groups. However, they are too stable to regenerate the carboxyl groups at relatively low temperatures. Although their thermal dissociation can be accelerated in the presence of strong acid as a catalyst, it does not give satisfying results. The hemiacetal ester structure is obtained by the acid-catalyzed addition reaction of vinyl ethers with carboxylic acids and is commonly used in recent polymer chemistry.[21-27] Thermal properties of hemiacetal esters are fascinating. The ease of the cleavage of central carbon-oxygen bond in hemiacetal ester structure is attributed to the reduced energy derived from the presence of an electron-donating substituent and an electron-withdrawing substituent at the both ends of the C-O bonds. As hemiacetal ester structure has a weak covalent bond, it is useful as a building block for reworkable resins.

Polymers with hemiacetal ester linkages in the side chain were developed by Endo et al (Scheme 1-7).[23-26] The thermal dissociation behavior of the polymers was controllable by a simple molecular design. Furthermore, regeneration of carboxylic acids and vinyl ethers in the thermolysis of hemiacetal esters was confirmed. Poly(hemiacetal ester)s having thermally

dissociative units in the main chain were also reported (Scheme 1-8).[27] The reworkable poly(hemiacetal ester)s having different alkyl chain length were obtained successfully. The polymers possessed significant thermal dissociation abilities and their dissociation occurred at 150 - 200 °C.

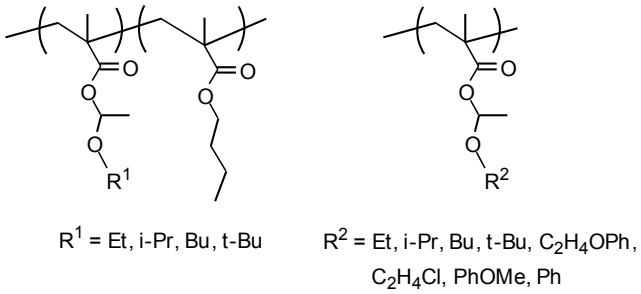

Scheme 1-7. Polymers with hemiacetal ester linkages.

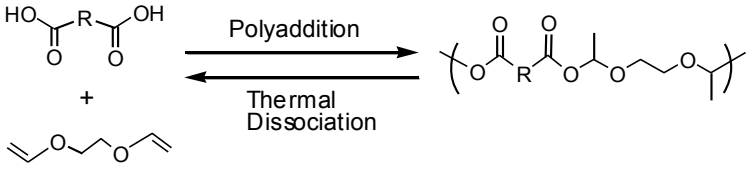

Scheme 1-8. Synthesis and thermal dissociation of poly(hemiacetal ester).

1-3. Role of UV curable resins with reworkable property

1-3-1. UV curable resins and environmental aspects

Photoinduced polymerization is a rapidly expanding technology. UV curing systems using multifunctional monomers have the advantages such as low volatile organic compounds, solvent-free process, saving energy and cost, and high productivity compared with conventional thermosets. Thus, UV curing systems are widely used in various applications, e. g., coatings, printing inks, adhesives, composite materials, photoresists, and solder masks.[6-8] Since the photochemically crosslinked materials show excellent physical and/or thermal properties, it is difficult or impossible to thoroughly remove them without damaging underlying materials.

Recently, much attention has been paid to recovery or recycling of polymeric materials due to environmental regulations and interests in environmentally friendly materials.[9-11] It is well-known that lower modulus thermoplastic polymers can be easily removed by an appropriate choice of solvent or heat. However, in many applications, cured resins are used and they are insoluble and infusible. Thus, the recycling of UV cured resins is one of the most challenging targets. Therefore, if a material would be designed for disassembly on a molecular scale, many of the disadvantages of crosslinked networks might be addressed without losing their positive attributes. In this point of view, UV curing materials which have thermally or chemically degradable property are effective for waste prevention and conservation of petroleum resources. In order to construct sustainable human society, a good design of materials with recyclability is highly desired.

1-3-2. Promising applications

An increasingly prevalent area of UV cured resins with reworkable property and the subject of much active research are observed in electronic component manufacturing.

Reworkable resin can be applied to the mounting of electronic components in the assembly of printed circuit boards or the temporary fixing of optical components such as lenses and prisms. This approach means that defective parts may be easily replaced or components may be held firmly in place during manufacture but may be removed if so desired. For example, manufacturing losses due to defective semiconductor components are ranged up to several percent for single chip packages. This is increased to 30 % or even higher for multi-chip configurations depending on the assembly complexity.[28] Given these percentages coupled with the high volume of chip assemblies produced, huge cost savings could be realized by the development of a cheap and effective packaging materials that support rework and replacement.

Recently, in addition to conventional photolithographic techniques, UV nanoimprint lithography (UV-NIL) has attracted much attention as one of the most promising nano-patterning technologies for the next generation of devices.[34-39] In UV-NIL, a photopolymerizable liquid monomer is pressurized between the nanopatterned master mold and a substrate, and then exposed to light for a short period of time to convert the liquid monomer into a solid polymer. Then, the master mold is removed to release the nanopatterned polymer substrate. Although UV-NIL possesses various advantages such as low cost, high resolution, and rapid formation of stable features, there are some issues to be solved.[40-44] Shrinkage of the UV imprinted patterns is a serious problem for micrometer- and nanometer-sized patterning of original features. Generally, acrylates and methacrylates are known to shrink in the range of 3~16 % in volume during UV curing and the shrinking property of UV cured materials is strongly dependent on the curing conditions. However, the effect of UV imprinting conditions on shrinkage of UV imprinted patterns has not been studied up to now. The shrinkage may cause product failures such as mismatch of the original mold. Another issue in UV-NIL is the fouling of quartz mold by cured resins. It is difficult to remove the cured resins remained on the quartz mold and the mold contaminated cannot be applied to UV-NIL process again. The

above-mentioned problems are crucial for UV-NIL process to be used in various applications. The fouling of quartz mold can be eliminated using reworkable monomers instead of conventional UV curable monomers for UV-NIL.

1-4. Objective of this work

Although several reworkable resins were investigated earlier[9-11], studies on UV curable resin with reworkable property are still not so many compared with those on reworkable thermosets. According to the basis of background mentioned above, this work has been focused on the development of new UV curable monomers and oligomers with reworkable property. Some applications of reworkable resins were also studied. This thesis is divided into 6 Chapters.

In Chapter 2, synthesis of difunctional (meth)acrylates bearing tertiary ester groups, their UV and thermal curing properties, and their ability as a reworkable resin are described. The difunctional (meth)acrylates containing radical initiator and photoacid generator (PAG) became insoluble in solvents. The cured films became soluble in solvents after UV irradiation followed by baking. The re-dissolution behaviors of the cured resin were strongly affected by the structures of reworkable monomers and the type of PAG.

In Chapter 3, synthesis of oligo(hemiacetal ester)s having methacrylate units and tertiary ester units in the side chains, their UV curing property, and degradation property of UV cured oligo(hemiacetal ester)s are described. Two types of oligo(hemiacetal ester)s were synthesized. Reworkable resin having degradable units in the main chain and side chain has not been reported up to now and has potential ability for reworkable UV curing system. The oligo(hemiacetal ester)s containing a photoradical initiator and a PAG became insoluble in solvents after irradiation. Although insolubilization behavior was not influenced by main-chain structure, the solubilization behavior of UV cured resins was significantly affected

by the oligomer structure.

In Chapter 4, synthesis of difunctional methacrylates which have hemiacetal ester unit in the molecule, the application of reworkable dimethacrylates to UV-NIL, and the effect of UV imprinting conditions on shrinkage of UV imprinted patterns are described. By applying these monomers to UV-NIL, fine line / space patterns were obtained in good form. To obtain the kinetic chain length for the UV imprinted resin, the linear polymers obtained from the degradation of UV imprinted reworkable resins were analyzed by SEC. It was found that degree of shrinkage of UV imprinted patterns was significantly affected by the kinetic chain length. The effect of UV imprint conditions on kinetic chain length was investigated. A relationship between kinetic chain length and shrinkage of UV imprinted patterns was clarified.

In Chapter 5, a reworkable resin was applied to make a replicated resin mold for UV-NIL. A mixture of reworkable resin, photoradical generator, and PAG was used as a resist for UV-NIL and primary patterns were obtained. Conventional UV-NIL was carried out using the primary patterns composed of UV cured reworkable resin as a mold. By degrading the primary patterns, the replicated resin mold with grooves of varying widths from 1 μm to 100 μm was fabricated. UV-NIL using the replicated resin mold was accomplished.

Finally, in Chapter 6, the results obtained in this work are summarized.

References

1. R. W. J. Westerhout, J. A. M. Kuipers, W. P. M. van Swaaij, *Ind. Eng. Chem. Res.*, 37, 841 (1998).
2. W. Kaminsky, B. Schlesselmann, C. Simon, *J. Anal. Appl. Pyrolysis*, 32, 19 (1995).
3. K. Suyama, M. Kubota, M. Shirai, H. Yoshida, *Polym. Degrad. Stabil.*, 91, 983 (2006).
4. M. Goto, M. Sasaki, T. Hirose, *J. Mater. Sci.,* 41, 1509 (2006).
5. M. Goto, *J. Supercrit. Fluids*, 47, 500 (2009).
6. E. Andrzejewska, *Prog. Polym. Sci.*, 26, 605 (2001).
7. C. Decker, *Prog. Polym. Sci.*, 21, 593 (1996).
8. S. Jönsson, P. -E. Sundell, J. Hultgren, D. Sheng, C. E. Hoyle, *Prog. Org. Coat.*, 27, 107 (1996).
9. M. Shirai, *Prog. Org. Coat.*, 58, 158 (2007).
10. C. J. Kloxin, T. F. Scott, B. J. Adzima, C. N. Bowman, *Macromolecules*, 43, 2643 (2010).
11. T. Maeda, H. Otsuka, A. Takahara, *Prog. Polym. Sci.*, 34, 581 (2009).
12. G. C. Tesoro, V. J. Sastri, *J. Appl. Polym. Sci.,* 39, 1425 (1990).
13. V. J. Sastri, G. C. Tesoro, *J. Appl. Polym. Sci.,* 39, 1439 (1990).
14. S. Yang, J. -S. Chen, H. Korner, T. Breiner, C. K. Ober, *Chem. Mater.*, 10, 1475 (1998).
15. J. -S. Chen, C. K. Ober, M. D. Poliks, *Polymer.*, 43, 131 (2002).
16 S. Chikaoka, T. Takata, T. Endo, *Macromolecules*, 24, 331 (1991).
17 M. Hitomi, F. Sanda, T. Endo, *J. Polym. Sci., Part A, Polym. Chem.*, 36, 2823 (1998).
18. M. Hitomi, F.Sanda, T. Endo, *Macromol. Chem. Phys.*, 200, 1268 (1999).
19. M. Watanabe, N. Yoshie, *Polymer*, 47, 4946 (2006).
20. S. L. Buchwalter, L. L. Kosber, *J. Polym. Sci., Part A, Polym. Chem.*, 34, 249 (1996).

21. H. Zhang, E. Ruckenstein, *Macromolecules*, 31, 7575 (1998).

22. E. Ruckenstein, H. Zhang, *Macromolecules*, 31, 9127 (1998).

23. Y. Nakane, M. Ishidoya, T. Endo, *J. Polym. Sci., Part A, Polym. Chem.*, 37, 609 (1999).

24. H. Otsuka, H. Fujiwara, T. Endo, *J. Polym. Sci., Part A, Polym. Chem.*, 37, 4478 (1999).

25. H. Komatsu, T. Hino, T. Endo, *J. Polym. Sci., Part A, Polym. Chem.*, 43, 4260 (2005).

26. H. Komatsu, T. Hino, T. Endo, *J. Polym. Sci., Part A, Polym. Chem.*, 44, 3966 (2006).

27. H. Otsuka, T. Endo, *Macromolecules*, 32, 9059 (1999).

28. J. Malik, S. J. Clarson, *Polym. Degrad. Stabil.*, 76, 241 (2002).

29. K. Yamamoto, M. Higuchi, H. Kanazawa, *Chem. Lett.*, 31, 692 (2002).

30. J. Malik, S. J. Clarson, *Polym. Degrad. Stabil.*, 79, 21 (2003).

31. H. Kanazawa, M. Higuchi, K. Yamamoto, *Macromolecules,* 39, 138 (2006).

32. H. Nandivada, X. Jiang, J. Lahann, *Adv. Mater.*, 19, 2197 (2007).

33. J. A. Johnson, M. G. Finn, J. T. Koberstein, N. J. Turro, *Macromolecules*, 40, 3589 (2007).

34. S. Y. Chou, P. R. Krauss, P. J. Renstrom, *J. Appl. Phys. Lett.*, 67, 3114 (1995).

35. S. Y. Chou, P. R. Krauss, P. J. Renstrom, *J. Vac. Sci. Technol.*, B14, 4129 (1996).

36. B. D. Gates, Q. Xu, M. Stewart, D. Ryan, C. G. Willson, G. M. Whitesides, *Chem. Rev.*, 105, 1171 (2005).

37. D. J. Resnick, S. V. Sreenivasan, C. G. Willson, *Mater. Today*, 8, 34 (2005).

38. H. Schift, *J. Vac. Sci. Technol.*, B26, 458 (2008).

39. B. K. Long, B. K. Keitz, C. G. Willson, *J. Mater. Chem.*, 17, 3575 (2007).

40. W. K. Neo, M. B. Chan-park, *Macromol. Rapid Commun.,* 26, 1008 (2005).

41. M. F. Montague, C. J. Hawker, *Chem. Mater.*, 19, 526 (2007).

42. A. del Campo, E. Arzt, *Chem. Rev.*, 108, 911 (2008).

43. A. Khan, M. Malkoch, M. F. Montague, C. J. Hawker, *J. Polym. Sci., Part A, Polym. Chem.*, 46, 6238 (2008).

44. W. H. Heath, F. Palmieri, J. R. Adams, B. K. Long, J. Chute, T. W. Holcombe, S. Zieren, M. J. Truitt, J. L. White, C. G. Willson, *Macromolecules*, 41, 719 (2008).

Chapter 2

Reworkable system based on di(meth)acrylates bearing tertiary ester groups

2-1. Introduction

Multifunctional (meth)acrylate resins have been widely used as photosensitive materials for printing plates, inks, photoresists, coatings and photo-curable adhesives. Photochemically crosslinked resins consist of insoluble and infusible networks and have many desirable properties for these applications including high strength, very low moisture absorption, and rapid curing. Scratching or chemical treatments with strong acid or base must be applied to remove these networks from substrates. However, crosslinked resins are difficult or impossible to be thoroughly removed without damaging the underlying materials.

Recently, reworkable resins, which are thermosets having thermally or chemically degradable properties under a given condition, have been reported.[1-3] These reworkable resins have attracted much attention in terms of environmental aspects. Among the reworkable resins, cleavable di(meth)acrylates have been studied most extensively due to their high reactivity and wide variety of monomer structures.[4-12] Cleavable monomers having tertiary ester, acetal and acid anhydride linkages have been reported.[6-12] Above all, a tertiary ester is subject to breakdown into carboxylic acid and alkene by simple thermal treatment. The molecular design including tertiary esters as degradable groups enables the well-controlled and selective decomposition. Another aspect of reworkable resins is to develop new methods of rework as well as the chemical structure.

This chapter describes an extensive study of the synthesis, curing and degradation properties of difunctional (meth)acrylates having aromatic units and tertiary ester units. This system consists of (1) thermal curing and thermal degradation, (2) thermal curing and

photoinduced degradation, and (3) photo-curing and thermal degradation as shown in Scheme 2-1. The reworkable behaviors are discussed in terms of the structures of the difunctional (meth)acrylates and photoacid generators used. A mechanism of curing and thermal degradation is discussed based on Fourier transform infrared (FTIR) and ^{1}H NMR analyses, TGA, mass spectrometry (MS) and SEC. This system is of importance as a photo-curable material which can be removed from substrates after use.

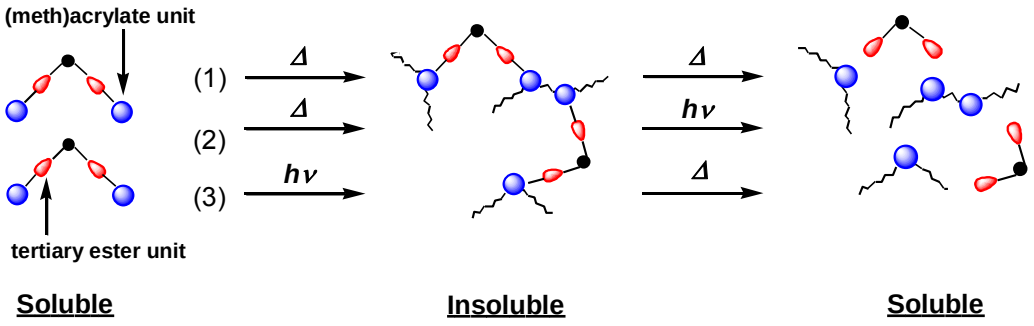

Scheme 2-1. Schematic representation of the concept of reworkable resins: (1) thermal curing and thermal degradation; (2) thermal curing and photoinduced degradation; (3) photo-curing and thermal degradation.

2-2. Experimental

2-2-1. Measurements

^{1}H NMR spectra were obtained at 300 MHz using a JEOL LA-300 spectrometer. UV-visible spectra were recorded with a Shimadzu UV-2400 PC. FTIR measurements were carried out using a JASCO FT/IR-410. Elemental analysis was carried out using a Yanaco CHN corder MT-3. Thermal decomposition behavior was investigated with a Shimadzu TGA 50 thermogravimetric analyzer and a DTA 50 differential thermal analyzer. These measurements were carried out under nitrogen flow and the heating rate was 10 ^{o}C min^{-1}. The thickness of the films was measured by interferometry (Nanometrics Japan, Nanospec/AFT M3000). The insoluble fraction of the films was determined by comparing the film thickness before and after dissolution in solvents. SEC was carried out in tetrahydrofuran using a JASCO PU-980 chromatograph equipped with polystyrene gel columns (Shodex GMN$_{HR}$-H + GMN$_{HR}$-N; 8.0 mm i.d. × 30 cm each) and a JASCO RI 1530 differential refractometer. The number-average molecular weight (*Mn*) and dispersity (*Mw/Mn*) were estimated on the basis of a polystyrene calibration. Mass spectra were measured using a Shimadzu GCMS-QP2010 equipped with a DI-2010 direct injection (DI) instrument. Irradiation at 365 nm was performed using a medium-pressure mercury lamp (Ushio UM-102, 115W) with a bandpath filter for 365 nm. The intensity of the light was measured with an Orc Light Measure UV-M02.

2-2-2. Materials

Methacryloyl chloride, acryloyl chloride, 2,2-dimethoxy-2-phenylacetophenone (DMPA), trifluoromethanesulfonyloxy-1,8-naphtalimide (NITf), *p*-toluenesulfonyl-*N*-methyl-*N*-nitroso-amide and 1,4- and 1,3-bis(2-hydroxy-2-propyl)benzene were obtained from Tokyo Kasei and used as received. 2,2'-Azobisisobutyronitrile (AIBN) was purchased from Aldrich and purified by recrystallization from ethanol. Toluenesulfonic acid 2-isopropylthioxanthone oxime ester (ITXTS) was prepared as described previously. [13]

The chemical structures of reworkable monomers, radical initiators, and photoacid generators are shown in Schemes 2-2, 2-3, and 2-4.

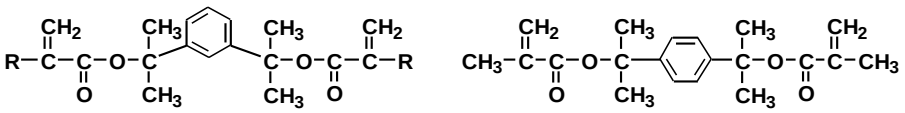

mTMBDMA (R = CH_3)
mTMBDA (R = H)

pTMBDMA

Scheme 2-2. Chemical structures of reworkable monomers.

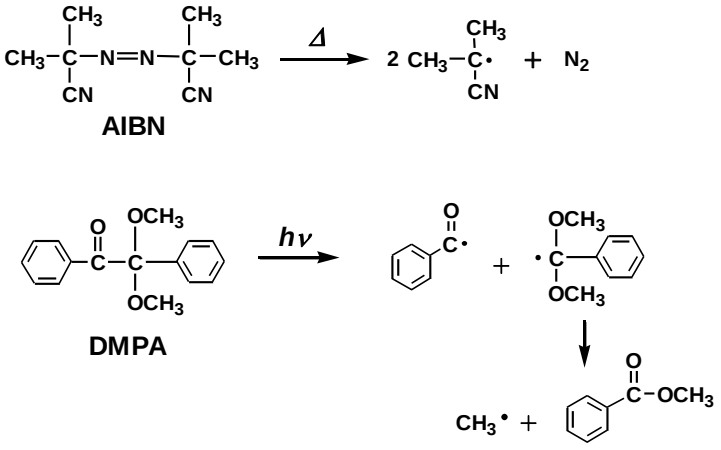

Scheme 2-3. Chemical structures and reactions of radical initiators.

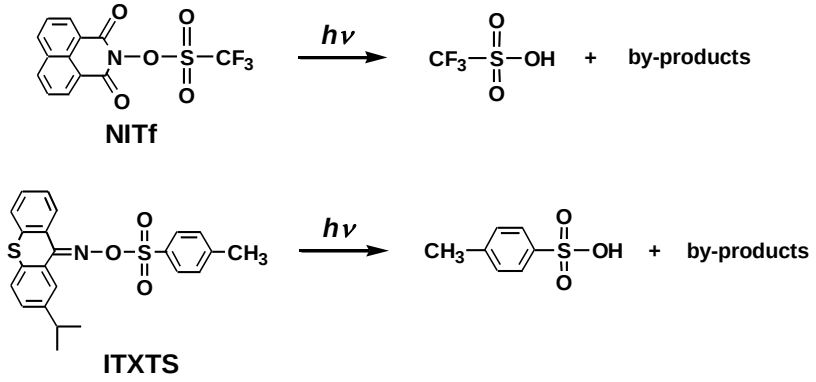

Scheme 2-4. Chemical structures and photoreactions of photoacid generators.

2-2-3. Synthesis of reworkable monomers

*Methacrylic acid 1,3-phenylenebis(1-methylethylidene) ester (**mTMBDMA**)*

To a cold (<5 ^{o}C) solution of 1,3-bis(2-hydroxy-2-propyl)benzene (4.0 g, 20.6 mmol) in a mixture of anhydrous pyridine (8.7 mL) and chloroform (60 mL) was slowly added a solution of 7.0 mL (53.6 mmol) of methacryloyl chloride in 7 mL of chloroform. The mixture was stirred at ambient temperature for 4 h. The solution was washed with saturated sodium bicarbonate solution and then with water. The organic layer was dried over anhydrous Na_2SO_4. The product was purified by column chromatography (eluent: $CHCl_3$/AcOEt = 9/1, v/v), giving a colorless viscous liquid in a yield of 2.2 g (32 %). ^{1}H NMR (300 MHz, $CDCl_3$; δ, ppm): 7.37 – 7.18 (4H, m, aromatic), 6.08 (2H, s, CH_2=C–), 5.51 (2H, s, CH_2=C–), 1.91 (6H, s, methacrylic CH_3), 1.79 (12H, s, tertiary CH_3). MS (EI): *m*/*z* 330 (M^+, 1.3), 159 (M^+ -171, 100). Analysis: calcd for $C_{20}H_{26}O_4$: C, 72.70; H, 7.93; found: C, 72.93; H, 7.85.

*Methacrylic acid 1,4-phenylenebis(1-methylethylidene) ester (**pTMBDMA**)*

pTMBDMA was prepared by a similar manner to mTMBDMA using 1,4-bis(2-hydroxy-2-propyl)benzene instead of 1,3-bis(2-hydroxy-2-propyl)benzene. Yield: 4.7 g (79 %). mp: 100.1 - 100.4 ^{o}C. ^{1}H NMR (300 MHz, $CDCl_3$; δ, ppm): 7.24 (4H, m, aromatic), 6.02 (2H, s, CH_2=C–), 5.45 (2H, s, CH_2=C–), 1.85 (6H, s, methacrylic CH_3), 1.72 (12H, s, tertiary CH_3). MS (EI): *m*/*z* 330 (M^+, 6.7), 245 (M^+ -85, 100).

*Acrylic acid 1,3-phenylenebis(1-methylethylidene) ester (**mTMBDA**)*

A synthetic procedure similar to that of mTMBDMA was followed. To a cold (<5 ^{o}C) solution of 1,3-bis(2-hydroxy-2-propyl)benzene (4.0 g, 20.6 mmol) in a mixture of anhydrous pyridine (8.7 mL) and chloroform (60 mL) was slowly added a solution of 4.2 mL (51.7 mmol)

of acryloyl chloride in 7 mL of chloroform. The mixture was stirred at ambient temperature for 4 h. The solution was washed with saturated sodium bicarbonate solution and then with water. The organic layer was dried over anhydrous Na_2SO_4. The product was purified by column chromatography (eluent: $CHCl_3$/AcOEt = 8/2, v/v), giving a pale yellow viscous liquid in a yield of 3.1 g (50 %). ^{1}H NMR (300 MHz, DMSO-d_6; δ, ppm): 7.31–7.21 (4H, m, aromatic), 6.24 (2H, d, CH_2=CH–), 6.13 (2H, m, CH_2=CH–), 5.89 (2H, d, CH_2=CH–), 1.72 (12H, s, tertiary CH_3). MS (EI): *m*/*z* 302 (M^+, 4.5), 159 (M^+ -143, 100). Analysis: calcd for $C_{18}H_{22}O_4$: C, 71.50; H, 7.33; found: C, 71.33; H, 8.21.

2-2-4. Curing behavior of reworkable monomers and degradation of cured resins

Thermal curing and thermal degradation of cured reworkable resin

All sample films were prepared on silicon wafer by spin-casting from solutions of cyclohexanone containing di(meth)acrylates and known amounts of AIBN. The sample films were dried on a hot plate at 90 ^{o}C for 1 min. The thickness of the films was 1 - 2 μm. Baking the sample using a hot plate was performed under nitrogen atmosphere. The insoluble fraction was determined by comparing the film thickness before and after development in methanol or tetrahydrofuran. The cured reworkable resins were baked at given temperatures to decompose the cured resins. The remaining film thickness was determined by comparing the film thickness before and after development in organic solvents.

Thermal curing and photo-induced degradation of cured reworkable resin

In this case the sample films consisted of reworkable di(meth)acrylates, AIBN, and a photoacid generator was prepared and the films were baked as shown above to yield cured resins. The cured reworkable resins were baked at given temperatures after irradiation at 365

nm to decompose the cured resins. The remaining film thickness was determined by comparing the film thickness before and after development in organic solvents.

Photo-curing and thermal degradation of cured reworkable resin

All sample films were prepared on silicon wafer by spin-casting from solutions of cyclohexanone containing di(meth)acrylates and known amounts of photoradical initiator and photoacid generator. The sample films were dried on a hot plate at 90 ^{o}C for 1 min. The thickness of the films was 1 - 2 μm. The sample films were irradiated at 365 nm under N_2 atmosphere. The cured reworkable resins were baked at given temperatures to decompose the cured resins. After the resins were immersed in organic solvents, the remaining film thickness was determined.

Methylation of decomposed product [14]

Thermally cured mTMBDMA was baked at 180 ^{o}C for 10 min in air. The product was immersed in chloroform. The solid was recovered after filtration of the mixture. To the suspension of the solid (1.5 mg) in benzene/diethyl ether solution (5/1 v/v; 6 mL) was added an excess amount of diazomethane, which was prepared using 100 mg of *p*-toluenesulfonyl-*N*-methyl-*N*-nitrosoamide and 1 mL of 5 mol L^{-1} KOH in water. The reaction was carried out at ambient temperature for 3 h. The reaction mixture was poured into a large amount of methanol. The product was purified by reprecipitation from chloroform/methanol. The polymer thus obtained (in a yield of 0.9 mg) was confirmed to be poly(methyl methacrylate) using FTIR and ^{1}H NMR spectroscopy.

2-3. Results and Discussion

2-3-1. Synthesis and properties of thermally degradable di(meth)acrylates

On the basis of the concept shown in Scheme 2-1, reworkable di(meth)acrylates mTMBDA, mTMBDMA and pTMBDMA which have both (meth)acrylate groups and tertiary ester linkages in their molecular structures were prepared. The di(meth)acrylates were prepared by the reaction of corresponding 1,3- or 1,4-bis(2-hydroxy-2-propyl)benzene and (meth)acryloyl chloride in moderate yields (32 - 79 %). Di(meth)acrylates containing aromatic units are stiff and stable to chemical reagents compared to aliphatic ones. The (meth)acrylate units work as a photoinduced crosslinking site if they were used in combination with free radical-generating photoinitiators. Tertiary esters are known to decompose to carboxylic acid and alkene by thermal treatment at temperatures lower than those required for primary or secondary esters.[6, 15] Furthermore, the temperature for tertiary ester cleavage is lowered in the presence of strong acids.[15]

The melting points of reworkable monomers were 40 ^{o}C for mTMBDMA and 100 ^{o}C for pTMBDMA, respectively. Thus, mTMBDMA and mTMBDA have a good film-forming property due to low melting point and low crystallinity. In contrast, pTMBDMA has a poor film-forming property, which makes it difficult to evaluate the reworkable properties in the film state, as discussed below. It is very important to evaluate the light absorption region of the resins for their application as photosensitive reworkable resins. Figure 2-1 shows the UV-visible spectra of mTMBDA, mTMBDMA, and pTMBDMA in acetonitrile. Peaks were observed around 250 nm due to $\pi - \pi^*$ transitions of the phenyl ring in the di(meth)acrylates. Reworkable di(meth)acrylates are transparent above 350 nm. Thus, the di(meth)acrylates were applicable as i-line or g-line sensitive materials.

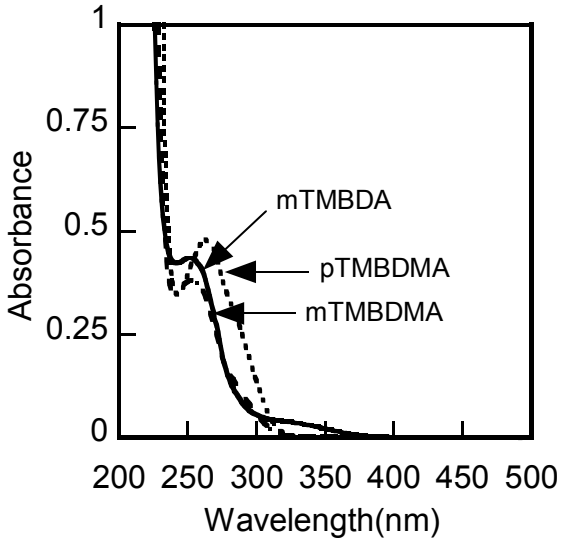

Figure 2-1. UV-visible spectra of mTMBDA (solid curve), mTMBDMA (dashed curve) and pTMBDMA (dotted curve) in acetonitrile (at a concentration of 5.0×10^{-4} mol L^{-1}).

2-3-2. Thermal curing and thermal degradation of cured reworkable resins

When mTMBDA and mTMBDMA films containing 1 wt% AIBN were heated at 120 ^{o}C for 15 min under nitrogen atmosphere, the films became completely insoluble in methanol. Simple thermal degradation of these cured resins was conducted without using PAGs. Figure 2-2 shows the dissolution of cured mTMBDA and mTMBDMA on baking at 120 – 200 ^{o}C for 10 min. A decreased film thickness was observed at 160 ^{o}C for the cured mTMBDA and 170 ^{o}C for the cured mTMBDMA. The cured mTMBDMA showed complete dissolution when baked at 180 ^{o}C. Figure 2-3 shows the FTIR spectral changes of the thermally cured mTMBDMA on baking. The reaction mechanism is shown in Scheme 2-5. The peak due to ester carbonyl (1724 cm^{-1}) showed slightly shift to 1707 cm^{-1} and the peak ascribed to carboxylic acid anhydride groups (1759 cm^{-1}, 1803 cm^{-1}) appeared. The shift of ester carbonyl groups indicated that the network structures were degraded by baking. The appearance of carboxylic acid anhydride groups also indicated the formation of the partially re-crosslinked materials. The content of the re-crosslinked materials is quite low because the degraded products dissolved completely. On the other hand, the cured mTMBDA did not show complete dissolution after thermolysis, which may be due to side reactions such as abstraction of methine proton on the main chain and successive radical coupling. Figure 2-4 shows the thermogravimetric analysis (TGA) profiles of the cured mTMBDA and cured mTMBDMA resins. Thermal decomposition temperature (T_d) of cured mTMBDA and cured mTMBDMA was 171 ^{o}C and 196 ^{o}C, respectively. Therefore, their thermal decomposition profiles of the cured mTMBDA and mTMBDMA were consistent with their dissolution profiles. The cured mTMBDMA showed higher stability than cured mTMBDA.

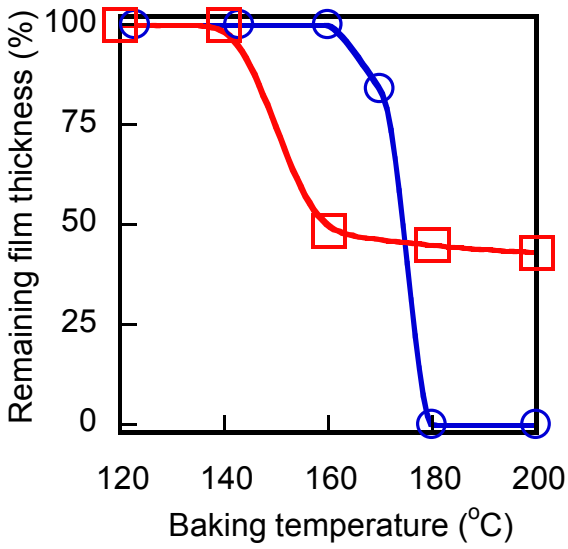

Figure 2-2. Degradation profiles of thermally cured mTMBDA (□) and mTMBDMA (○). Curing condition: baked at 120 °C for 15 min under nitrogen. Baking condition for degradation: 10 min in air. Dissolution: in methanol for 10 min. Film thickness: 1.0 μm.

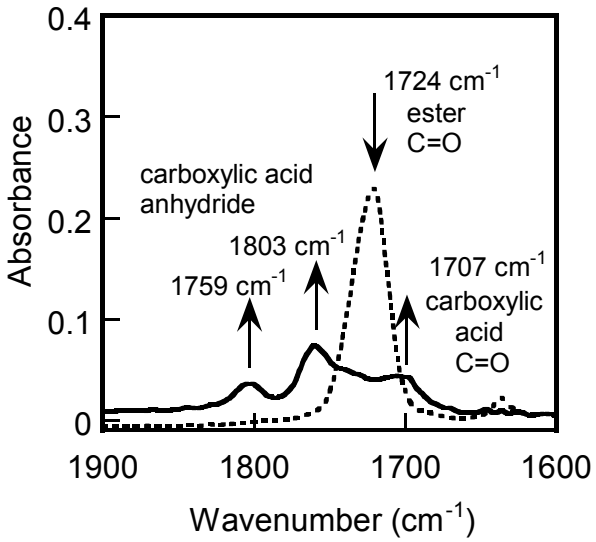

Figure 2-3. IR spectral changes of thermally cured mTMBDMA resin on baking. Curing condition: baked at 120 °C for 15 min under nitrogen. Dotted line: before baking. Solid line: after baking at 180 °C for 10 min. Film thickness: 1.0 μm.

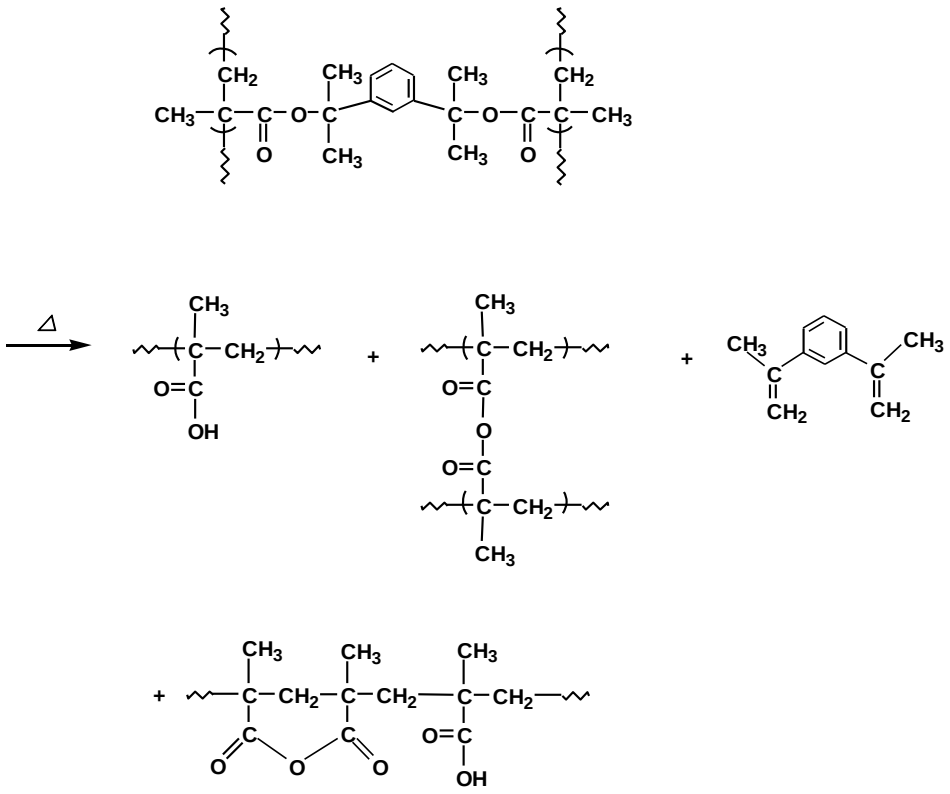

Scheme 2-5. Proposed mechanism for thermal degradation of thermally cured mTMBDMA.

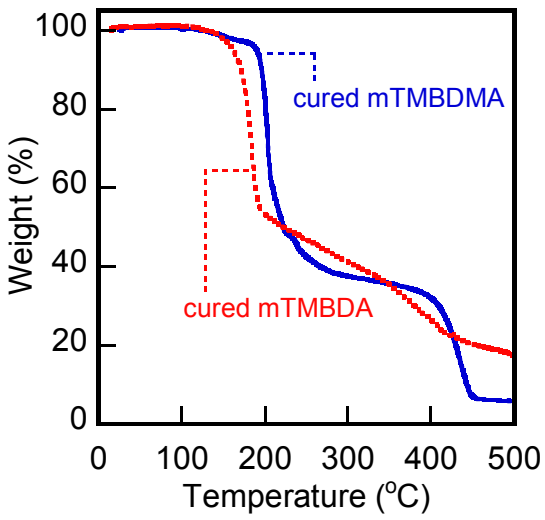

Figure 2-4. TGA profiles of cured mTMBDMA and cured mTMBDA resin. Curing condition: baked at 140 °C for 10 min under nitrogen. Heating rate: 10 °C/min.

2-3-3. Thermal curing and photoinduced degradation of cured reworkable resins

The di(meth)acrylates are thermally curable in the presence of a radical initiator AIBN. The PAGs included in the system do not affect the free radical polymerization process because their degradation temperature is much higher than the processing temperature. Figure 2-5 (a) shows the insoluble fraction of mTMBDA and mTMBDMA films containing 1 wt% AIBN and 1 wt% NITf. The insoluble fraction increased with baking temperature, and complete insolubilization was observed for these films when baked at 140 ^{o}C for 10 min. On baking, the peak at 1636 cm^{-1} due to C=C stretching in IR spectra decreased. Figure 2-5 (b) shows the effect of conversion of (meth)acrylate units on baking. The effective polymerization for these monomers occurred and the conversion for mTMBDA and mTMBDMA after baking at 140 ^{o}C for 10 min was observed to be 76 and 78%, respectively. Reactivity of mTMBDA was similar to that of mTMBDMA. Addition of i-line sensitive PAGs, NITf and ITXTS did not affect the thermal curing reaction of mTMBDA and mTMBDMA as was expected.

Figure 2-6 (a) shows the effect of baking time at 120 ^{o}C on insolubilization of the reworkable monomers. The insoluble fraction increased with baking time, and complete insolubilization was observed for these films when baked at 120 ^{o}C for 15 min. Figure 2-6 (b) shows the effect of baking time on conversion of (meth)acrylate units. The conversion of (meth)acrylate units increased with baking time and both mTMBDA and mTMBDMA showed similar curing behavior.

Thermal properties of the cured di(meth)acrylates were studied using TGA. Figure 2-7 shows the TGA profiles of the cured mTMBDMA under neutral or acidic conditions and their values of T_d are summarized in Table 2-1. When the cured resins were heated under nitrogen at a heating rate (10 ^{o}C / min), cured mTMBDMA resin under neutral condition started to lose its weight at 196 ^{o}C as shown in Figure 2-4. On the other hand, values of T_d for cured mTMBDMA with *p*-toluenesulfonic acid generated from ITXTS and with triflic acid generated

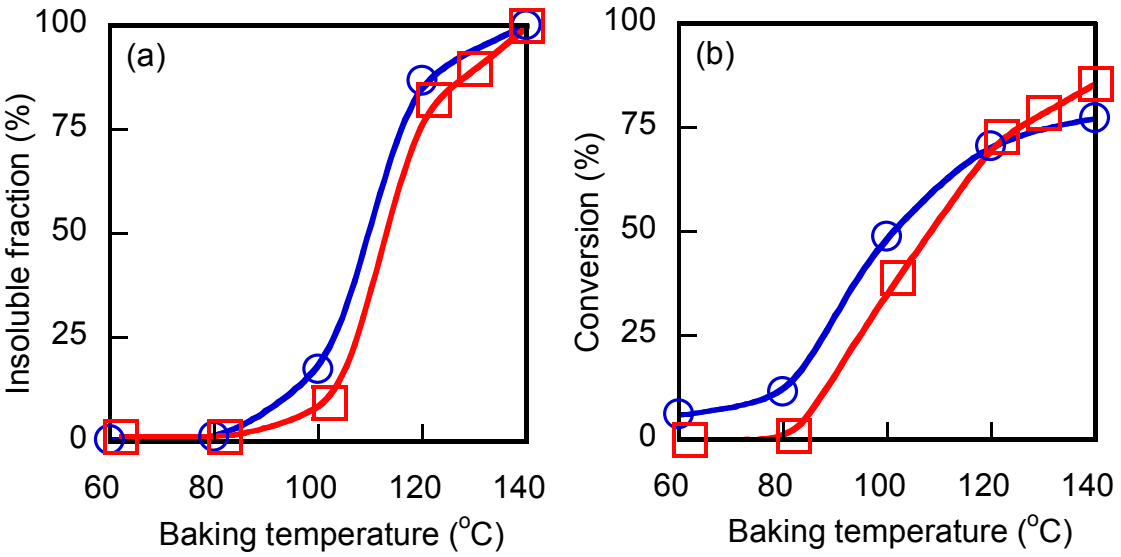

Figure 2-5. Effect of baking temperature on insolubilization (a) and conversion of (meth)acrylate unit (b) of monomers containing 1 wt% AIBN and 1 wt% NITf. Monomer: mTMBDMA (○) and mTMBDA (□). Dissolution: in methanol for 10 min. Film thickness: 1.0 -2.0 μm. Bake time: 10 min.

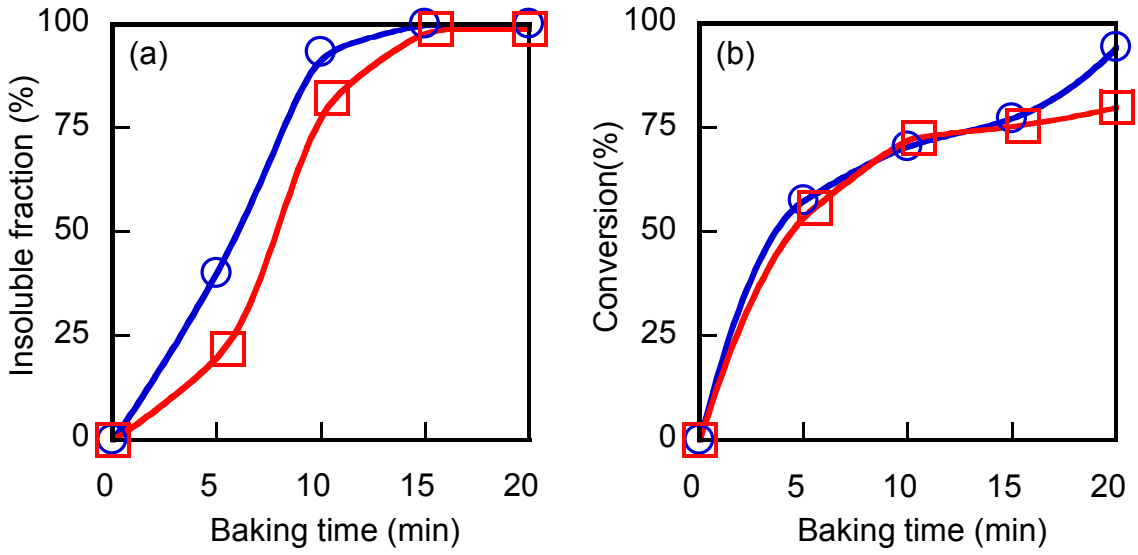

Figure 2-6. Effect of baking time on insolubilization (a) and conversion of (meth)acrylate unit (b) of monomers containing 1 wt% AIBN and 1 wt% NITf. Monomer: mTMBDMA (○) and mTMBDA (□). Baking temperature: 120 °C. Dissolution: in methanol for 10 min. Film thickness: 1.0 -2.0 μm.

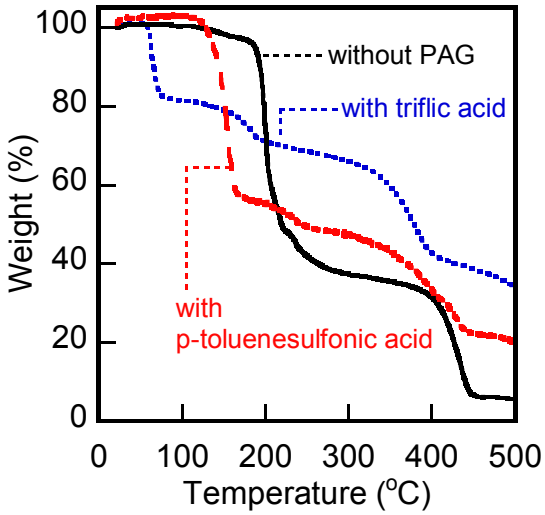

Figure 2-7. TGA profiles of cured mTMBDMA resin. PAG; dotted line: NITf, dashed line: ITXTS, and solid line: without PAG. Curing condition: baked at 140 °C for 10 min under nitrogen. Irradiation dose at 365 nm: 500 mJ/cm^2. Heating rate: 10 °C/min.

Table 2-1. Thermal decomposition temperatures of the cured resins with or without acid generated from PAGs in the system.

Resin	T_d (°C)	T_d (°C) [a] with *p*-TSA[b]	T_d (°C)[a] with triflic acid
Cured mTMBDMA	196	142	65
Cured mTMBDA	171	137	58

a) PAG concentration: 1.0 wt%. Irradiation dose: 500 mJ/cm^2.
b) *p*-toluenesulfonic acid.

from NITf were 142 ^{o}C and 65 ^{o}C, respectively. Structure of PAGs affected the thermal decomposition behavior of the cured reworkable resin. Similar thermal decomposition behavior was also observed when the cured mTMBDA was analyzed by TGA.

Figure 2-8 shows the solubility change of thermally cured mTMBDA and mTMBDMA resins. Although the cured resins are thermally stable up to 140 ^{o}C without irradiation, complete dissolution of the cured mTMBDMA containing 1 wt% ITXTS was observed when the cured films were irradiated at 365 nm and baked at 130 - 140 ^{o}C. The effect of the structure of PAG on the decomposition properties was also investigated. With NITf instead of ITXTS as a PAG, thermally cured mTMBDMA resin dissolved in methanol after irradiation at 365 nm and followed by baking at 100 – 140 ^{o}C. The structure of the PAG affected the baking temperature for complete dissolution. On irradiation at 365 nm, NITf and ITXTS generate triflic acid and *p*-toluenesulfonic acid, respectively. Triflic acid catalyzed the cleavage of tertiary ester linkages more effectively than *p*-toluenesulfonic acid as shown in Table 2-1. Thus, the temperature for the photo-induced degradation of the cured materials can be settled by choosing PAGs. The insoluble fraction of cured mTMBDMA coincided with remaining tertiary ester linkages. Thus, quantitative decomposition of tertiary ester linkages was needed for complete dissolution of the cured films. On the other hand, the cured mTMBDA did not show complete dissolution behavior.

Analysis of the decomposition products enables clarification of the degradation mechanism. FTIR, ^{1}H NMR, GC-MS, and SEC analyses were carried out. Figure 2-9 shows FTIR spectral changes of thermally cured mTMBDMA resin on irradiation at 365 nm and followed by baking at 140 ^{o}C for 10 min. The peak at 1140 cm^{-1} due to ester C-O-C bonds disappeared when exposed to 365-nm light and followed by baking. On the other hand, the peak due to ester carbonyl (1724 cm^{-1}) showed slightly shift to 1707 cm^{-1} and the peak ascribed to hydroxyl groups (2800 – 3600 cm^{-1}) appeared, which is due to the formation of carboxylic acid groups.

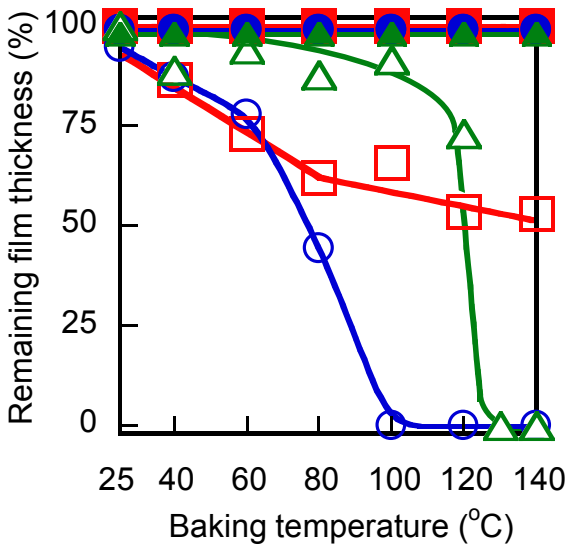

Figure 2-8. Dissolution profiles of thermally cured mTMBDA (□, ■) and mTMBDMA (○, ●, △, ▲) films. Additive: (□, ■, ○, ●) 1 wt% AIBN and 1 wt% NITf; (△, ▲) 1 wt% AIBN and 1 wt% ITXTS. Curing condition: baked at 120 °C for 15 min under nitrogen. Open symbol: exposed at 365 nm with 200 mJ/cm^2. Solid symbol: unexposed at 365 nm. Dissolution: in methanol for 10 min. Bake condition: 10 min in air. Film thickness: 1.0 μm.

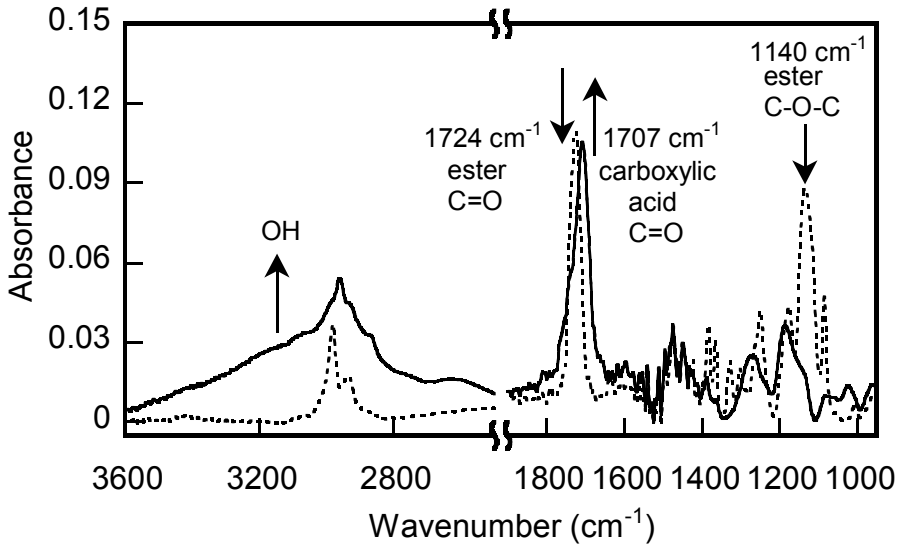

Figure 2-9. IR spectral changes of thermally cured mTMBDMA resin containing 1 wt% AIBN and 1 wt% NITf on irradiation. Curing condition: baked at 120 °C for 15 min under nitrogen. Dotted line: before irradiation. Solid line: after irradiation at 365 nm with 200 mJ/cm^2 and followed by baking at 140 °C for 10 min. Film thickness: 0.7 μm.

No carboxylic acid anhydride groups were observed because the baking for degradation of reworkable resin was conducted at relatively mild condition. Another product, 1,3-bis(1-methylethenyl)benzene was identified from DI-mode GC-MS and ^{1}H NMR analyses. Figure 2-10 (a) shows the DI-mode GC-MS spectrum of thermally cured mTMBDMA containing 1 wt% AIBN. The spectrum of authentic 1,3-bis(1-methylethenyl)benzene is shown in Figure 2-10 (b). The peak at *m/z* = 158 and a series of fragment peaks due to 1,3-bis(1-methylethenyl)benzene generated by thermolysis was almost vaporized and was observed. ^{1}H NMR analysis of the mTMBDMA monomer in d_6-DMSO on heating also reveals the formation of 1,3-bis(1-methylethenyl)benzene as confirmed by the olefinic peaks at 5.1 and 5.4 ppm.

In particular, SEC is a powerful method for investigating the chain length of photo-cured (meth)acrylates.[12,14] We consider that an 'unzipping' reaction of the poly(methacrylate) chains does not occur for the acid-catalyzed degradation of the network structure, because the degradation temperature is not high (120 - 140 ^{o}C). Figure 2-11 shows the SEC profile of thermally cured mTMBDMA containing 1 wt% AIBN after thermal degradation and followed by methylation of poly(methacrylic acid) as a decomposition product. *Mn* and *Mw/Mn* were 1.8×10^{4} gmol^{-1} and 3.5, respectively.

The reaction mechanism is shown in Scheme 2-6. The radicals thermally generated from AIBN initiated the polymerization of the dimethacrylates. The networks formed are degraded by thermolysis with or without photogenerated acid. The networks are converted into liner poly(methacrylic acid) and 1,3-bis(1-methylethenyl)benzene. Photogenerated acid lowers the decomposition temperature of the networks.

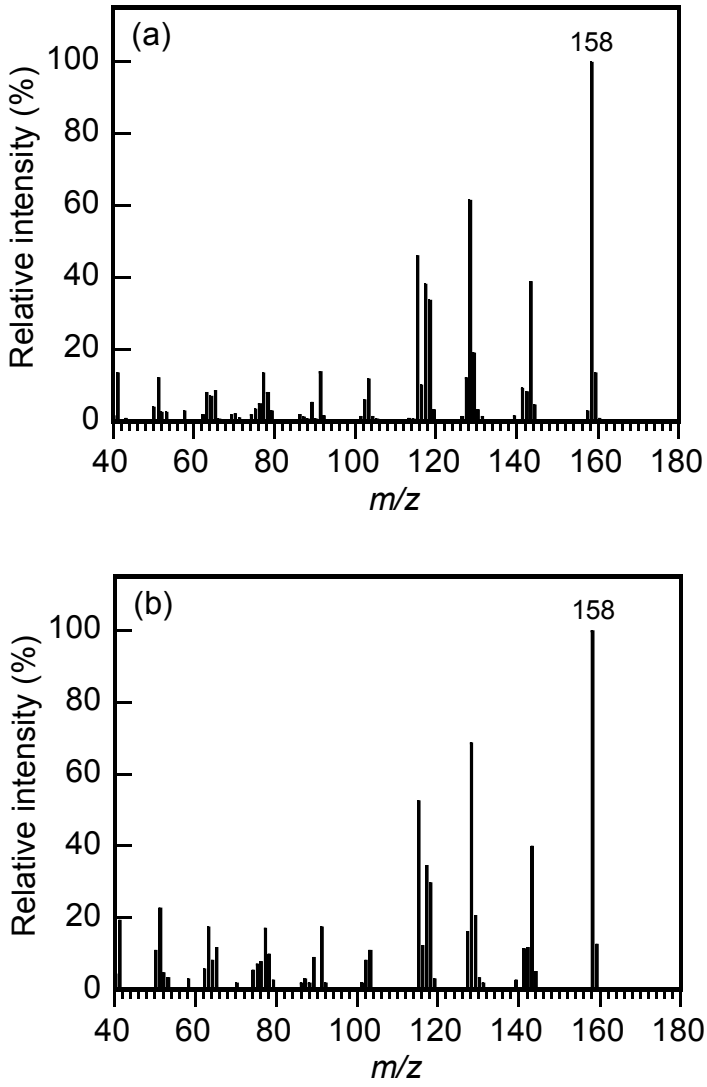

Figure 2-10. DI-mode GC-MS spectra of (a) thermally cured mTMBDMA and (b) 1,3-bis(1-methylethenyl)benzene. Curing condition: baked at 120 ^{o}C for 15 min under nitrogen. Probe temperature: 220 ^{o}C.

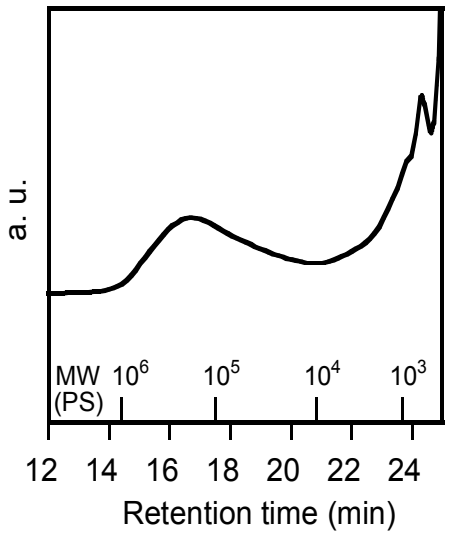

Figure 2-11. SEC profile of thermally cured mTMBDMA after thermal degradation and followed by methylation. Curing condition: baked at 120 °C for 15 min under nitrogen. Thermal degradation condition: heating at 180 °C for 10 min in air.

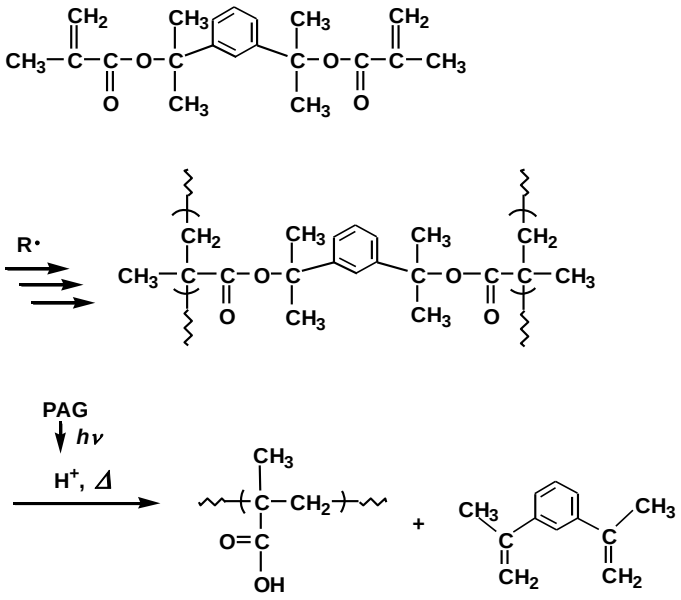

Scheme 2-6. Reaction mechanism of the curing and photoinduced thermal degradation of mTMBDMA.

Figure 2-12 shows the effect of irradiation dose at 365 nm on decomposition behaviors of cured reworkable resins. The remaining film thickness of cured resins decreased with irradiation dose, and complete solubilization of the cured mTMBDMA was observed when irradiated at 365 nm with 20 mJ/cm^2 and baked at 140 ^{o}C for 10 min. It was confirmed that the cured mTMBDMA was very sensitive to the acids generated in the system. The effect of AIBN concentration on dissolution of cured mTMBDA was also studied. Regretfully, the cured mTMBDA did not show complete dissolution behavior. Compared with lower concentration (0.5 – 1.0 wt% of AIBN), cured mTMBDA containing 1.5 wt% AIBN showed lower dissolution behavior into methanol. It is considered that relatively high crosslink density and chain transfer activity prevent the complete dissolution of the cured mTMBDA.

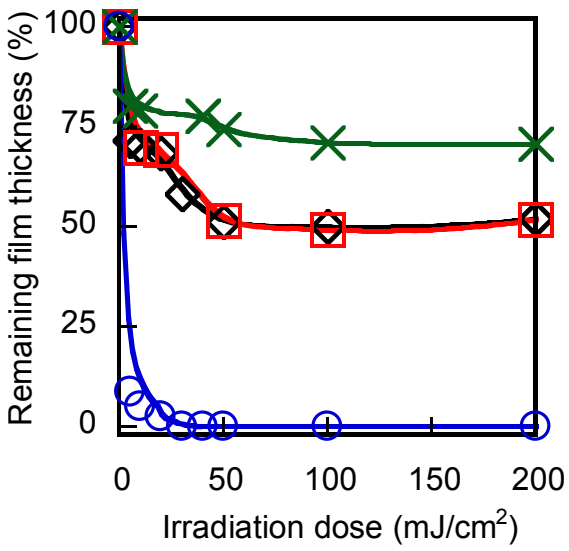

Figure 2-12. Effect of irradiation dose on dissolution of thermally cured resins containing 1 wt% NITf. Resin: (○) mTMBDMA and (□, ◇, ×) mTMBDA. Additive: (□, ○) 1 wt% AIBN and 1 wt% NITf; (◇) 0.5 wt% AIBN and 1 wt% NITf, and (×) 1.5 wt% AIBN and 1 wt% NITf. Curing condition: (○) baked at 120 ^{o}C for 15 min and (□, ◇, ×) baked at 140 ^{o}C for 10 min under nitrogen. Degradation condition: irradiated at 365 nm in air and followed by baking at 140 ^{o}C for 10 min. Dissolution: in methanol for 10 min. Film thickness: 1.0 μm.

2-3-4. Photo-curing and thermal degradation of cured reworkable resins

As mentioned above, an i-line sensitive photoinitiator, DMPA, was used for photo-curing of mTMBDA and mTMBDMA. DMPA generates radical species on irradiation at 365 nm. Figure 2-13 shows photo-induced insolubilization behaviors of mTMBDA and mTMBDMA containing 1 wt% DMPA. Insoluble fraction increased with increasing irradiation dose and reached a constant value. Insoluble fractions of mTMBDA and mTMBDMA at the irradiation dose of 200 mJ/cm^2 were 66 % and 70 %, respectively.

Figure 2-14 shows the IR spectral changes of mTMBDMA containing 1 wt% DMPA on irradiation. The peak at 1636 cm^{-1} due to C=C stretching in IR spectra decreased on irradiation at 365-nm light. Figure 2-15 shows the conversions of (meth)acrylate units of mTMBDA and mTMBDMA on irradiation. The effective polymerization occurred and the conversion at the exposure dose of 200 mJ/cm^2 of mTMBDA and mTMBDMA were observed to be 51 % and 44%, respectively. mTMBDMA was more reactive than mTMBDA. The results disagreed with those of thermal curing shown in Figure 2-5 (b). It is known that the propagation rate of methacrylates is lower than acrylates. The disagreement may be due to high chain transfer activity or unspecified reactions of mTMBDA.

The thermal degradation of photo-cured mTMBDA and mTMBDMA was investigated. Figure 2-16 shows the dissolution of photo-cured mTMBDA and mTMBDMA on baking. Complete dissolution was observed for photo-cured mTMBDMA when the film was baked at 180–190 ^{o}C for 10 min. Photo-cured mTMBDA did not show complete dissolution. The decomposition profiles of thermally cured films (see Figure 2-2) and photo-cured films were in good agreement. The degradation products of cured mTMBDMA became insoluble in methanol after baking above 200 ^{o}C. Figure 2-17 shows the FTIR spectral changes of the photo-cured mTMBDMA on baking. The peak due to ester carbonyl (1724 cm^{-1}) showed

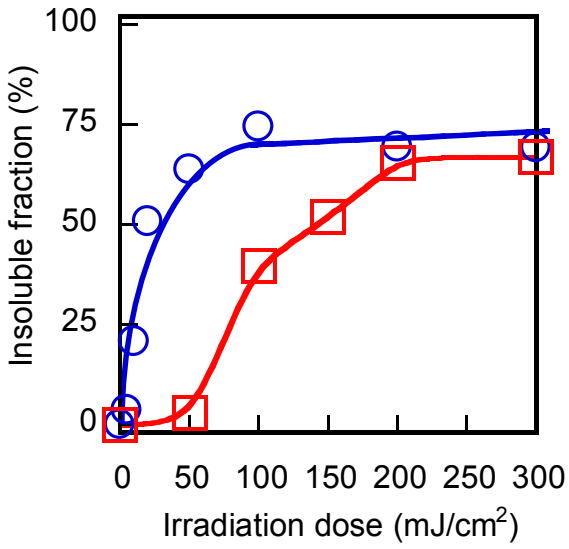

Figure 2-13. Effect of irradiation dose at 365 nm on insolubilization of mTMBDA (□) and mTMBDMA (○) containing 1 wt% DMPA. Irradiation condition: at room temperature under nitrogen. Dissolution: in methanol for 10 min. Film thickness: 1.0 μm.

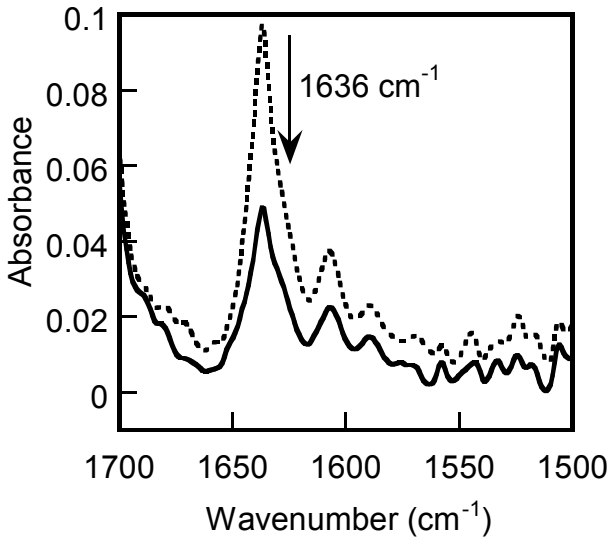

Figure 2-14. IR spectral changes of mTMBDMA containing 1 wt% DMPA on irradiation at 365 nm under nitrogen. Dotted line: before irradiation. Solid line: after irradiation at 365 nm with 100 mJ/cm^2. Film thickness: 2.0 μm.

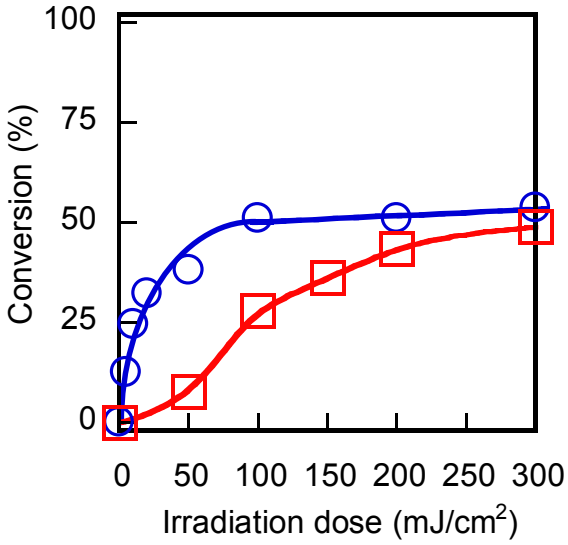

Figure 2-15. Effect of irradiation dose at 365 nm on conversion of mTMBDA (□) and mTMBDMA (○) containing 1 wt% DMPA. Irradiation condition: at room temperature under nitrogen. Dissolution: in methanol for 10 min. Film thickness: 1.0 μm.

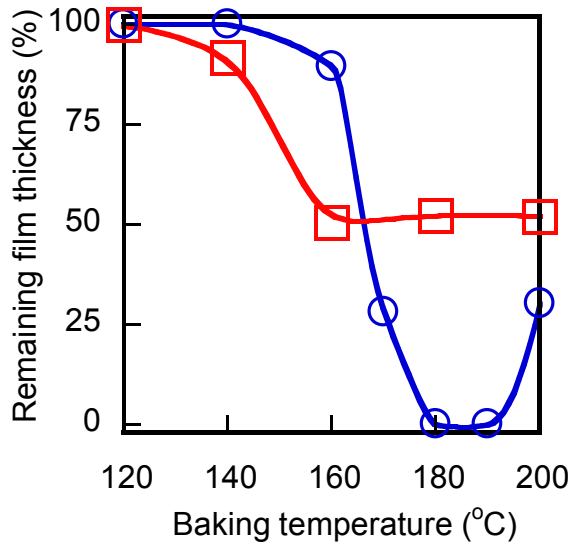

Figure 2-16. Degradation profiles of thermally cured mTMBDA (□) and mTMBDMA (○). Curing condition: irradiated at 365 nm with 200 mJ/cm^2 under nitrogen. Baking condition for degradation: 10 min in air. Dissolution: in methanol for 10 min. Film thickness: 1.0 μm.

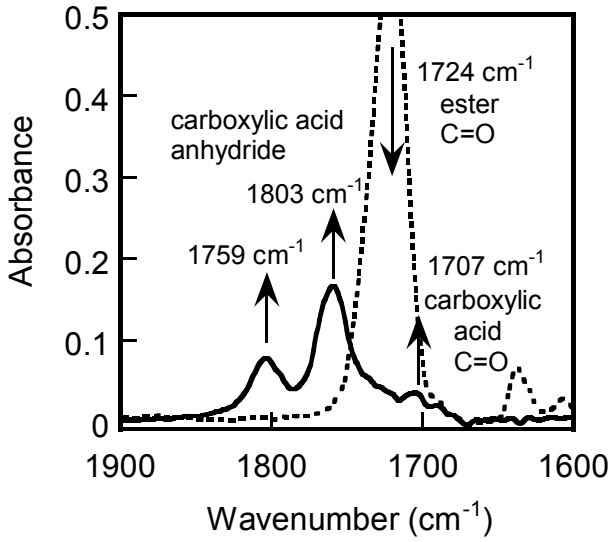

Figure 2-17. IR spectral changes of photo-cured mTMBDMA resin on baking. Curing condition: irradiated at 365 nm with 200 mJ/cm^2 under nitrogen. Dotted line: before baking. Solid line: after baking at 200 ^{o}C for 10 min. Film thickness: 2.0 μm.

slightly shift to 1707 cm^{-1} and the peak ascribed to carboxylic acid anhydride groups (1759 cm^{-1}, 1803 cm^{-1}) appeared. The re-insolubilization above 200 ^{o}C was due to the crosslinking of poly(methacrylic acid) generated from degradation of the cured mTMBDMA via formation of carboxylic acid anhydride groups.

2-4. Conclusion

Novel difunctional (meth)acrylates bearing tertiary ester groups were synthesized. Thermal curing and thermal degradation, thermal curing and photoinduced degradation, and photo-curing and thermal degradation of di(meth)acrylates having aromatic units and thermally degradable units were reported.

The difunctional (meth)acrylates containing a thermally induced radical initiator AIBN or an AIBN and a PAG were cured by baking. These di(meth)acrylates became completely insoluble in methanol. The cured di(meth)acrylates were dissolved in solvents after thermolysis of tertiary esters. Complete dissolution was observed for the cured mTMBDMA. The dissolution behaviors were strongly affected by the structures of the PAGs and with or without acids generated in the system. The temperature for the photo-induced degradation of the cured materials can be settled by choosing PAGs.

The difunctional (meth)acrylates containing a photoradical initiator were cured on irradiation. The cured di(meth)acrylates were dissolved in solvents after thermolysis. Complete dissolution was observed for the cured mTMBDMA. The dissolution behaviors were strongly affected by the structures of the reworkable monomers.

A mechanism for the photo- or thermally curing and photoinduced thermal degradation was studied using FTIR and ^{1}H NMR analyses, TGA, MS and SEC. Tertiary ester was subject to breakdown into carboxylic acid and alkene by simple thermal treatment. Poly(methacrylic acid) and 1,3- bis(1-methylethenyl)benzene were identified as decomposition products.

References

1. M. Shirai, *Prog. Org. Coat.*, 58, 158 (2007).
2. T. Maeda, H. Otsuka, A. Takahara, *Prog. Polym. Sci.*, 34, 581 (2009).
3. C. J. Kloxin, T. F. Scott, B. J. Adzima, C. N. Bowman, *Macromolecules*, 43, 2643 (2010).
4. K. Ogino, J. -S. Chen, C. K. Ober, *Chem. Mater.*, 10, 3833 (1998).
5. M. F. Montague, C. J. Hawker, *Chem. Mater.*, 19, 526 (2007).
6. S. Yang, J. -S. Chen, H. Korner, T. Breiner, C. K. Ober, *Chem. Mater.*, 10, 1475 (1998).
7. J. -S. Chen, C. K. Ober, M. D. Poliks, *Polymer.*, 43, 131 (2002).
8. L. Kilian, Z. -H. Wang, T. E. Long, *J. Polym. Sci., Part A, Polym. Chem.*, 41, 3083 (2003).
9. S. B. Jhaveri, K. R. Carter, *Macromolecules,* 40, 7874 (2007).
10. S. L. Buchwalter, L. L. Kosber, *J. Polym. Sci., Part A, Polym. Chem.*, 34, 249 (1996).
11. E. Ruckenstein, H. Zhang, *Macromolecules*, 32, 3979 (1999).
12. J. A. Burdick, T. M. Lovestead, K. S. Anseth, *Biomacromolecules*, 4, 149 (2003).
13. H. Okamura, K. Sakai, M. Tsunooka, M. Shirai, T. Fujiki, S. Kawasaki, M. Yamada, *J. Photopolym. Sci. Technol*., 16, 87 (2003).
14. M. Shirai, K. Mitsukura, H. Okamura, *Chem. Mater.*, 20, 1971 (2008).
15. H. Okamura, K. Shin, M. Shirai, *Polym. J.*, 38, 1237 (2006).

Chapter 3

Reworkable system based on main- and side-chain scission of photocurable oligo(hemiacetal ester)s

3-1. Introduction

It is known that the hemiacetal ester linkages are stable up to 150 – 200 ^{o}C under neutral or basic conditions and decomposes readily under acidic conditions.[1-2] Thus, the hemiacetal ester linkage is very useful as a degradable unit for reworkable resins. Acidolysis of hemiacetal ester linkage is shown in Scheme 3-1. Recently, polymers that contain acid-cleavable backbone structures have been reported.[3-5] Otsuka and Endo reported the syntheses and thermal dissociation behavior of poly(hemiacetal ester)s with various alkyl spacers.[3] The dissociation temperature of the polymers can be controlled by molecular design of the dicarboxylic acid components. Hashimoto et al. also reported the syntheses of poly(acetal)s with various main-chain structures.[4] The polymers exhibited stability under neutral or basic conditions and were smoothly degraded with aqueous acids. Felix and Ober reported the syntheses of poly(acetal)s and their applications to positive-tone photoresists developable in supercritical CO_2.[5] Chain-scission type resists can give positive-tone pattern by both aqueous alkaline solution and supercritical CO_2 development.

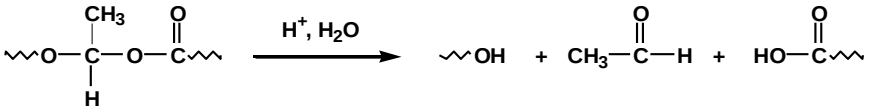

Scheme 3-1. Acidolysis of a hemiacetal ester linkage.

Chapter 3

This chapter describes the synthesis of novel oligo(hemiacetal ester)s having methacrylate units as UV crosslinkable groups and both main-chain hemiacetal ester units and tertiary ester units in the side chains as degradable linkages. The oligo(hemiacetal ester)s were prepared by polyaddition of corresponding dicarboxylic acid with divinyl ether. The concept of the present system is shown in Scheme 3-2. On irradiation at 365-nm light, network formation occurs by radical species generated from photoradical initiator. On irradiation at 254-nm light and followed by baking, the network decomposes by acid-catalyzed decomposition reaction of hemiacetal ester linkages and tertiary ester linkages. The UV curing and degradation behaviors were investigated.

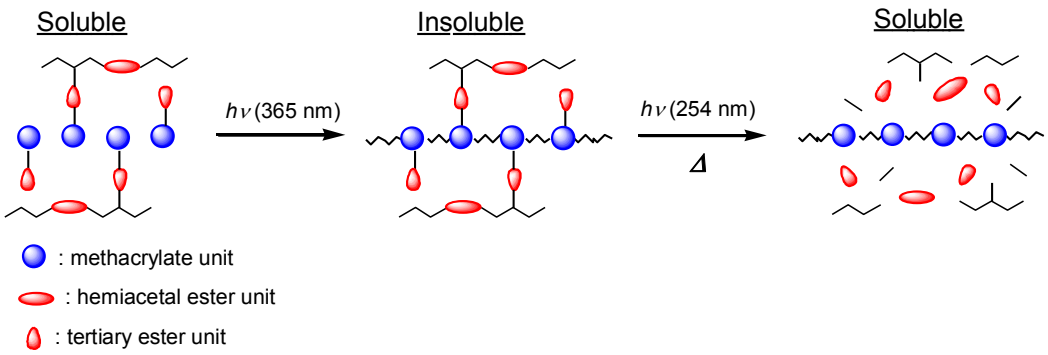

Scheme 3-2. Design concept of photocrosslinkable oligomers having degradable property.

3-2. Experimental

3-2-1. Measurements

^{1}H NMR spectra were observed at 400 MHz using a JEOL LA-400 spectrophotometer and at 300 MHz using a JEOL LA-300 spectrophotometer. FTIR measurements were carried out using a JASCO FT/IR-4200. Size exclusion chromatography (SEC) was performed in tetrahydrofuran by use of a SEC system (JASCO PU-2080Plus) with polystyrene gel columns, TSKgel GMH_{HR}-N and TSKgel GMH_{HR}-H. Molecular weights for the polymers were calibrated for polystyrene standards. Irradiation was performed at 254 and 365 nm using a low-pressure Hg lamp (Ushio ULO-6DQ, 6W) and a high-pressure Hg lamp (Ushio UM 102) with a filter UVD36B, respectively. The intensity of the light was measured by an Orc Light Measure UV-M02.

3-2-2. Materials

Chloroform and triethylamine were purchased and distilled over CaH_2 before use. Propylene glycol 1-monomethyl ether 2-acetate (PGMEA), triphenylsulfonium triflate (TPST), and 1,4-bis[(vinyloxy)methyl]-cyclohexane (CHDVE) were of reagent grade and used without further purification. Other solvents and reagents were purchased and used as received.

3-2-3. Synthesis of dicarboxylic acids having tertiary ester groups

*3-(t-Butyldimethylsilyloxy)-1,1-dimethylpropanol (**1**)*[6]

Dimethylaminopyridine (2.50 g, 20.4 mmol), *t*-butyldimethylsilyl chloride (80.0 g, 530 mmol), chloroform (630 mL), and triethylamine (75.0 mL, 530 mmol) were placed in a three-necked round-bottom flask fitted with an efficient magnetic stirrer and a thermometer

under nitrogen atmosphere. 3-Methyl-1,3-butanediol (50.0 mL, 470 mmol) was added dropwise. The mixture was stirred at ambient temperature for 20 h and then thoroughly washed with water, saturated ammonium chloride. The chloroform layer was separated and dried over anhydrous Na_2SO_4. After removal of the solvent on a rotary evaporator, **1** was purified by distillation under reduced pressure (bp: 45.3 ^oC at 3.0 mmHg), giving a colorless liquid in a yield of 95.7 g (91 %). ^1H NMR (300 MHz, DMSO-d_6; δ, ppm) 4.16 (1H, s, -OH), 3.68 (2H, t, -CH_2-O), 1.56 (2H, t, C(CH_3)$_2$-CH_2-), 1.05 (6H, s, tertiary CH_3), 0.82 (9H, s, Si-C(CH_3)$_3$), 0.00 (6H, s, O-Si(CH_3)$_2$-). Anal. Calcd for $C_{11}H_{26}O_2Si$: C 60.49, H 12.00. Found: C 59.73, H 11.86.

*3-(t-Butyldimethylsilyloxy)-1,1-dimethylpropyl methacrylate (**2**)*

Dimethylaminopyridine (4.30 g, 35.2 mmol), 2,6-di-*t*-butyl-*p*-cresol (0.10 g, 0.45 mmol), **1** (95.7 g, 438 mmol), chloroform (300 mL), and triethylamine (88.0 mL, 630 mmol) were placed in a four-necked round-bottom flask fitted with an efficient magnetic stirrer and a thermometer under nitrogen atmosphere. The flask was cooled to 0 - 5 ^oC using an ice-water bath. Methacryloyl chloride (61.0 mL, 630 mmol) was added slowly to the solution and the reaction was continued for 50 h. The chloroform layer was washed with water twice, saturated $NaHCO_3$ three times, and then with water twice. The organic layer was separated and dried over anhydrous Na_2SO_4. After removal of the solvent on a rotary evaporator, **2** was purified by column chromatography (silica gel, eluent: ethyl acetate/hexane = 3/7, v/v) to obtain a colorless liquid in a yield of 95.2 g (75 %). ^1H NMR (400 MHz, $CDCl_3$; δ, ppm) 5.95, 5.44 (2H, s, CH_2=C-), 3.69 (2H, t, -CH_2-O), 2.00 (2H, t, C(CH_3)$_2$-CH_2-), 1.85 (3H, s, methacrylic CH_3), 1.46 (6H, s, O-C(CH_3)$_2$-), 0.84 (9H, s, -C(CH_3)$_3$), 0.00 (6H, s, O-Si(CH_3)$_2$-). Anal. Calcd for $C_{15}H_{30}O_3Si$: C 62.89, H 10.55. Found: C 61.81, H 10.57.

*1,1-Dimethyl-3-hydroxypropyl methacrylate (**3**)*[7]

Into a three necked round-bottom flask was placed 370 mL of 1 M tetrabutylammonium fluoride in tetrahydrofuran (THF). The flask was cooled to 0 - 5 ^{o}C using an ice-water bath. **2** (52.0 g, 181 mmol) was added slowly to the solution. The reaction mixture was stirred at ambient temperature for 3 h. After removal of THF on a rotary evaporator, excessive chloroform was added and the chloroform solution was washed with water three times and dried over anhydrous Na_2SO_4. After removal of the solvent, **3** was purified by column chromatography (silica gel, eluent: ethyl acetate/hexane = 3/2, v/v) to obtain a colorless liquid in a yield of 27.1 g (86 %). ^{1}H NMR (400 MHz, $CDCl_3$; δ, ppm) 6.06, 5.54 (2H, s, C*H*$_2$=C), 4.30 (2H, t, C*H*$_2$-O), 1.91 (3H, s, methacrylic C*H*$_3$), 1.87 (2H, t, C(CH$_3$)$_2$-C*H*$_2$-), 1.26 (s, 6H, tertiary C*H*$_3$). Anal. Calcd for $C_9H_{16}O_3$: C 62.77, H 9.36. Found: C 62.12, H 9.41.

*1,2,4-Benzenetricarboxylic acid 4-[3-methyl-3-[(2-methyl-1-oxo-2-propenyl)oxy]butyl]ester (**dicarboxylic acid A**)*

Into a three necked round-bottom flask was placed trimellitic anhydride chloride (5.60 g, 26.5 mmol) and toluene (30.0 mL). **3** (5.00 g, 29.0 mmol), 2,6-di-*t*-butyl-*p*-cresol (50.0 mg, 0.23 mmol), and pyridine (2.10 g, 26.5 mmol) in 15.0 mL of toluene was added slowly to the solution. The reaction mixture was stirred at 100 ^{o}C for 10 h. The mixture was cooled to room temperature, and then filtered. Excess amounts of diethyl ether were added and the ether layer was washed with saturated $NaHCO_3$ three times. The ether layer was separated and dried over anhydrous $MgSO_4$. After removal of the solvent, 4-[3-methyl-3-[(2-methyl-1-oxo-2-propenyl)-oxy]butyl]trimellitic anhydride was purified by recrystallization from hexane/toluene (8/2, v/v) in a yield of 4.40 g (48 %). mp: 76.0 - 77.0 ^{o}C. ^{1}H NMR (400 MHz, $CDCl_3$; δ, ppm) 8.54 - 8.05 (3H, m, aromatic), 6.03, 5.50 (2H, s, C*H*$_2$=C), 4.31 (2H, t, O-C*H*$_2$-), 2.36 (2H, t, O-CH$_2$-C*H*$_2$-), 1.87 (3H, s, methacrylic C*H*$_3$), 1.67 (6H, s, tertiary C*H*$_3$). MS (EI) *m/z* 346

(M^+, 2.5).

4-[3-Methyl-3-[(2-methyl-1-oxo-2-propenyl)-oxy]butyl]trimellitic anhydride (2.00 g, 5.8 mmol), water (1.00 g, 56.0 mmol), and 2-butanone (18.0 mL) were placed in a two-necked round-bottom flask and stirred at ambient temperature for 48 h. Then, the reaction mixture was evaporated to dryness to obtain dicarboxylic acid A in a yield of 2.00 g (98 %). mp: 110.0 – 111.0 °C. ^{1}H NMR (400 MHz, $(CD_3)_2CO$; δ, ppm) 8.34 - 7.84 (3H, m, aromatic), 5.97, 5.53 (2H, s, C*H*$_2$=C), 4.35 (2H, t, O-C*H*$_2$-), 2.38 (2H, t, O-CH$_2$-C*H*$_2$-), 1.83 (s, 3H, methacrylic C*H*$_3$), 1.68 (s, 6H, tertiary C*H*$_3$).

1,2,4-benzenetricarboxylic acid 2-[3-methyl-3-[(2-methyl-1-oxo-2-propenyl)oxy]butyl]ester and 1,3,4-benzenetricarboxylic acid 4-[3-methyl-3-[(2-methyl-1-oxo-2-propenyl)oxy]butyl ester] ***(dicarboxylic acid B)***

Trimellitic anhydride (5.10 g, 26.5 mmol), **3** (5.00 g, 29.0 mmol), 2,6-di-*t*-butyl-*p*-cresol (7.8 mg, 35 μmol), PGMEA 10.0 g, and *N,N*-dimethylbenzylamine (0.25 mL, 1.7 mmol) were placed in a four-necked round-bottom flask fitted with an efficient magnetic stirrer and a thermometer under nitrogen atmosphere. The reaction mixture was stirred at 100 °C for 24 h. Then, additional 2,6-di-*t*-butyl-*p*-cresol (7.8 mg, 35 μmol) in 0.1 mL of PGMEA was added and the reaction was continued for 1 h at 120 °C. After removal of solvent, excessive saturated $NaHCO_3$ was added and the solution was washed with chloroform three times. The $NaHCO_3$ aqueous solution was separated and 90 mL of 1.2 N HClaq was added dropwise to obtain white solid. The solid was purified by recrystallization from ethanol/water (1/3, v/v) in a yield of 2.60 g (26 %). mp: 175.0 - 178.0 °C. ^{1}H NMR (400 MHz, DMSO-d_6; δ, ppm) 8.27 - 7.67 (3H, m, aromatic), 5.95, 5.90, 5.60, 5.52 (2H, s, C*H*$_2$=C), 4.35, 4.21 (2H, t, O-C*H*$_2$-), 2.21 (2H, m, O-CH$_2$-C*H*$_2$-), 1.81, 1.76 (3H, s, methacrylic C*H*$_3$), 1.55, 1.48 (6H, s, tertiary C*H*$_3$). Anal. Calcd for $C_{18}H_{20}O_8$: C 59.34, H 5.53. Found: C 59.20, H 5.53.

1,2,4-Benzenetricarboxylic acid 2-ethyl ester and 1,3,4-benzenetricarboxylic acid 4-ethyl ester ***(dicarboxylic acid C)***

Trimellitic anhydride (27.1 g, 141 mmol) and ethanol (100 mL, 1.71 mol) were placed in a four-necked round-bottom flask fitted with an efficient magnetic stirrer and a thermometer under nitrogen atmosphere. The reaction mixture was stirred at 80 ^{o}C for 1.5 h. After removal of solvent, white solid was obtained. The solid was purified by recrystallization from acetone/hexane (4/5, v/v) in a yield of 13.4 g (40 %). mp: 198.0 - 200.5 ^{o}C. ^{1}H NMR (400 MHz, DMSO-d_6; δ, ppm) 8.27 - 7.73 (3H, m, aromatic), 4.29 (2H, q, O-CH_2-CH_3), 1.30 (3H, t, O-CH_2-CH_3). Anal. Calcd for $C_{11}H_{10}O_6$: C 55.90, H 4.38. Found: C 55.66, H 4.11.

3-2-4. Synthesis of oligomers[3]

The typical polymerization procedures are shown as follows.

Oligomer A

Dicarboxylic acid A (250 mg, 0.7 mmol), CHDVE (140 mg, 0.7 mmol), cyclohexanone (0.4 mL), and 2,6-di-*t*-butyl-*p*-cresol (1.50 mg, 6.8 μmol) were placed in a two-necked round-bottom flask. The polyaddition reaction was carried out at 60 ^{o}C for 10 min under air-bubbling. Then, 1.5 mL of acetone and 1.6 mL of cyclohexanone were added to the reaction mixture. The solution was cooled to -78 ^{o}C. Diazomethane which was generated from *p*-toluenesulfonyl-*N*-methyl-*N*-nitrosoamide and ethanol under alkaline condition was introduced into the oligomer solution for 80 min at -78 ^{o}C using N_2 gas as a carrier.[8] The methylated oligomer A was purified by reprecipitation from cyclohexanone/hexane in a yield of 42 mg (11 %). A complete methylation was confirmed by ^{1}H NMR spectrum and thermogravimetric analysis.

Oligomer B

Dicarboxylic acid B (500 mg, 1.4 mmol), CHDVE (270 mg, 1.4 mmol), cyclohexanone (1.2 mL), and 2,6-di-*t*-butyl-*p*-cresol (2.40 mg, 11 μmol) were placed in the two-necked round-bottom flask. The polyaddition reaction was carried out at 120 ^{o}C for 10 min under air-bubbling. Then, 1.0 mL of acetone and 0.8 mL of cyclohexanone were added to the reaction mixture and the solution was cooled to -78 ^{o}C. The methylation of the terminal COOH groups was carried out using the same procedure as described for the synthesis of oligomer A. The methylated oligomer B was purified by reprecipitation from cyclohexanone/hexane in a yield of 210 mg (27 %).

Optimization of oligomerization condition

Dicarboxylic acid C (500 mg, 2.1 mmol), CHDVE (420 mg, 2.1 mmol), and solvent (tetrahydrofuran or cyclohexanone, 1.2 mL) were placed in the two-necked round-bottom flask. When the oligomerization was conducted under acidic condition, pyridinium *p*-toluenesulfonate (10.5 mg, 0.04 mmol) was added to the solution. The reaction mixture was kept at given temperatures and time. Then, analysis of polyaddition behavior by SEC was carried out. To prepare the sample solution for SEC analysis, a drop of the reaction mixture was dissolved in tetrahydrofuran and filtered with a membrane filter (pore size: 0.5 μm).

3-2-5. Photo-curing and degradation of resins

Sample films (0.5 - 1.0 μm) were prepared on silicon wafer by spin-casting of the cyclohexanone solution containing a oligomer, a monofunctional monomer 2-methyl-2-adaman-tyl methacrylate (MADMA), a photoradical initiator DMPA, and a photoacid generator TPST. The UV curing was carried out by irradiation at 365-nm light under nitrogen atmosphere. The insoluble fraction was determined by comparing the film thickness before and after dissolution

in acetone. Then the UV cured films were irradiated at 254 nm and followed by baking at given temperatures to decompose the network structures. After the film was immersed in acetone, the remaining film thickness was determined by comparing the thickness before and after dissolution in acetone.

3-3. Results and Discussion

3-3-1. Synthesis and thermal properties of oligo(hemiacetal ester)s

On the basis of the concept shown in Scheme 3-2, oligomer A and oligomer B were prepared. In this system, photo-crosslinking occurs by the polymerization of methacrylate units in the side chain. On the other hand, the degradation occurs at the main chain and side chain of the crosslinked polymers. Thus, dicarboxylic acids which have both methacrylate groups and tertiary ester linkages in a molecule were prepared (see Scheme 3-3). Dicarboxylic acid A was a phthalic acid derivative and dicarboxylic acid B was a mixture of structural isomers, isophthalic and terephthalic acid derivatives. The isomers could not be isolated by purification using flash chromatography or recrystallization. Thus, dicarboxylic acid B including structural isomers was used as a dicarboxylic acid monomer.

Optimization of polyaddition reaction was carried out using model dicarboxylic acid, i.e., dicarboxylic acid C and CHDVE. The reaction mechanism is shown in Scheme 3-4. Figure 3-1 shows the SEC profiles of the model oligomers. When equimolar amounts of dicarboxylic acids and divinyl ethers in tetrahydrofuran were stirred at ambient temperature in the presence of 2 mol% of pyridinium *p*-toluenesulfonate as an acid catalyst, the model oligomer with a molecular weight of 1,500 was obtained (see Figure 3-1 (a)). The SEC curve shifted to lower molecular weight region as increasing reaction time, suggesting the degradation of the oligomer formed. So, this oligomerization condition was not suitable to obtain oligomers. When

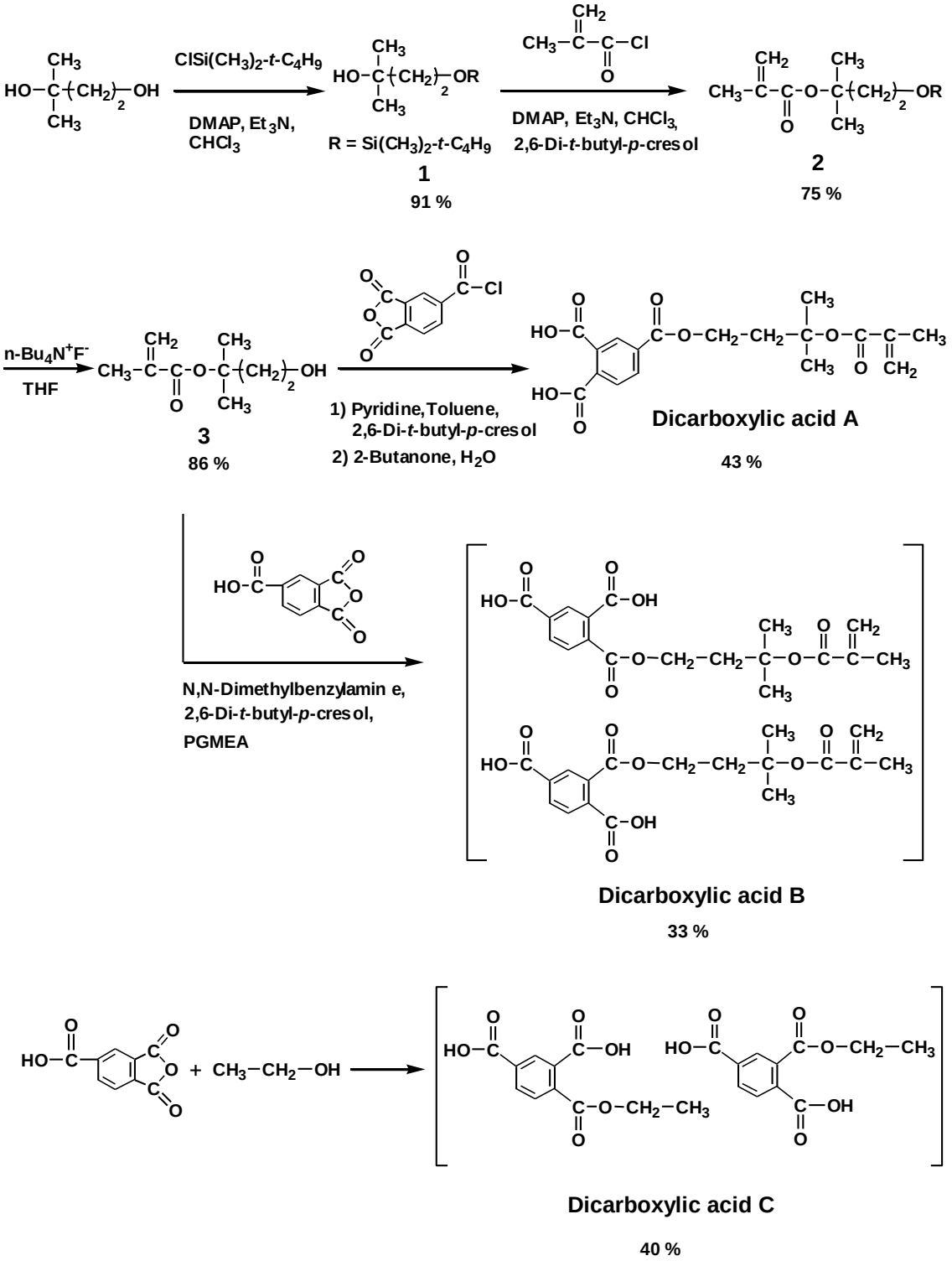

Scheme 3-3. Synthesis of dicarboxylic acids A, B, and C.

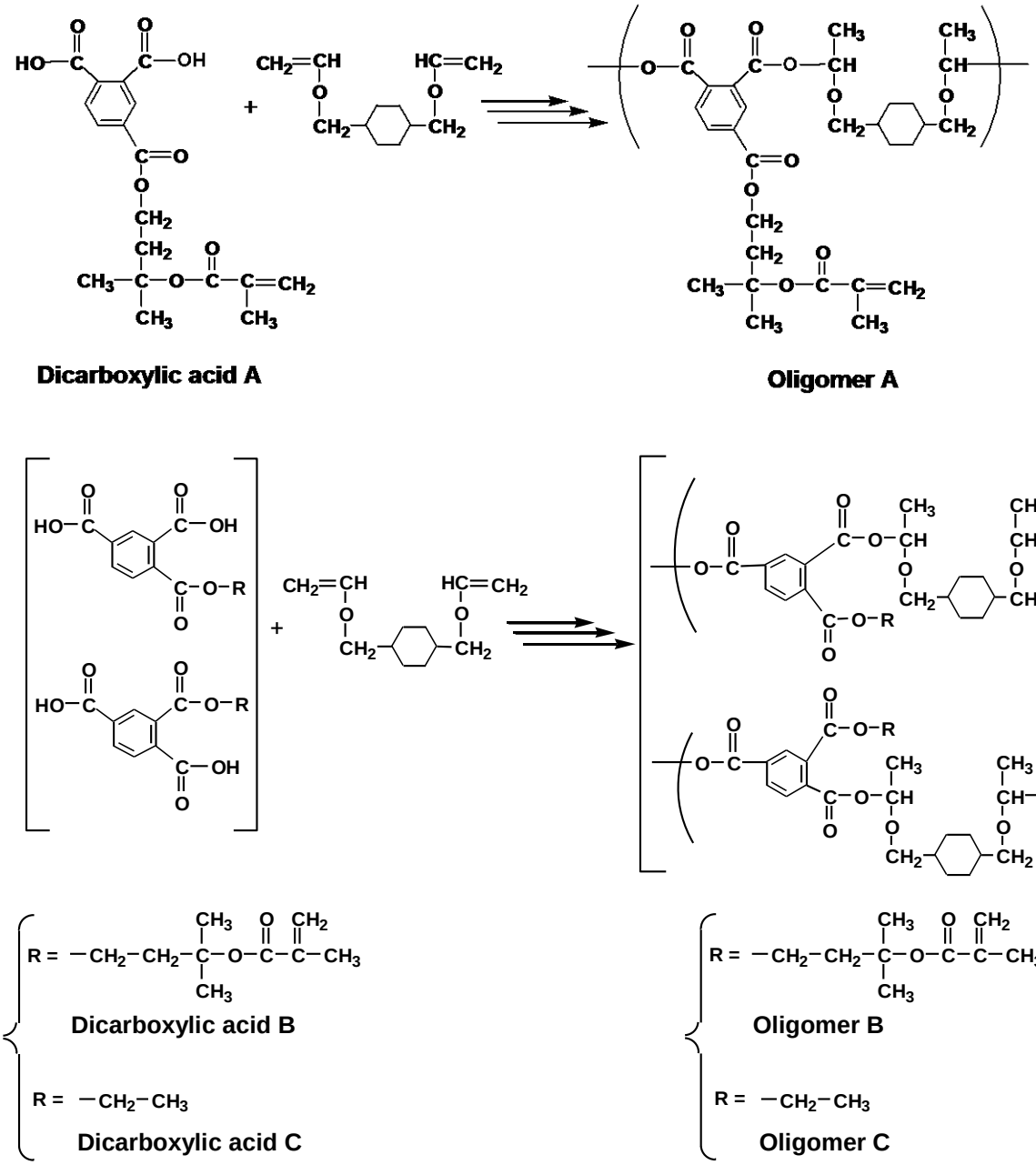

Scheme 3-4. Synthesis of oligo(hemiacetal ester)s.

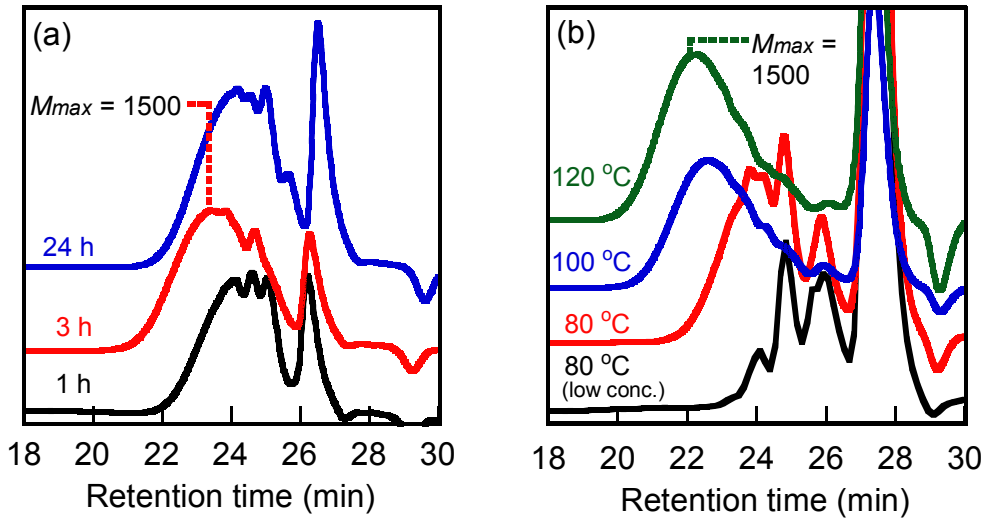

Figure 3-1. SEC profiles of oligomer C. (a) Solvent: tetrahydrofuran, temperature: room temperature. (b) Solvent: cyclohexanone, reaction time: 10 min.

equimolar amounts of dicarboxylic acids and divinyl ethers in cyclohexanone were stirred at various temperatures in the absence of an acid catalyst, the molecular weight of the oligomers formed shifted to higher molecular weight region as increasing reaction temperatures (see Figure 3-1 (b)). The effect of concentration of reaction mixture was also investigated at 80 ^{o}C. The normal concentration of reaction mixture (0.84 mmol / mL) yielded higher molecular weight oligomers than that of lower concentration of reaction mixture (0.41 mmol / mL).

Figure 3-2 shows the effect of reaction time at 100 ^{o}C (a) and 120 ^{o}C (b) on SEC profiles of oligomers. Using cyclohexanone as a solvent and heating at 100 ^{o}C for 10 min, the oligomer with M_{max} of 3,000 was obtained. Similar to the former case, the longer reaction time induced partial degradation of the oligomer formed as seen by the increase in the SEC peak attributed to low molecular weight compound (retention time: 26.2 min). In the case of reaction at 120 ^{o}C, the SEC curve shifted to higher molecular weight region as increasing reaction time until 10 min and M_{max} of 3,900 was obtained. The longer reaction time (20 min or 30 min) also induced partial degradation of the oligomer formed. Furthermore, oligomerization did not proceed successfully at lower temperatures as shown in Figure 3-1 (b). It was suggested that oligomerization conditions, i.e., solvent, temperature and reaction time, strongly affected the molecular weight of oligomers.

The polyaddition reaction was carried out at 60 ^{o}C for 10 min for oligomer A and 120 ^{o}C for 10 min for oligomer B. The reaction was monitored by ^{1}H NMR and SEC analyses. Polyaddition of dicarboxylic acid B with divinyl ether was carried out at optimized reaction conditions and oligomer B was successfully obtained. In contrast, in the case of oligomer A, the reaction was carried out under mild conditions because the oligomer formed was degraded at high reaction temperatures (above 80 ^{o}C) and the formation of acetaldehyde was confirmed by ^{1}H NMR spectrum. This difference of polyaddition behavior was caused by the difference of main-chain structures. It was confirmed that optimum reaction temperature was needed to

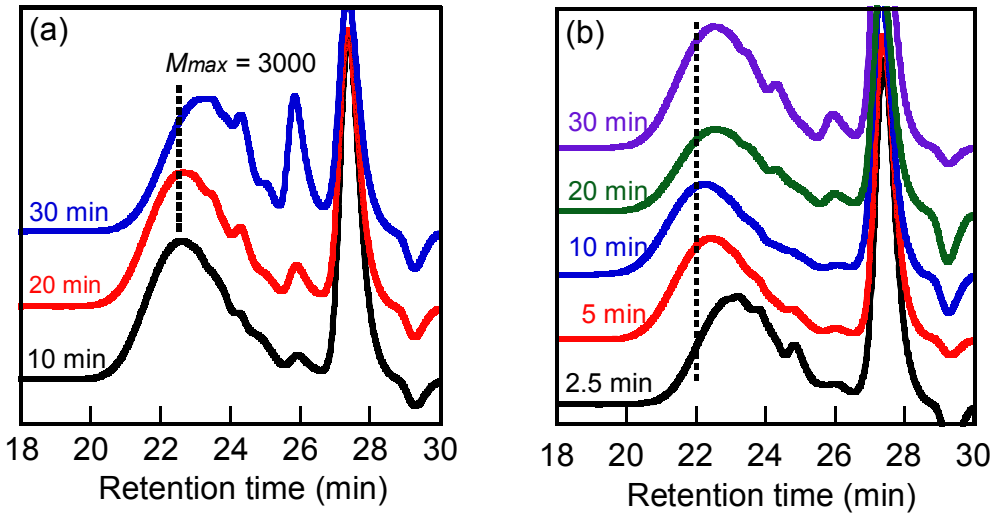

Figure 3-2. SEC profiles of oligomer C. Solvent: cyclohexanone. Reaction temperature: (a) 100 ^{o}C and (b) 120 ^{o}C.

obtain the oligomers.

Figures 3-3 (a) and (b) show the ^{1}H NMR spectra of the oligomer A and oligomer B, respectively. Only methoxycarbonyl terminal end was observed in the structure of oligomer A. On the other hand, the end groups of oligomer B were 40 % of vinyloxy groups and 60 % of methyl ester groups. The peaks attributed to the methine hydrogen of hemiacetal ester unit in the main chain (6.13 ppm) and terminal methyl ester groups (3.95 ppm) were confirmed. Figures 3-4 (a) and (b) show IR spectra of the oligomer A and oligomer B, respectively. The peaks attributed to vinyl groups of the oligomers (1637 cm^{-1}) were confirmed in both oligomers. Figure 3-5 shows SEC diagrams of the oligomers A and B and the properties of the oligomers A and B were summarized in Table 3-1. It was confirmed that oligomers A and B were monodispersed, respectively. Number average molecular weights (M_n) of the oligomers A and B were 3,200 and 3,000, respectively. The M_n values of the oligomers A and B obtained by SEC were in good agreement with the corresponding values calculated from ^{1}H NMR spectra.

The stability of the oligomers A and B that have terminal COOH group was relatively low and they were degraded at ambient temperature for several days. The degradation of COOH terminated oligomers was confirmed by SEC analysis. Thus, enhanced stabilization of oligomers was needed. Figure 3-6 shows the SEC profile changes of oligomer B on methylation of terminal carboxyl groups. The M_n values of the oligomer before methylation and after methylation were 2,400 and 3,000, respectively. This difference was due to the change of polarity of the oligomer by methylation. It was confirmed that the methylation process did not degrade the oligomer formed.

The thermal decomposition behavior of the oligomers was studied using TGA. Figure 3-7 shows the TGA profiles of the oligomers A and B. The conversion of the terminal COOH groups into methyl ester groups enhanced the thermal stability and their thermal decomposition temperature was higher than 130 ^{o}C. When the oligomers were heated under nitrogen

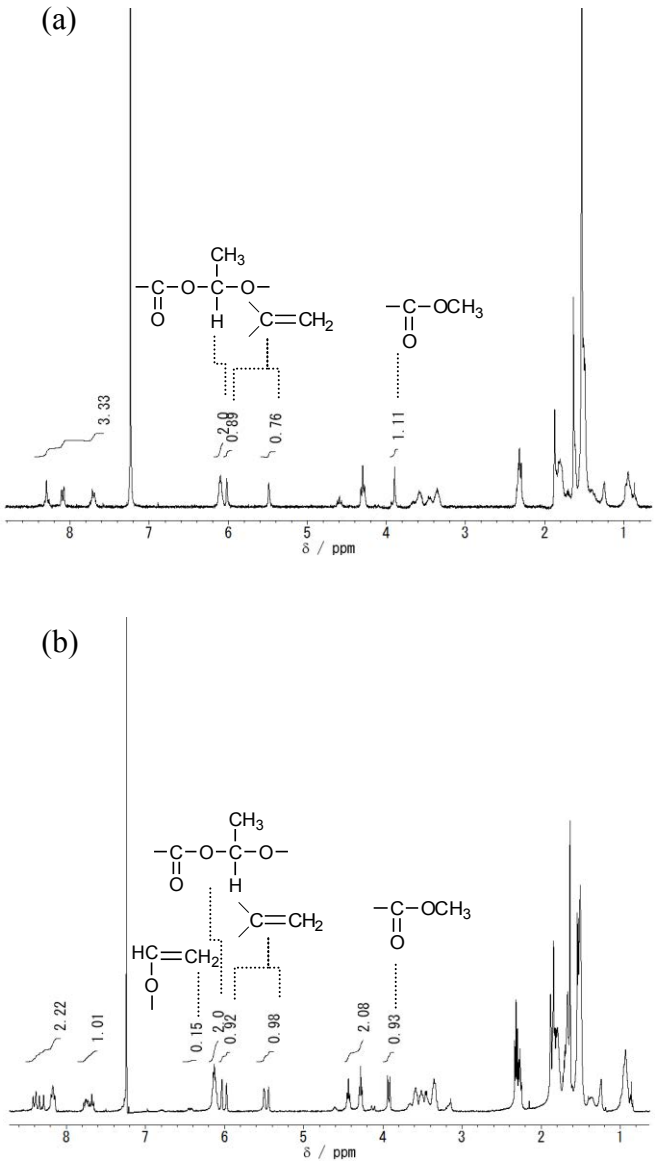

Figure 3-3. ^{1}H NMR spectra (400 MHz, $CDCl_3$) of (a) oligomer A and (b) oligomer B.

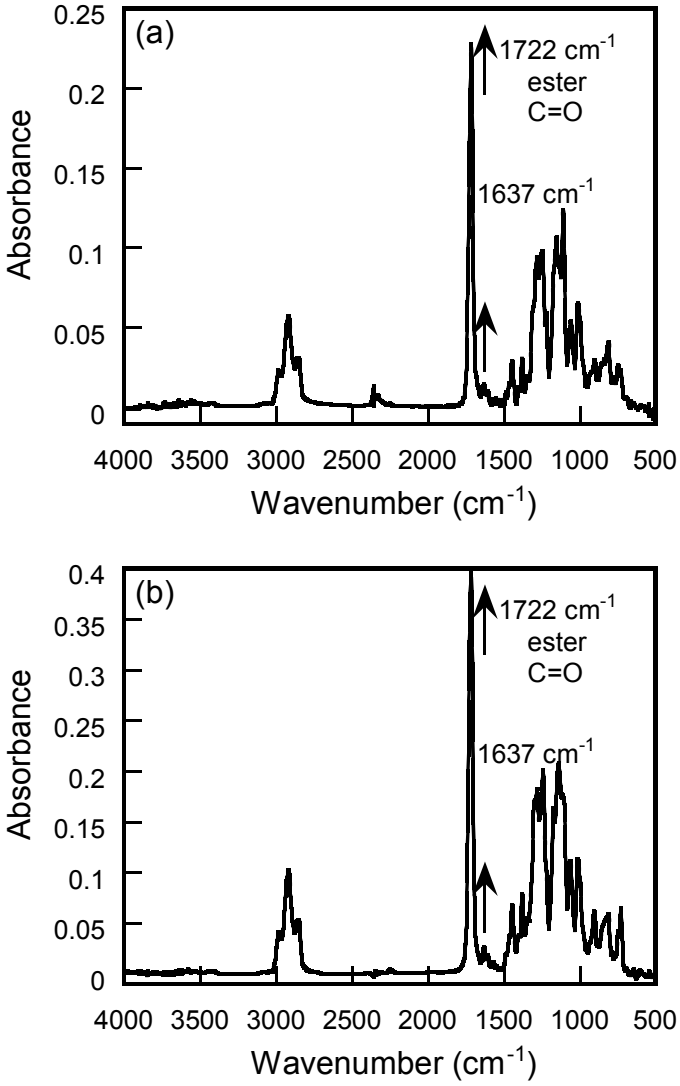

Figure 3-4. IR spectra (neat) of (a) oligomer A and (b) oligomer B.

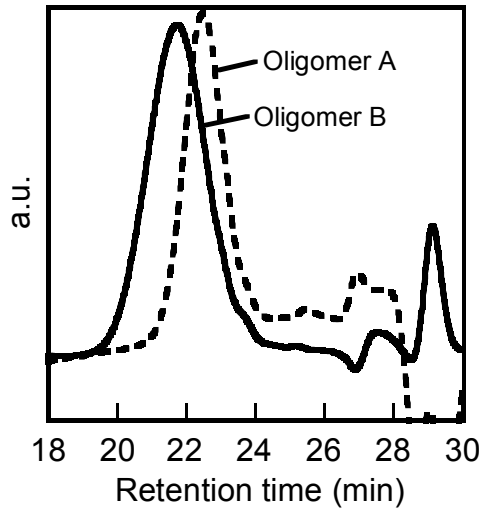

Figure 3-5. SEC profiles of the oligomer A and oligomer B.

Table 3-1. Properties of oligomers.

Oligomer	M_n [a)]	M_n [b)]	M_w/M_n [b)]	T_d (°C)[c)]
Oligomer A	3,200	2,400	1.3	138
Oligomer B	2,800	3,000	2.1	164

a) Determined by ^{1}H NMR.
b) Determined by SEC (THF, polystyrene standards).
c) Thermal decomposition temperature determined from TGA.

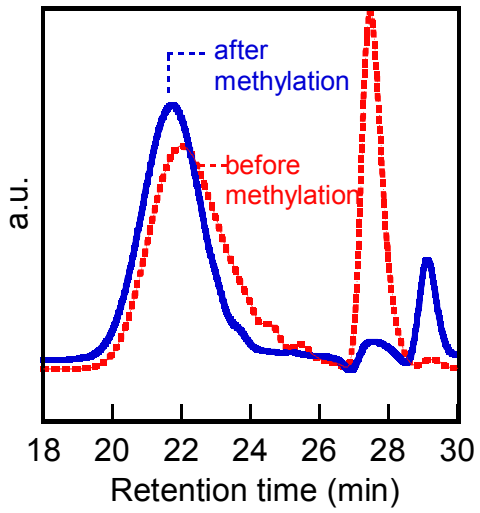

Figure 3-6. SEC profiles of oligomer B. Dotted line: before methylation. Solid line: after methylation.

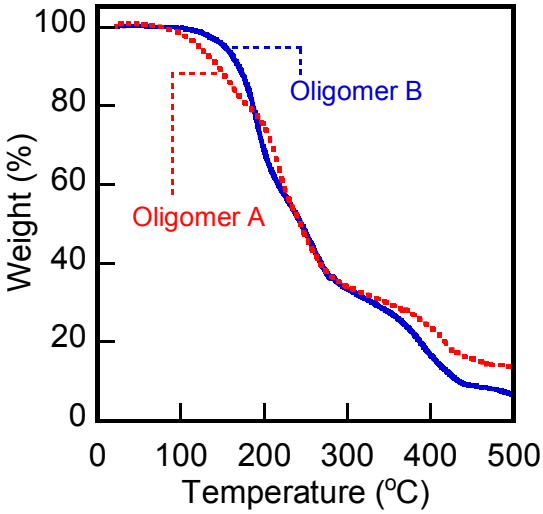

Figure 3-7. TGA profiles of oligomer A and oligomer B. Heating rate: 10 °C/min.

atmosphere at a heating rate (10 ^{o}C/min), oligomer A started to lose its weight at 138 ^{o}C and oligomer B started to lose its weight at 164 ^{o}C. Scheme 3-5 shows the thermolysis of oligomer B. Hemiacetal esters are known to decompose to corresponding vinyl ether and carboxylic acid by thermal treatment.[9-10] On the other hand, acetaldehyde, carboxylic acid, and alcohol derivatives are the products of acid-catalyzed degradation (see Scheme 3-1).[8] Tertiary esters of carboxylic acids[11-13] are known to decompose to carboxylic acid and alkene by thermal treatment. Additionally, the degradation temperature of hemiacetal esters is lower than that of tertiary esters. Since oligomers A and B are structural isomers, they should be degraded in a similar manner. However, in the early stage of thermal degradation, the degradation behavior of oligomers slightly differed from each other (see Figure 3-7). The weight loss of oligomer A at 210 ^{o}C was 36 %, which was consistent with the calculated value for the removal of divinyl ether derivatives formed by degradation of hemiacetal ester units in the oligomer A (35 %). The weight loss of the oligomer A at 280 ^{o}C (62 %) was consistent with the value calculated for the degradation of both tertiary ester and primary ester linkages (63 %). The weight loss of oligomer B at 200 ^{o}C was 35 %, which was consistent with the value calculated for the removal of corresponding divinyl ether (35 %), suggesting the complete cleavage of hemiacetal ester linkages in oligomer B. The weight losses of oligomer B at 240 ^{o}C and at 280 ^{o}C were 49 % and 63 %, respectively. The values were consistent with the calculated values for degradation of tertiary ester linkages (50 %) and primary ester linkages (63 %).

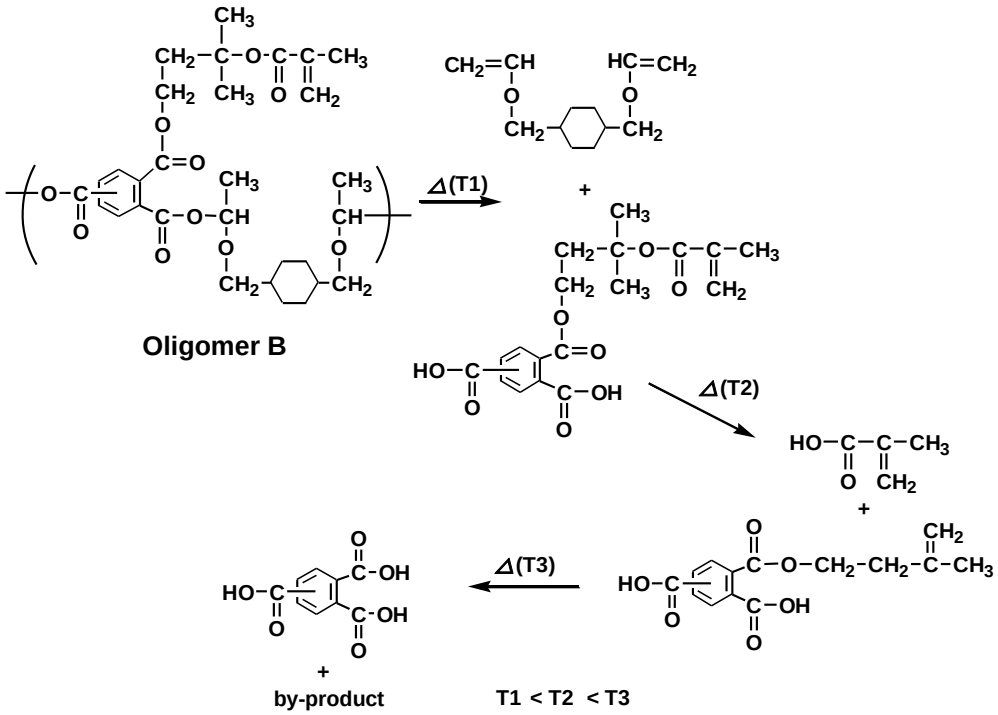

Scheme 3-5. Thermolysis of oligomer B.

3-3-2. Photo-induced insolubilization of oligo(hemiacetal ester)s

The oligomer B film was applied to UV curing system. Figure 3-8 shows the UV curing behaviors of oligomer B on irradiation. The oligomer B film containing 2 wt% of DMPA did not become insoluble in acetone on irradiation at 365 nm under nitrogen atmosphere. Changes of C=C double bonds (1636 cm^{-1}) were monitored by IR spectroscopy and it was ascertained that the methacrylate groups in the side chains did not radically polymerize on irradiation. This may be due to the restrictive mobility of the methacrylate units in the side chain.

When mono-functional methacrylate monomer MADMA was blended with oligomer B, photo-induced insolubilization occurred. MADMA was chosen as a comonomer because MADMA had high boiling point (301 ^{o}C) and tertiary ester groups in the chemical structure. Figure 3-9 shows the insolubilization profiles of oligomer B / MADMA blended films containing 2 wt% of DMPA and 1 wt% of TPST on irradiation at 365 nm under nitrogen atmosphere. If the irradiation was carried out in air, no insolubilization was observed. DMPA was used as photoradical initiator which can generate radical species on irradiation at 365 nm. TPST was unreactive to 365 nm irradiation because TPST has no absorption peak at 365 nm. Effective photo-induced polymerization occurred. The insoluble fraction increased as increasing irradiation dose and MADMA contents. The insoluble fractions for the oligomer B / MADMA ratios at 1 / 1, 1 / 10, and 1 / 20 (mole / mole) were 8, 62, and 62 %, respectively at the irradiation dose of 200 mJ/cm^2. Scheme 3-6 shows the photo-induced curing of oligomer B / MADMA blended system. The radical species generated from DMPA induced crosslinking reaction of oligomer B / MADMA via free-radical polymerization. Figure 3-10 shows the IR spectral changes of oligomer B / MADMA = 1 / 10 (molar ratio) containing 1 wt% DMPA and 1 wt% TPST on irradiation. The peak at 1636 cm^{-1} due to C=C stretching in IR spectra decreased on irradiation at 365-nm light. Figure 3-11 shows the conversion of methacrylate units of oligomer B / MADMA blended film on irradiation. The effective

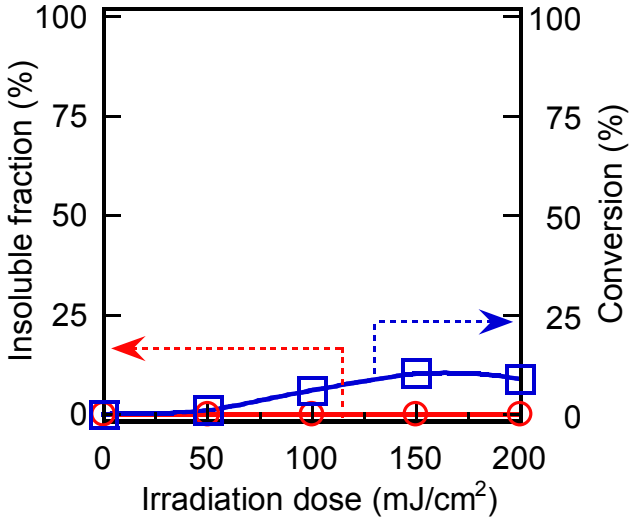

Figure 3-8. Effect of irradiation dose at 365 nm on insolubilization (○) and conversion of methacrylate unit (□) of oligomer B containing 2 wt % DMPA. Dissolution: in acetone for 10 min. Irradiation condition: at room temperature under nitrogen. Film thickness: 1.0 μm.

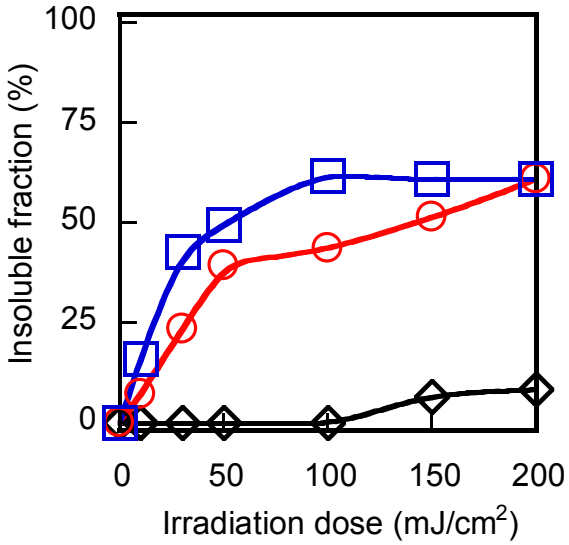

Figure 3-9. Effect of irradiation dose at 365 nm on insolubilization of oligomer B / MADMA blended film containing 2 wt % DMPA and 1 wt% TPST. Oligomer B / MADMA (molar ratio): (◇) 1 / 1, (○) 1 / 10, and (□) 1 / 20. Irradiation condition: at room temperature under nitrogen. Dissolution: in acetone for 10 min. Film thickness: 1.0 μm.

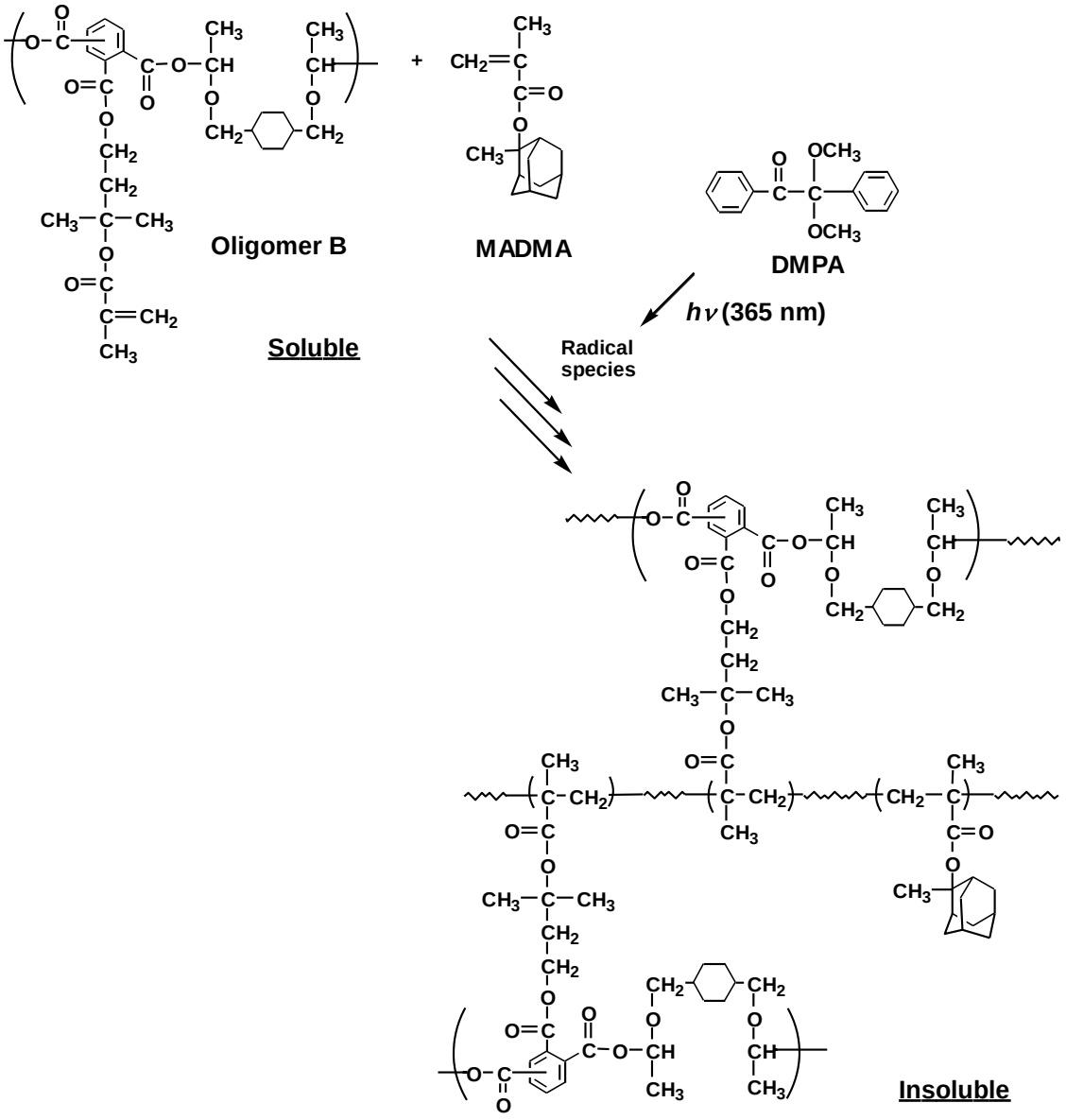

Scheme 3-6. Proposed mechanism for crosslinking of oligomer B / MADMA.

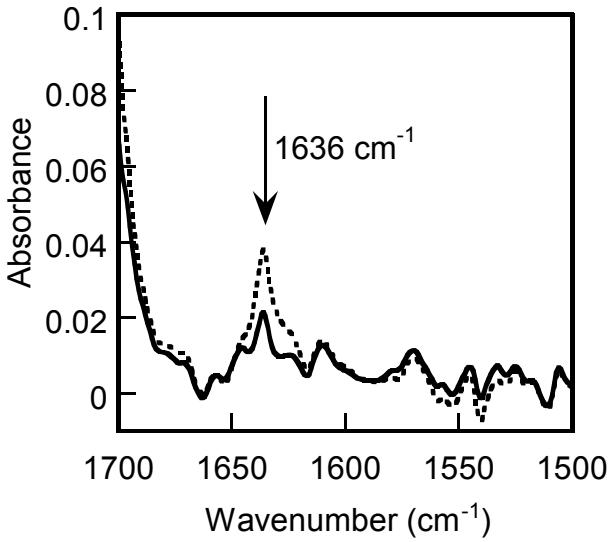

Figure 3-10. IR spectral changes of oligomer B / MADMA blended (1 / 10, molar ratio) film containing 2 wt % DMPA and 1 wt% TPST on irradiation. Dotted line: before irradiation. Solid line: after irradiation at 365 nm with 200 mJ/cm^2. Irradiation condition: at room temperature under nitrogen. Film thickness: 1.0 μm.

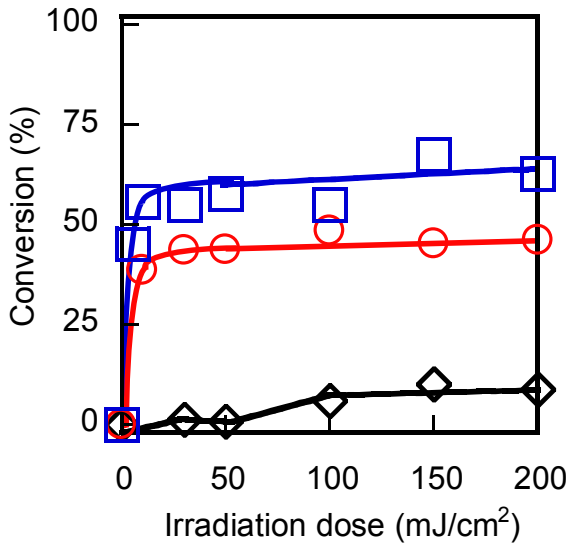

Figure 3-11. Effect of irradiation dose at 365 nm on conversion of oligomer B / MADMA blended film containing 2 wt % DMPA and 1 wt% TPST. Oligomer B / MADMA (molar ratio): (◇) 1 / 1, (○) 1 / 10, and (□) 1 / 20. Irradiation condition: at room temperature under nitrogen. Film thickness: 1.0 μm.

polymerization was confirmed and the conversions of the oligomer B / MADMA ratios at 1 / 1, 1 / 10, and 1 / 20 (mole / mole) were 9, 46, and 63 %, respectively at the exposure dose of 200 mJ/cm^2. The conversion of the methacrylate groups increased with increasing irradiation dose and MADMA content. Photo-induced insolubilization behavior of oligomer B was improved by adding MADMA as comonomer due to the high reactivity and high mobility of MADMA.

The UV curing behavior of oligomer A / MADMA and oligomer B / MADMA was investigated. Figure 3-12 (a) shows the photo-induced insolubilization behavior of oligomer / MADMA (1 / 20, molar ratio). Photo-induced insolubilization occurred with increasing irradiation dose and reached a constant value. The insoluble fractions of the oligomer A / MADMA blended film reached 62 % and the oligomer B / MADMA film reached 62 %, respectively. The insolubilization behavior of oligomer A was similar to that of oligomer B. Figure 3-12 (b) shows the conversion of methacrylate units of oligomer / MADMA (1 / 20, molar ratio) on irradiation at 365 nm. When the oligomers were exposed at 365 nm with 200 mJ/cm^2, the conversion of oligomers was observed to be about 60 %. If the oligomer / MADMA blended film irradiated at 365 nm was immersed into cyclohexanone instead of acetone, the insoluble fractions were 45 % for cyclohexanone and 61 % for acetone, respectively. Thus, there might be a small amount of MADMA homopolymer in the system, but most of insoluble fractions were crosslinked oligomer / MADMA networks. The difference of main-chain structures of the oligomers A and B did not affect the photo-curing behavior.

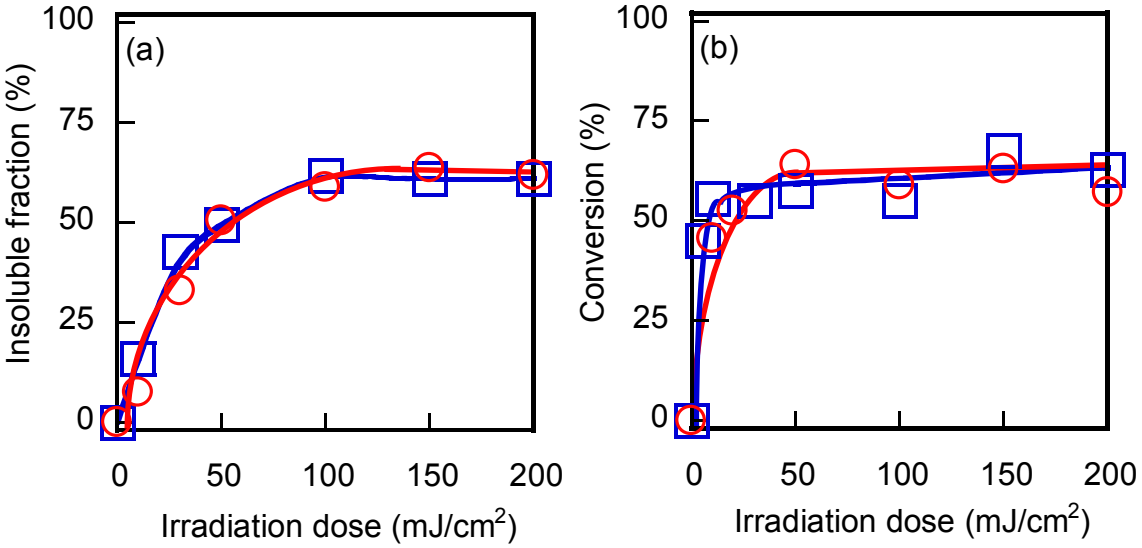

Figure 3-12. Effect of irradiation dose at 365 nm on insolubilization (a) and conversion of methacrylate unit (b) of oligomer / MADMA blended (1 / 20, molar ratio) film containing 2 wt% DMPA and 1 wt% TPST. Oligomer: (○) oligomer A and (□) oligomer B. Irradiation condition: at room temperature under nitrogen. Dissolution: in acetone for 10 min. Film thickness: 1.0 μm.

3-3-3. Photo and thermal degradation of UV crosslinked resins

Figure 3-13 shows the dissolution of the cured films containing 1 wt% of TPST when baked at given temperatures after irradiation at 254 nm. In this experiment, the film thickness of cured resins was kept at 0.5 μm to keep the transparency at 254-nm light. On irradiation at 254 nm, complete dissolution of oligomer A / MADMA blended film was observed. The hemiacetal ester linkages of the network were decomposed by acid-catalyzed hydrolysis on irradiation at 254 nm. The tertiary ester units of the resins were decomposed after baking above 120 ^{o}C. Without 254 nm irradiation, oligomer A / MADMA blended film became soluble in acetone after baked at 40 − 100 ^{o}C. On irradiation at 254 nm and followed by baking at 120 − 160 ^{o}C, complete dissolution of oligomer B / MADMA blended film was observed. Because the degradation products of oligomer B / MADMA blended films were meta or para linked carboxylic acid derivatives, they might be insoluble in acetone. So, complete dissolution of the films indicated the degradation of both hemiacetal ester and tertiary ester linkages. Without 254-nm light irradiation, the remaining film thickness of oligomer B / MADMA blended film was about 10 % after baked at 140 - 200 ^{o}C. This was due to the thermal dissociation of hemiacetal ester units, which induced the degradation of tertiary ester linkages. From the view point of solubility, oligomer A was more degradable than oligomer B. Figure 3-14 shows the IR spectral changes of UV cured oligomer B / MADMA on irradiation at 254 nm and followed by baking at 120 ^{o}C for 10 min. The peaks due to ester C-O groups and acetal O-C-O groups (1178 cm^{-1}) disappeared. On the other hand, the peak due to ester carbonyl (1723 cm^{-1}) showed slight shift to 1698 cm^{-1} and the peak due to hydroxyl groups (2800 - 3600 cm^{-1}) appeared, which may be due to the formation of carboxylic acid groups. When the UV cured films containing TPST were exposed to 254-nm light, triflic acid was generated and the acid-catalyzed cleavage of the hemiacetal ester units and tertiary ester units occurred.

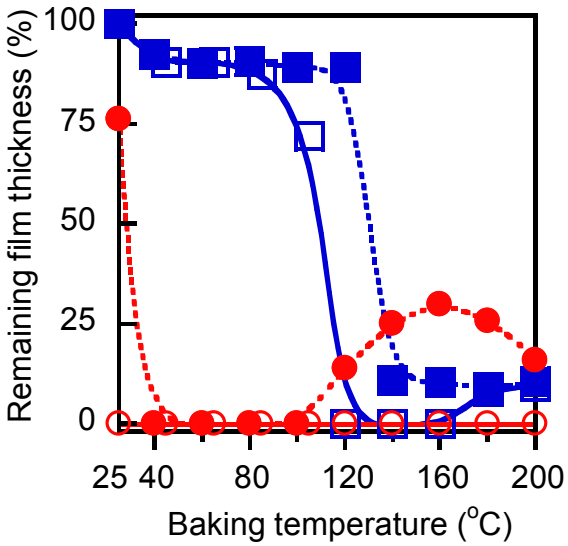

Figure 3-13. Effect of baking temperature on dissolution of photo-cured oligomer / MADMA blend (1 / 20, molar ratio) film containing 2 wt% DMPA and 1 wt% TPST. Oligomer: (○, ●) oligomer A and (□, ■) oligomer B. Open symbol: exposed at 254 nm with 200 mJ/cm^2. Solid symbol: unexposed at 254 nm. Curing condition: irradiated at 365 nm with 200 mJ/cm^2 under nitrogen. Dissolution: in acetone for 10 min. Film thickness: 0.5 μm.

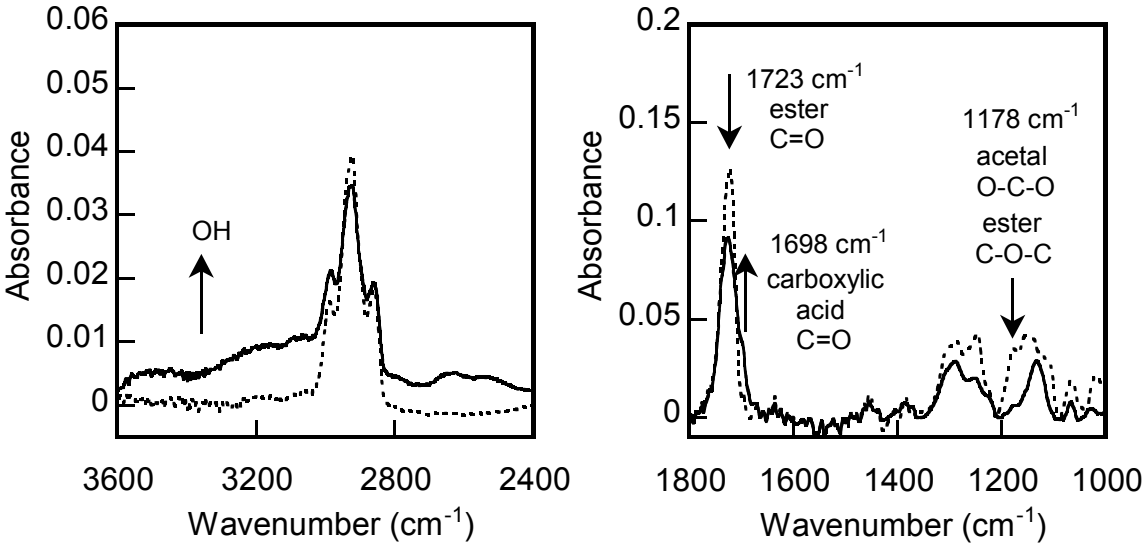

Figure 3-14. IR spectral changes of UV cured oligomer B / MADMA = 1 / 20 (molar ratio) containing 2 wt% DMPA and 1 wt% TPST on irradiation. Curing condition: irradiated at 365 nm with 200 mJ/cm^2 at room temperature under nitrogen. Dotted line: before irradiation at 254 nm. Solid line: after irradiation at 254 nm with 200 mJ/cm^2 in air and followed by baking at 120 °C for 10 min. Film thickness: 0.5 μm.

After decomposition of UV cured oligomer B / MADMA by irradiation at 254 nm and followed by baking at 120 ^{o}C for 10 min, the film was dissolved in $CHCl_3$. Soluble and insoluble fractions were recovered as 63 % and 33 % yields, respectively. Additionally, the fraction insoluble in $CHCl_3$ completely dissolved in acetone. Thus, the decomposition reaction proceeded almost quantitatively. The expected weight loss (6 %) was nearly identical to the observed value (4 %). Figure 3-15 shows the ^{1}H NMR spectrum of soluble fraction in $CDCl_3$. It revealed that aromatic peaks, olefinic peaks, and aliphatic peaks due to adamantyl unit supported the generation of the products shown in Scheme 3-7. The fraction insoluble in $CHCl_3$ was suggested to be poly(methacrylic acid) by IR spectrum (Figure 3-16). Furthermore, ^{1}H NMR measurement using deuterated acetone also suggested that the molecular weight of poly(methacrylic acid) may exceed 5,000 as judged by the broadness and lack of the terminal ends in the spectrum. Acetaldehyde might be vaporized during the decomposition reaction.

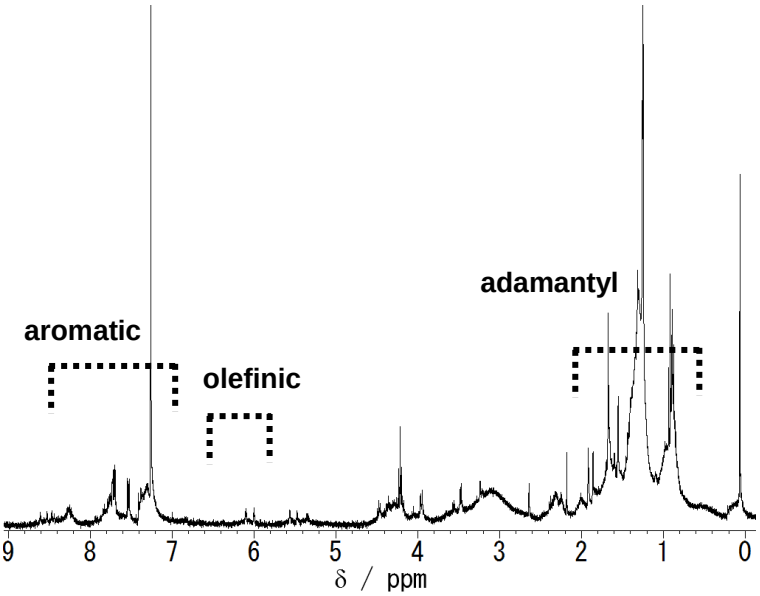

Figure 3-15. ^{1}H NMR spectrum (400 MHz, $CDCl_3$) of soluble fraction in $CHCl_3$ obtained from degradation of UV cured oligomer B / MADMA = 1 / 20 (molar ratio) containing 2 wt% DMPA and 1 wt% TPST on irradiation. Curing condition: irradiated at 365 nm with 200 mJ/cm^2 at room temperature under nitrogen. Degradation condition: irradiated at 254 nm with 200 mJ/cm^2 in air and followed by baking at 120 ^{o}C for 10 min. Film thickness: 0.5 μm.

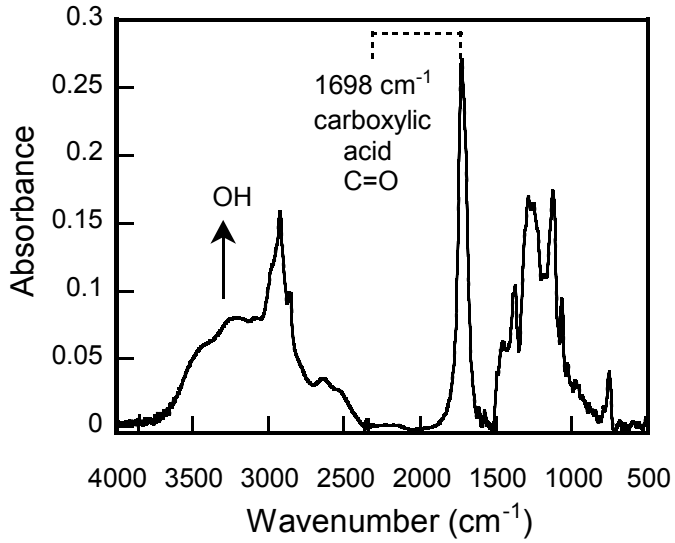

Figure 3-16. IR spectrum (KBr) of insoluble fraction in $CHCl_3$ obtained from degradation of UV cured oligomer B / MADMA = 1 / 20 (molar ratio) containing 2 wt% DMPA and 1 wt% TPST on irradiation. Curing condition: irradiated at 365 nm with 200 mJ/cm^2 at room temperature under nitrogen. Degradation condition: irradiated at 254 nm with 200 mJ/cm^2 in air and followed by baking at 120 ^{o}C for 10 min. Film thickness: 0.5 μm.

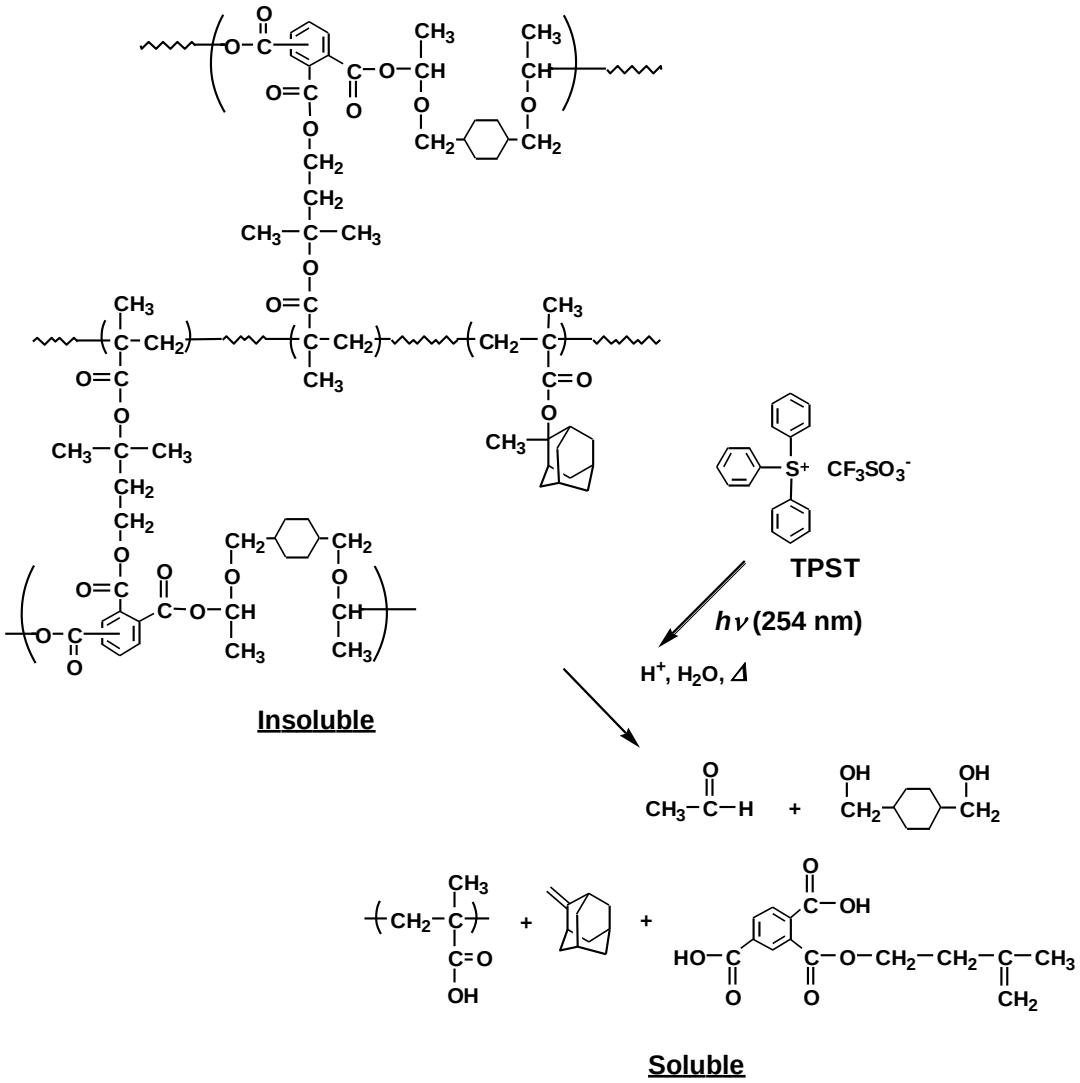

Scheme 3-7. Proposed mechanism for decrosslinking of cured oligomer B / MADMA.

A reaction mechanism of oligomer B / MADMA blended system is shown in Scheme 3-8. On irradiation at 365 nm, DMPA was photolyzed to generate radical species which initiate the polymerization of methacrylate units. On irradiation at 254 nm, TPST generated trifluoromethanesulfonic acid which induced the acid-catalyzed cleavage of hemiacetal ester linkages and tertiary ester linkages. The decomposition of resins gave poly(methacrylic acid) together with acetaldehyde and alcohol derivatives.

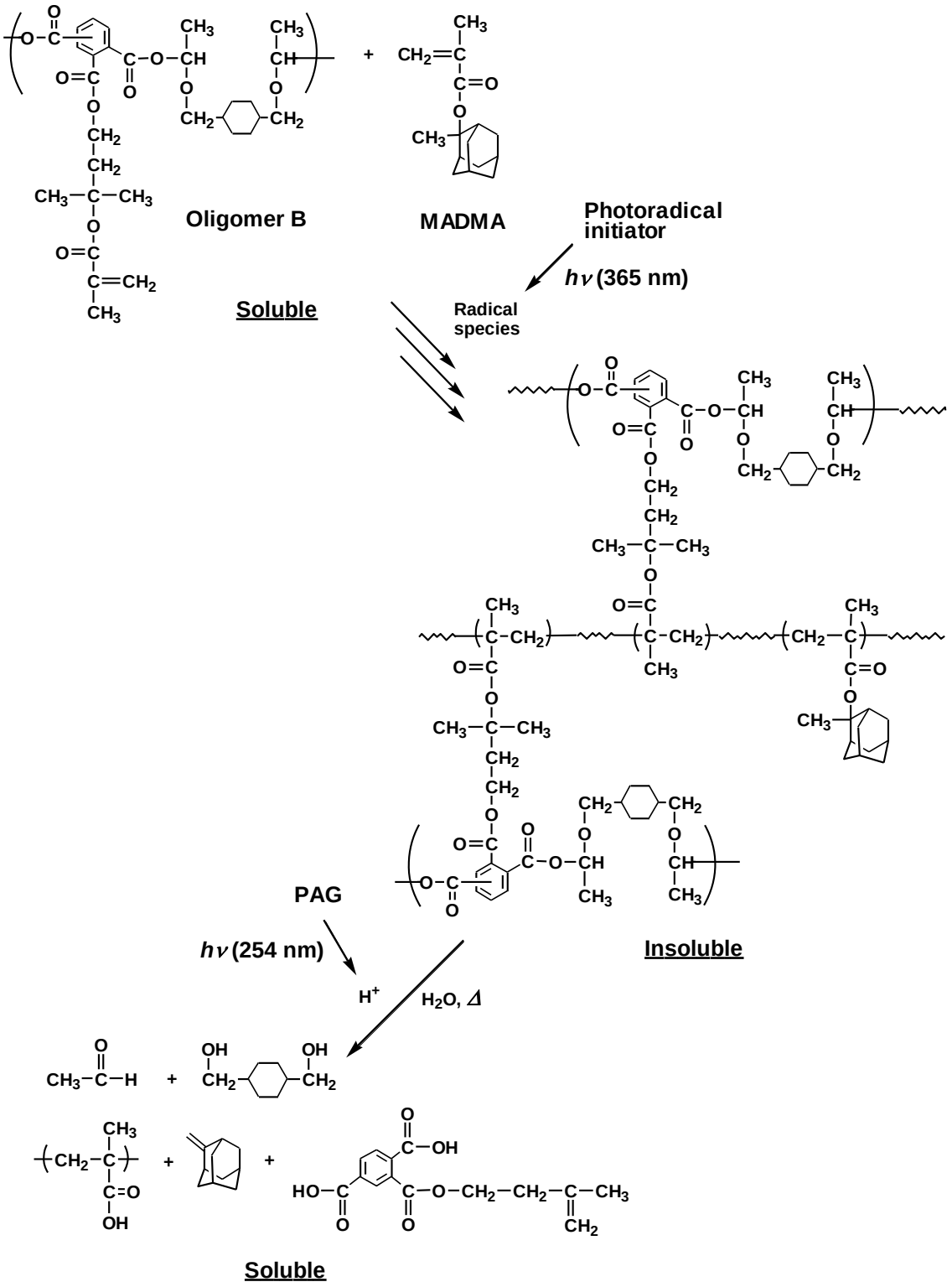

Scheme 3-8. A reaction mechanism of oligomer B / MADMA blended system.

3-4. Conclusion

Two oligo(hemiacetal ester)s which have methacrylate units and tertiary ester linkages in the side chains were synthesized by polyaddition of corresponding dicarboxylic acids with a divinyl ether. Terminal carboxyl groups of oligomers were methylated by diazomethane, which enhanced the thermal stability of the oligomers. UV curing of oligomer or oligomer / MADMA blended system was investigated. Oligomer / MADMA films containing a photoradical initiator DMPA and a photoacid generator TPST were cured on irradiation at 365 nm under nitrogen. Photo-induced insolubilization behavior was not influenced by the difference of main-chain structure of oligomers. The UV cured oligomer A / MADMA blended film became soluble in acetone after irradiation at 254 nm. The oligomer B / MADMA blended film became soluble in acetone after irradiation at 254 nm and followed by baking at 120 - 160 ^{o}C for 10 min. The solubilization of the degraded film may be affected by the main-chain structure of oligomers and degradation products. It was confirmed that de-crosslinking occurred by the cleavage of hemiacetal ester linkages and tertiary ester linkages. The oligomers can be applied to photocrosslinkable materials with degradable property.

References

1. H. Zhang, E. Ruckenstein, *Macromolecules*, 31, 7575 (1998).
2. E. Ruckenstein, H. Zhang, *Macromolecules*, 31, 9127 (1998).
3. H. Otsuka, T. Endo, *Macromolecules*, 32, 9059 (1999).
4. T. Hashimoto, K. Ishizuka, A. Umehara, T. Kodaira, *J. Polym. Sci., Part A, Polym. Chem.*, 40, 4053 (2002).
5. N. Felix, C. K. Ober, *Chem. Mater.*, 20, 2932 (2008).
6. S. K. Chaudhary, O. Hernandez, *Tetrahedron Lett.*, 20, 99 (1979).
7. E. J. Corey, A. Venkateswarlu, *J. Am. Chem. Soc.*, 94, 6190 (1972).
8. M. Shirai, K. Mitsukura, H. Okamura, *Chem. Mater.*, 20, 1971 (2008).
9. Y. Nakane, M. Ishidoya, T. Endo, *J. Polym. Sci., Part A, Polym. Chem.*, 37, 609 (1999).
10. H. Otsuka, H. Fujiwara, T. Endo, *J. Polym. Sci., Part A, Polym. Chem.*, 37, 4478 (1999).
11. K. Ogino, J. -S. Chen, C. K. Ober, *Chem. Mater.*, 10, 3833 (1998).
12. D. Matsukawa, H. Okamura, M. Shirai, *Chem. Lett.*, 36, 1290 (2007).
13. M. F. Montague, C. J. Hawker, *Chem. Mater.*, 19, 526 (2007).

Chapter 4

Reworkable system based on dimethacrylates with low shrinkage and their application to UV nanoimprint lithography

4-1. Introduction

Since imprint lithography is a cost-effective high-resolution patterning technology that does not require expensive optical elements, imprint lithography has emerged as a promising technology for device manufacturing.[1-5] Scheme 4-1 shows the schematic diagram of UV nanoimprint lithography (UV-NIL). Especially, UV-NIL does not involve heating and cooling steps and is generally operated at lower pressures. Therefore, the process has faster cycle times and can select a lot of UV curable monomers having different functional groups.[6] Acrylates and methacrylates are widely used for UV-NIL because of their commercial availability, low viscosity, and rapid photopolymerization via radical propagation.[6]

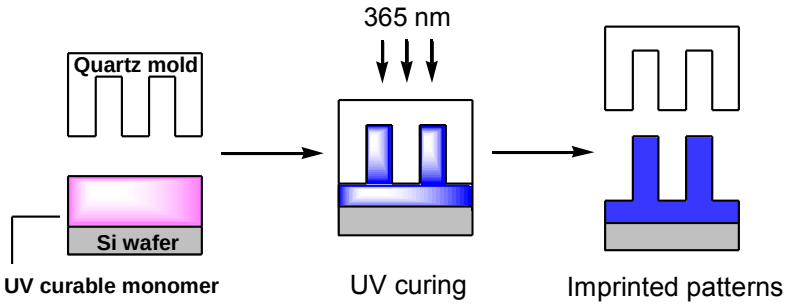

Scheme 4-1. Schematic diagram of UV imprinting.

However, the volume shrinkage in the UV imprinting process is a serious problem for micrometer- and nanometer-sized patterning of original features. Generally, acrylates and methacrylates are known to shrink 3~16 % in volume during UV curing and the shrinking

property of UV cured materials is strongly dependent on the curing conditions.[6,7] The shrinkage may cause product failures such as mismatch of the original mold. In general, the shrinking behavior depends on not only monomer structures but also UV curing conditions. Thus, it is important to elucidate the relationship between the UV curing conditions and the chemical structure of the UV cured resins. The photo-polymerization process has been extensively studied by many workers. The influence of polymerization conditions such as temperature, light intensity, concentration of initiator, and oxygen inhibition on UV curing has been investigated using various techniques such as real time infrared spectroscopy, photo-DSC, and solid-state NMR spectroscopy.[8-11] However, it is not easy to investigate the chemical structure of the cured resins because the cured materials have a network structure and they are insoluble in solvents and infusible. We have reported the synthesis of several types of reworkable resins and applied them to analyze the chemical structure of cured resins, i. e., the kinetic chain length of cured resins.[12] It was confirmed that the UV cured reworkable resin was very attractive for analyzing the chemical structure of UV cured materials because the kinetic chain length of cured resin was successfully obtained and this method gave a real kinetic chain length compared to other methods.

Another problem in UV-NIL is a fouling of master mold. Because UV-NIL uses UV curable resins, it is difficult or impossible to remove the cured resins adhered to the surface of the master mold. Therefore, development of UV curing resins for UV-NIL with reworkable property and low shrinkage is desired.

In this chapter, difunctional reworkable methacrylates with low shrinkage were designed and synthesized and applied to UV-NIL. Effects of light intensities, initiator concentration, monomer structure, and chain transfer reagent on shrinkage of UV imprinted patterns were studied. Furthermore, the effect of the kinetic chain length of the cured resin on the shrinkage was studied. The cured resin was degraded to yield a linear polymer whose molecular weight

was measured by size exclusion chromatography (SEC). The concept of the present system is shown in Scheme 4-2.

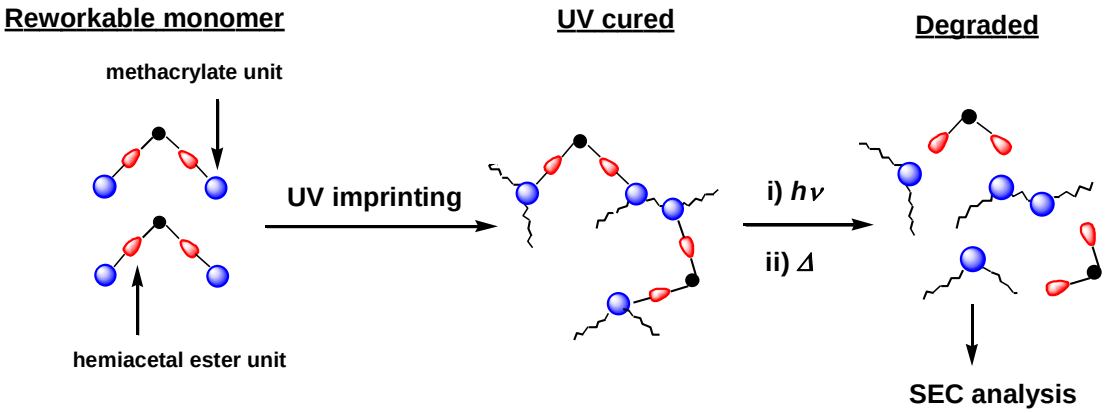

Scheme 4-2. Analysis of polymer chain length of cured resin.

4-2. Experimental

4-2-1. Measurements

UV imprinting was performed using a Maruni MNI-1000HC. The depth of line patterns of quartz mold and the height of UV imprinted patterns were measured using a Kosaka surfcorder ET 3000i. Irradiation was performed at 254 nm and 365 nm using a low pressure Hg lamp (Ushio ULO-6DQ, 6W) and a Xe lamp (ASAHI SPECTRA MAX-302, 300W) equipped with a filter, respectively. The wavelength of the transmitted light from Xe lamp was in the range of 350 - 380 nm with λ_{max} at 367 nm. Photo-DSC was performed using Shimadzu DSC 60 equipped with HAMAMATSU LC8. A Hg-Xe lamp equipped with a filter was used for irradiation. The transmitted light was in the range of 330 - 370 nm with λ_{max} at 347 nm. The incident light intensity at the sample pan position was measured to be 2.0 mW/cm^2. Scanning electron microscopy (SEM) images were taken using a HITACHI S-4300.

4-2-2. Materials

A photoacid generator di(4-*t*-butylphenyl)iodonium triflate (DITF) was of reagent grade and used without further purification. A release agent OPTOOL DSX (Daikin Industry) for UV-NIL was used as received. Other solvents and reagents were purchased and used as received. Reworkable monomer BPDMA was prepared as described previously.[12] 2-Vinyloxyethyl methacrylate was prepared as described previously.[13]

The chemical structures of reworkable monomers are shown in Scheme 4-3.

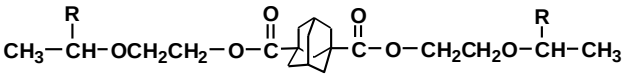

ADMA

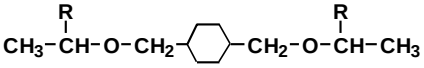

CDMA

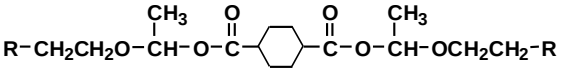

CDCMA

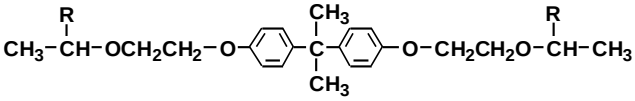

BPDMA

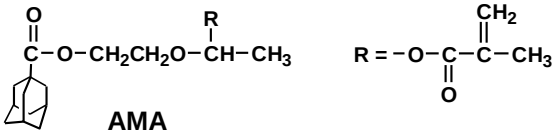

AMA

Scheme 4-3. Structures of reworkable monomers used.

4-2-3. Synthesis of reworkable monomers having hemiacetal ester groups

*2-Methyl-2-propenoic acid, tricyclo[3.3.1.1(3,7)]decane-1,3- dicarboxylic acid bis(oxy-2,1-ethanediyloxyethylidene) ester (**ADMA**)*

Difunctional methacrylate monomer (ADMA) was prepared as follows. 1,3-Adamantanedicarboxylic acid (1.9 g, 8.5 mmol) was mixed with 25 mL of $SOCl_2$ and the mixture was refluxed for 3 h. Excessive $SOCl_2$ was evaporated and 1,3-adamantanedicarbonyl dichloride was obtained as white solid in a yield of 2.1 g (95 %). mp: 74 - 75 ^oC.

Chloroform (10 mL), triethylamine (4.0 mL), and 2-vinyloxyethanol (2.0 g, 22.7 mmol) were placed in a three-necked round-bottom flask fitted with an efficient magnetic stirrer and a thermometer. 1,3-Adamantanedicarbonyl dichloride (2.1 g, 8.1 mmol) in 15 mL of chloroform was added dropwise at 5 ^oC under nitrogen atmosphere and reacted for 18 h at room temperature. The chloroform solution was washed with 1N-HCl, water, saturated $NaHCO_3$, and water and the chloroform layer was dried over anhydrous $MgSO_4$. 1,3-Adamantanedicarboxylic acid bis(2-vinyloxyethyl) ester was purified by column chromatography (silica gel, eluent: chloroform), giving a colorless viscous liquid in a yield of 1.5 g (56 %). ^1H NMR (300 MHz, $CDCl_3$; δ, ppm): 6.45 (2H, q, O-C*H*=CH_2), 4.27 (4H, t, -C(=O)-CH_2-), 4.17, 4.02 (4H, dd, -OCH=CH_2), 3.86 (4H, t, -CH_2-O-), 2.13 - 1.66 (14H, m, adamantane).

Into a three-necked round-bottom flask were placed *p*-toluenesulfonic acid (0.036 g, 0.21 mmol), tetrahydrofuran (THF) (6 mL), and methacrylic acid (1.08 g, 12.6 mmol) under nitrogen atmosphere. 1,3-Adamantanedicarboxylic acid bis(2-vinyloxyethyl) ester (1.53 g, 4.2 mmol) in 10 mL of THF was added dropwise at 5 ^oC and the reaction was continued for 6 h at 10 ^oC. After removal of THF, excessive diethyl ether was added and the ether solution was washed with saturated $NaHCO_3$ aqueous solution three times and dried over anhydrous $MgSO_4$. After removal of diethyl ether, the monomer ADMA was purified by column chromatography (silica

gel, eluent: chloroform), giving a colorless viscous liquid in a yield of 1.2 g (53 %). ^{1}H NMR (300 MHz, $CDCl_3$; δ, ppm): 6.13, 5.58 (4H, s, C*H*$_2$=C), 6.02 - 5.91 (2H, m, O-C*H*(CH_3)-O), 4.18 (4H, t, -C(=O)-C*H*$_2$), 3.88 - 3.66 (4H, m, -C*H*$_2$-O), 2.18 - 1.62 (14H, m, adamantane), 1.92 (6H, s, methacrylic C*H*$_3$), 1.42 (6H, m, -C*H*$_3$).

*2-Methyl-2-propenoic acid, 1,4-cyclohexyl-bis(methanediyloxyethylidene) ester (**CDMA**)*

The monomer CDMA was prepared by a similar method to the preparation of ADMA. Into a three-necked round-bottom flask were placed *p*-toluenesulfonic acid (0.026 g, 0.15 mmol), THF (18 mL), and methacrylic acid (3.9 g, 15 mmol) under nitrogen atmosphere. 1,4-Bis[vinyloxy(methyl)]cyclohexane (3.0 g, 15 mmol) in 18 mL of THF was added dropwise below 2 ^{o}C and the reaction was continued for 5 h at 5 ^{o}C. After removal of THF, excessive diethyl ether was added and the ether solution was washed with saturated $NaHCO_3$ aqueous solution five times and then saturated NaCl solution and dried over anhydrous Na_2SO_4. After removal of diethyl ether, the monomer CDMA was purified by column chromatography (silica gel, eluent: ethyl acetate/hexane=1:9, v/v), giving a colorless viscous liquid in a yield of 1.7 g (30 %). ^{1}H NMR (300 MHz, $CDCl_3$; δ, ppm): 6.12, 5.56 (4H, s, C*H*$_2$=C), 5.92 (2H, m, O-C*H*(CH_3)-O), 3.57 - 3.21 (4H, m, -C*H*$_2$-), 1.92 (6H, s, methacrylic C*H*$_3$), 1.87 - 1.29, 1.01 - 0.79 (10H, m, cyclohexyl), 1.40 (6H, m, -C*H*$_3$). Anal. Calcd for $C_{20}H_{32}O_6$: C 65.19, H 8.75. Found: C 65.03, H 8.55. MS (EI): *m/z* 368 (M^+, 0.84), 109 (M^+-259, 100).

*1,4-Bis-(1-[2-methacryloxyethyleneoxy]ethyl)1,4-cyclohexanedicarboxylate (**CDCMA**)*

Into a three-necked round-bottom flask was placed 1,4-cyclohexanedicarboxylic acid (0.602 g, 3.49 mmol) under nitrogen atmosphere. 2-Vinyloxyethyl methacrylate (1.36 g, 8.73 mmol) and radical inhibitor OH-TEMPO (0.068 g) in 9 mL of cyclohexanone was added dropwise and the reaction was continued for 3 h at 155 ^{o}C. After the reaction mixture was

cooled to room temperature, 200 mL of diethyl ether was added and the ether solution was washed with saturated $NaHCO_3$ aqueous solution twice and then dried over anhydrous Na_2SO_4. After removal of diethyl ether, the monomer CDCMA was purified by column chromatography (silica gel, eluent: chloroform), giving a colorless viscous liquid in a yield of 0.54 g (32 %). ^{1}H NMR (300 MHz, $CDCl_3$; δ, ppm): 6.11, 5.57 (4H, s, C*H*$_2$=C), 5.94 (2H, q, O-C*H*(CH_3)-O), 4.27, 3.80 (8H, t, O-C*H*$_2$C*H*$_2$-O), 2.29 - 1.43 (10H, m, cyclohexyl), 1.93 (6H, s, methacrylic C*H*$_3$), 1.38 (6H, d, -C*H*$_3$).

*1-Adamantanecarboxylic acid 2-(1-methacryloxyethoxy) ethyl (**AMA**)*

1-Adamantanecarbonyl chloride (13.5 g, 68.1 mmol), 34 mL of methyl isobutyl ketone, and pyridine (10.8 g, 136.2 mmol) were placed in a three-necked round-bottom flask fitted with an efficient magnetic stirrer and a thermometer under nitrogen. Ethylene glycol monovinyl ether (9.0 g, 102.1 mmol) was added dropwise at 5 ^{o}C and reacted for 24 h at room temperature. The methyl isobutyl ketone solution was washed with 1N-HClaq, water, saturated $NaHCO_3$, and water. Then the methyl isobutyl ketone layer was dried over anhydrous Na_2SO_4. 1-Adamantanecarboxylic acid 2-vinyloxyethyl ester was purified by distillation (2.0 mmHg, 122.1 – 123.5 ^{o}C), giving a colorless viscous liquid in a yield of 11.5 g (67 %). ^{1}H NMR (400 MHz, $CDCl_3$; δ, ppm): 6.47 (1H, q, O-C*H*=CH_2), 4.28 (2H, t, -C(=O)-C*H*$_2$-), 4.20, 4.03 (2H, dd, -OCH=C*H*$_2$), 3.87 (2H, t, -C*H*$_2$-O-), 2.08~1.64 (15H, m, adamantane). MS (EI): *m/z* 249 (M^+-H, 0.1), 207 (M^+-43, 100).

Into a three-necked round-bottom flask were placed p-toluenesulfonic acid (0.027 g, 0.16 mmol), tetrahydrofuran (THF) (18 mL), and methacrylic acid (2.0 g, 24.0 mmol) under nitrogen. 1-Adamantanecarboxylic acid 2-vinyloxyethyl ester (4.0 g, 16.0 mmol) in 5 mL of THF was added dropwise at 5 ^{o}C and the reaction was continued for 5 h at 10 ^{o}C. 100 mL of diethyl ether was added and the ether solution was washed with saturated $NaHCO_3$ aqueous solution

three times and dried over anhydrous Na_2SO_4. After removal of diethyl ether, the monomer AMA was purified by column chromatography (silica gel, eluent; chloroform:hexane = 7:3, v/v), giving a colorless viscous liquid in a yield of 2.2 g (41 %). ^{1}H NMR (300 MHz, $CDCl_3$; δ, ppm): 6.16, 5.61 (2H, s, C*H*$_2$=C), 6.00 (1H, m, O-C*H*(CH_3)-O), 4.19 (2H, t, -C(=O)-C*H*$_2$), 3.90 - 3.67 (2H, m, -C*H*$_2$-O), 2.06 - 1.64 (15H, m, adamantane), 1.89 (3H, s, -C*H*$_3$), 1.45 (3H, m, O-CH(C*H*$_3$)-O). MS (EI): *m/z* 335 (M^+-H, 8.0), 135 (M^+-201, 100).

4-2-4. UV imprinting of reworkable monomers

Samples for the UV imprinting were a mixture of a reworkable monomer, a photoradical initiator DMPA, and a photoacid generator DITF. The surface of Si wafer was treated with hexamethyldisilazane and the surface of quartz mold (Size: 2.5 x 2.5 cm, 20 μm line patterns with an aspect ratio of 1/20) was treated with OPTOOL DSX before use. The sample was put on Si wafer and a quartz mold was placed on the sample. The depth of line patterns of quartz mold was about 1 μm. The sample was pressed at 0.8 - 2.5 MPa and irradiated at 365 nm under vacuum (~120 mmHg). The quartz mold was removed to obtain the UV imprinted patterns of reworkable monomers (see Scheme 4-1). Degree of shrinkage in height of UV imprinted patterns was defined as $100 \times (h_1-h_2)/h_1$, where h_1 is the depth of line patterns of the mold and h_2 is the height of imprinted line patterns.

4-2-5. Photo-induced degradation of cured reworkable resin and analysis of kinetic chain length

The UV imprinting for the sample preparation of SEC analysis was performed as described above, except for using a quartz plate instead of quartz mold. The UV cured reworkable resin was irradiated at 254 nm and baked at given temperatures for 10 min. Then the sample was immersed in methanol for 10 min. The methanol solution was concentrated to dryness and the residue (1.0 mg) was suspended in 6 mL of a mixed solvent of benzene/ethyl ether (5/1, v/v).

Diazomethane which was freshly generated from *p*-toluenesulfonyl-*N*-methyl-*N*-nitrosoamide and ethanol under alkaline condition was introduced into the suspended solution for 2 h using N_2 gas as a carrier.[12] The reaction mixture was poured into excessive methanol to precipitate the methylated polymer (poly(methyl methacrylate), PMMA). To prepare the sample solution for SEC analysis, PMMA was dissolved in THF and filtered with a membrane filter (pore size: 0.5 μm) to remove small amounts of insoluble fraction.

4-2-6. UV curing by photo-DSC and analysis of kinetic chain length

The UV curing of reworkable monomers was also conducted by using photo-DSC. Accurately weighed (about 5 mg) samples of the UV curable composition were polymerized in aluminum DSC pans under nitrogen atmosphere by irradiating at 365 nm. The reaction heat liberated during the polymerization was hypothesized to directly proportion to the number of vinyl groups reacted. By integrating the area of the exothermic peak, the conversion of the vinyl groups (*C*) can be determined according to *eq 1*

$$C = \Delta H_t / \Delta H_0^{theor} \qquad (eq\ 1)$$

where ΔH_t is the reaction heat evolved at time t and ΔH_0^{theor} is the theoretical heat for complete conversion. ΔH_0^{theor} was estimated to be 55 kJ/mol for an methacrylic double bond.[14,15] The UV cured samples were taken out from aluminum pan and then dissolved in 10 mL of methanol / 1N-HClaq (9/1, v/v) for 12 hours at room temperature. After removal of the solvent, the products were methylated and analyzed by SEC as described above. This method afforded rapid UV curing and ease of recovery for degradation products compared to the method described above.

4-3. Results and Discussion

4-3-1. UV curing and degradation of cured reworkable resins

When reworkable monomers containing DMPA and DITF were irradiated with 365-nm light under reduced pressure, efficient curing was observed. If the irradiation was carried out in air, no curing was observed. DMPA was used as a photoradical initiator which can generate radical species on irradiation at 365 nm. DITF did not affect the radical polymerization process because it is unreactive to 365-nm light. Figure 4-1 shows the relationship between insoluble fraction and irradiation dose at 365 nm. Photo-induced insolubilization of reworkable monomers occurred with increasing irradiation dose. The effective UV curing for all monomers occurred. Especially, ADMA was highly curable on irradiation and the complete insolubilization of ADMA was observed at the exposure dose of 50 mJ/cm^2. Complete insolubilization for all monomers was observed at the exposure dose of 150 mJ/cm^2.

Figure 4-2 shows the IR spectral changes of ADMA containing 1 wt% DMPA and 1 wt% DITF on irradiation. The peak at 1636 cm^{-1} due to C=C stretching in IR spectra decreased on irradiation at 365-nm light. Figure 4-3 shows the conversion of methacrylate units of ADMA, CDMA, CDCMA, and BPDMA on irradiation. The effective polymerization for ADMA and CDCMA occurred and the conversion at the exposure dose of 200 mJ/cm^2 was observed to be about 75 %. On the other hand, BPDMA and CDMA exhibited a slow rate and the conversion at the exposure dose of 200 mJ/cm^2 was observed to be 50 %. The higher conversions of ADMA and CDCMA compared to others might be due to the enhanced flexibility of the methacrylate units and low viscosity.

It is known that the hemiacetal ester linkage is stable up to 150 - 200 ^oC under neutral or basic conditions and decomposes readily under acidic conditions.[16,17] Although UV cured reworkable resins were insoluble in methanol, it became soluble in methanol after exposure at

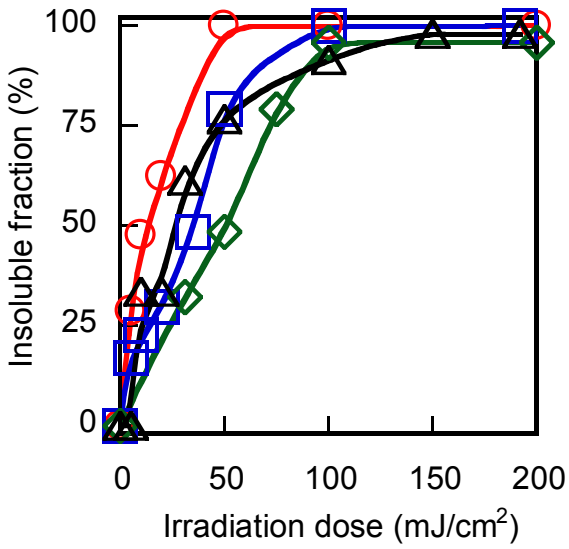

Figure 4-1. Effect of irradiation dose at 365 nm on insolubilization of monomers containing 1 wt% DMPA and 1 wt% DITF. Monomer: (○) ADMA, (□) CDMA, (◇) CDCMA, and (△) BPDMA. Applied pressure: 0.8 MPa. Irradiation condition: room temperature under reduced pressure (~120 mmHg). Dissolution: in methanol for 10 min. Film thickness: 1.0 μm.

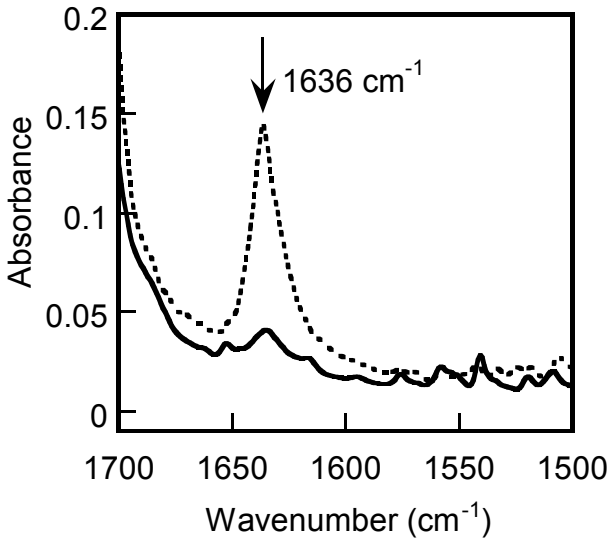

Figure 4-2. IR spectral changes of ADMA containing 1 wt% DMPA and 1 wt% DITF. Applied pressure: 0.8 MPa. Light intensity at 365 nm: 13.3 mW/cm^2. Dotted line: unexposed. Solid line: irradiated at 365 nm with 200 mJ/cm^2 under reduced pressure (~120 mmHg). Film thickness: 1.0 μm.

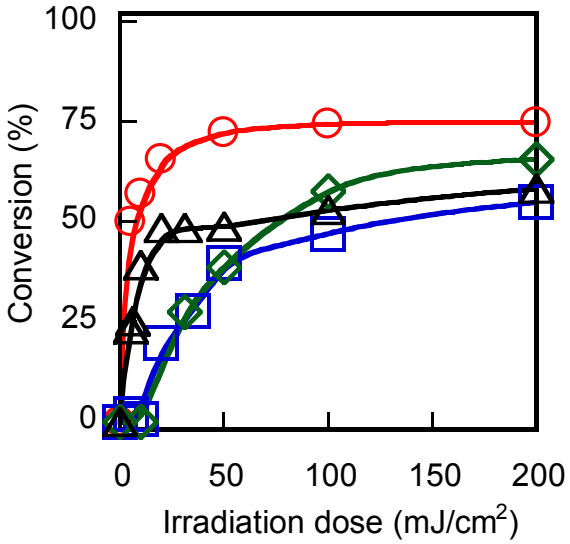

Figure 4-3. Effect of irradiation dose at 365 nm on conversion of monomers containing 1 wt% DMPA and 1 wt% DITF. Monomer: (○) ADMA, (□) CDMA, (◇) CDCMA, and (△) BPDMA. Applied pressure: 0.8 MPa. Irradiation condition: room temperature under reduced pressure (~120 mmHg). Dissolution: in methanol for 10 min. Film thickness: 1.0 μm.

254-nm light. Triflic acid generated from DITF induced acid-catalyzed hydrolysis of the hemiacetal esters of the cured resins and yielded poly(methacrylic acid) together with acetaldehyde and an alcohol derivative. A degradation mechanism of the cured ADMA is shown in Scheme 4-4. Here, water can be supplied from the atmospheric moisture if the UV cured film was thin (~1 μm). Cleavage of the hemiacetal ester units was confirmed by the FTIR spectroscopy. Figure 4-4 shows the IR spectral changes of UV cured ADMA on irradiation at 254 nm and followed by baking at 80 ^{o}C for 10 min. The peak at 1134 cm^{-1} due to -O-C-O- bonds disappeared when exposed to 254-nm light and followed by baking. On the other hand, the peak due to ester carbonyl (1727 cm^{-1}) showed slightly shift to 1704 cm^{-1} and the peak ascribed to hydroxyl groups (2800 – 3600 cm^{-1}) appeared, which is due to the formation of carboxylic acid groups.

Figure 4-5 shows the dissolution of the cured resins when baked at various temperatures after irradiation at 254 nm. More than 50 % of cured reworkable resins except for BPDMA became soluble after irradiation at 254 nm at room temperature. Complete dissolution of the cured resins was accomplished after baking at 80 ^{o}C. Especially, ADMA and CDMA became soluble in methanol after baking at lower temperatures. Since water is necessary for the degradation of the cured resins, the dissolution behavior was dependent on the hydrophilicity of the core structures of reworkable monomers. BPDMA having hydrophobic nature of the core structure showed poor degradability.

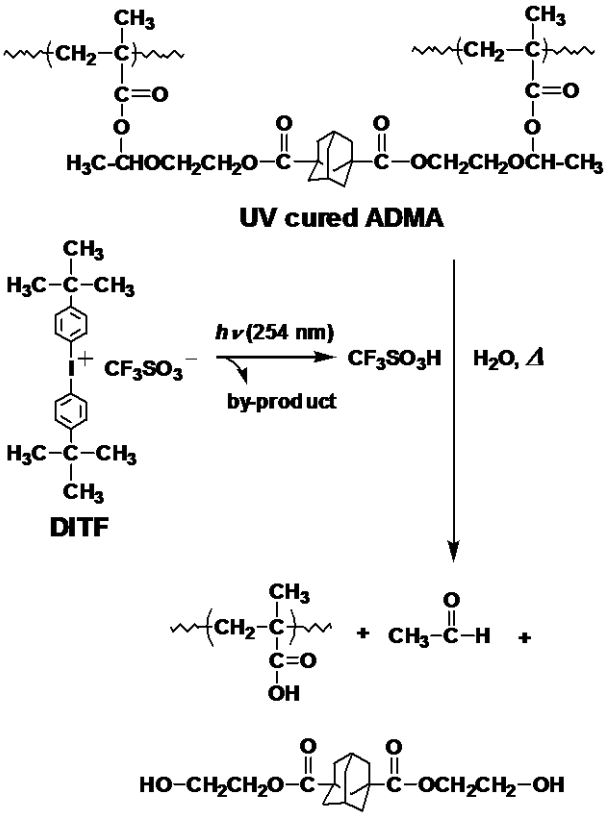

Scheme 4-4. Proposed mechanism for degradation of UV cured ADMA.

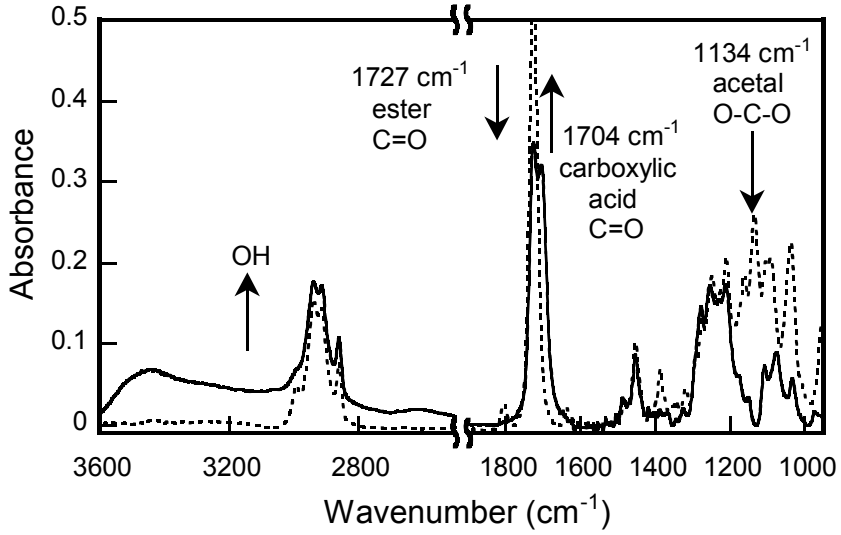

Figure 4-4. IR spectral changes of UV cured ADMA containing 1 wt% DMPA and 1 wt% DITF on irradiation. Applied pressure: 0.8 MPa. Irradiation dose for curing at 365 nm: 200 mJ/cm^2. Dotted line: before irradiation at 254 nm. Solid line: after irradiation at 254 nm with 200 mJ/cm^2 and followed by baking at 80 ^{o}C for 10 min. Film thickness: 2.0 μm.

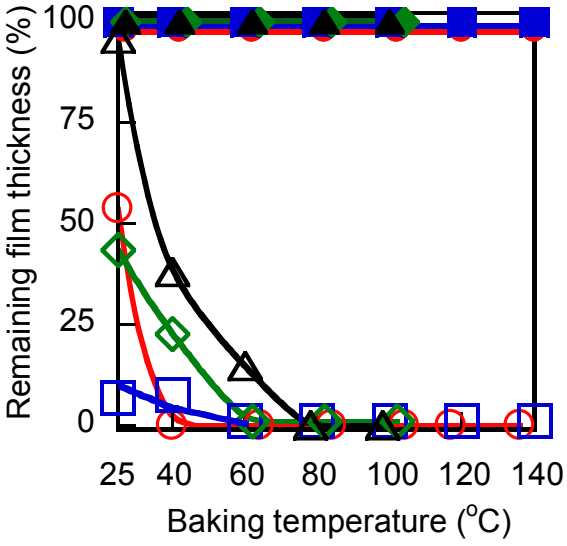

Figure 4-5. Effect of Baking temperature on dissolution of UV cured resins containing 1 wt% DMPA and 1 wt% DITF. Monomer: (○) ADMA, (□) CDMA, (◇) CDCMA, and (△) BPDMA. Applied pressure: 0.8 MPa. Irradiation dose for curing at 365 nm: 200 mJ/cm^2. Open symbol: exposed at 254 nm with 200 mJ/cm^2. Solid symbol: unexposed at 254 nm. Dissolution: in methanol for 10 min. Baking time: 10 min. Film thickness: 1.0 μm.

4-3-2. UV imprinting using reworkable monomers

Four types of reworkable resins were applied to UV-NIL. Figure 4-6 shows photographs of the UV imprinted patterns of reworkable resins (20 μm line width) on Si wafer. Patterns with the widths from 1 μm to 100 μm were prepared in good form. Figure 4-7 shows SEM images of the UV imprinted patterns of ADMA and Figure 4-8 shows SEM images of the UV imprinted patterns of CDMA on Si wafer. Patterns with the widths from 600 nm to 100 μm were prepared in good form. All reworkable monomers were useful to fabricate UV imprinted patterns in a similar manner. Therefore, application of reworkable resins to UV-NIL can prevent the fouling of the master mold.

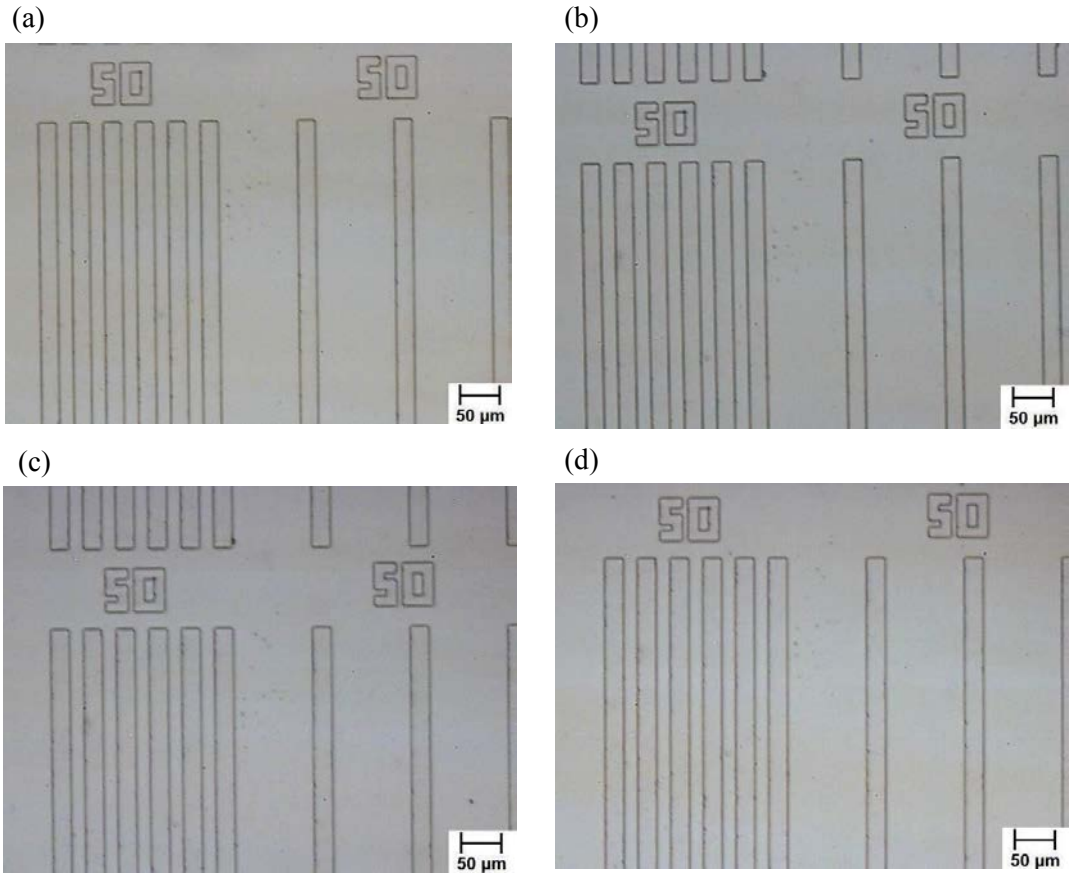

Figure 4-6. Optical micrographs of UV imprinted patterns of (a) ADMA, (b) CDMA, (c) CDCMA, and (d) BPDMA on Si wafer. Irradiation dose at 365 nm: 200 mJ/cm^2. Applied pressure: 0.8 MPa. Width of UV imprinted patterns: 20 μm. Height of UV imprinted patterns: 1 μm.

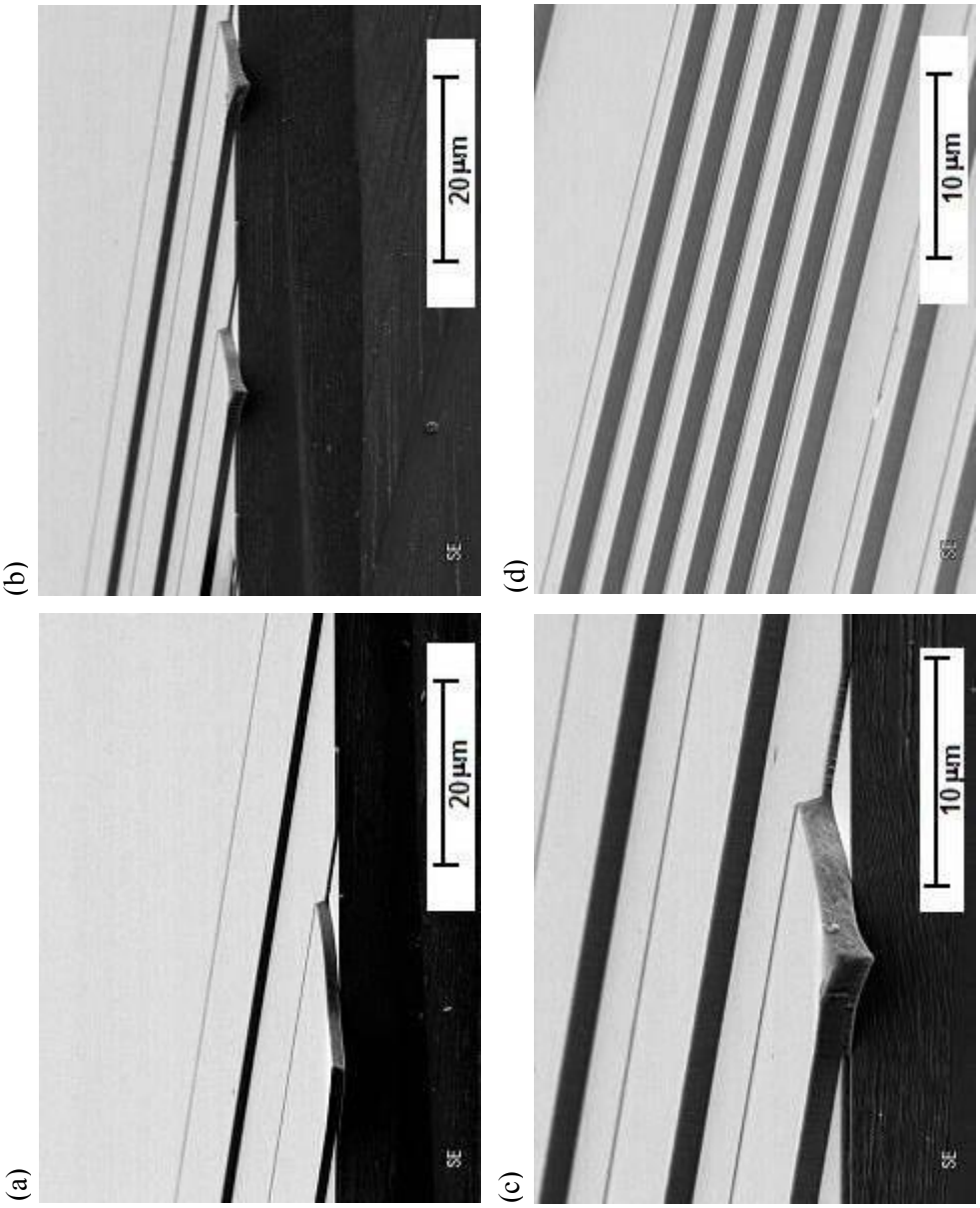

Figure 4-7. SEM photographs of UV imprinted patterns of ADMA on Si wafer. Irradiation dose at 365 nm: 600 mJ/cm^2. Applied pressure: 2.5 MPa. Width of UV imprinted patterns: (a) 20 μm, (b) 10 μm, (c) 10 μm, and (d) 3 μm. Height of UV imprinted patterns: 1 μm.

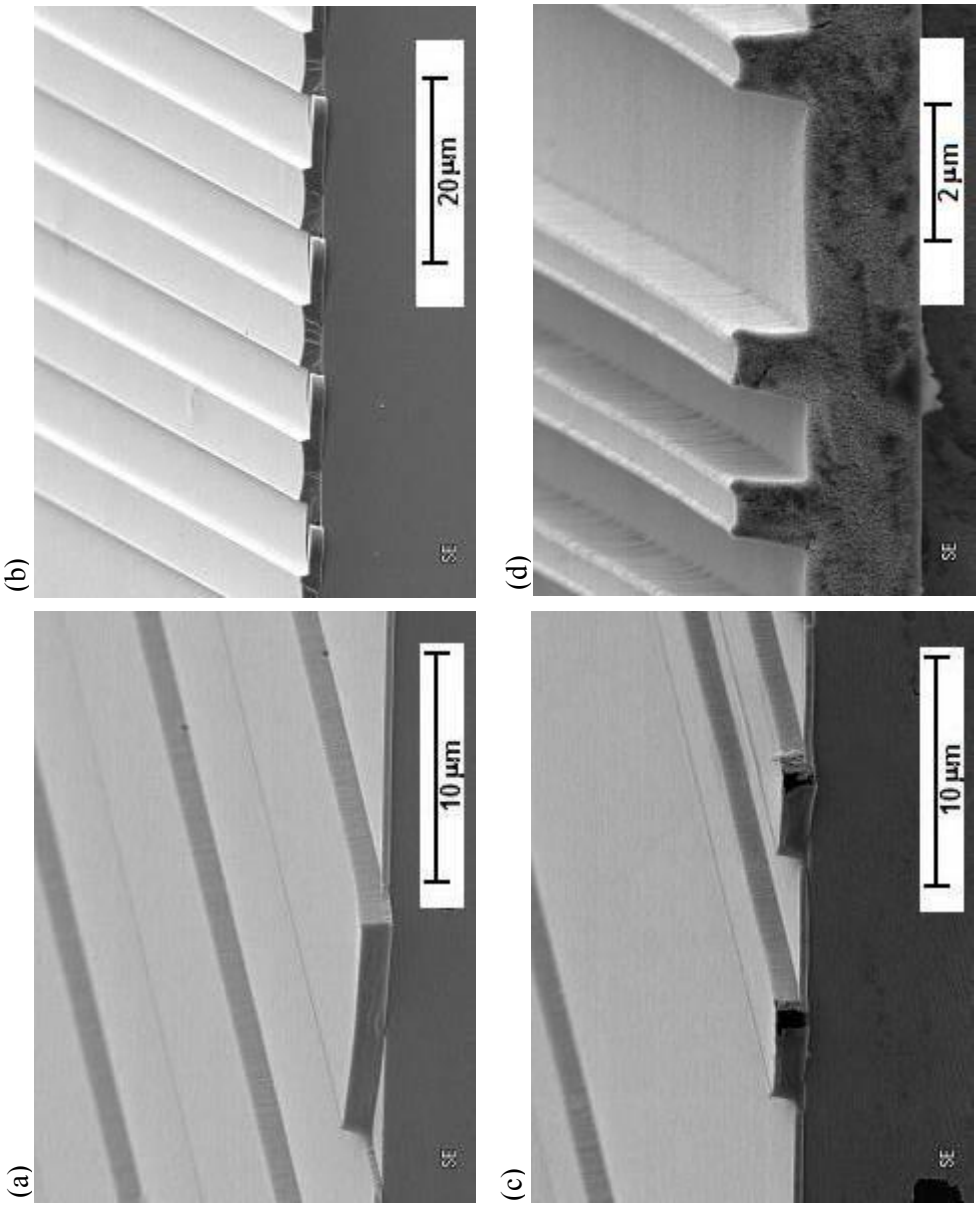

Figure 4-8. SEM photographs of UV imprinted patterns of CDMA on Si wafer. Irradiation dose at 365 nm: 600 mJ/cm^2. Applied pressure: 2.5 MPa. Width of UV imprinted patterns: (a) 10 μm, (b) 6 μm, (c) 4 μm, and (d) 600 nm. Height of UV imprinted patterns: 1 μm.

4-3-3. Effect of monomer structure

4-3-3-1. Shrinkage of UV imprinted patterns

Figure 4-9 shows the effect of the monomer structure on shrinkage in height of UV imprinted patterns. In this experiment, all reworkable monomers were irradiated at 365 nm with 200 mJ/cm^2 and the conversions of C=C bonds were in the range of 60 - 70 %. Degree of shrinkage decreased with increasing the bulkiness of middle part of the monomer. Figure 4-10 shows a relationship between acrylic equivalent value of the monomers and the shrinkage of UV imprinted patterns. In general, acrylic equivalent value is used as an indicator that exhibits bulkiness of relevant molecule. It was found that the monomer with high acrylic equivalent value induced small shrinkage of UV imprinted patterns.

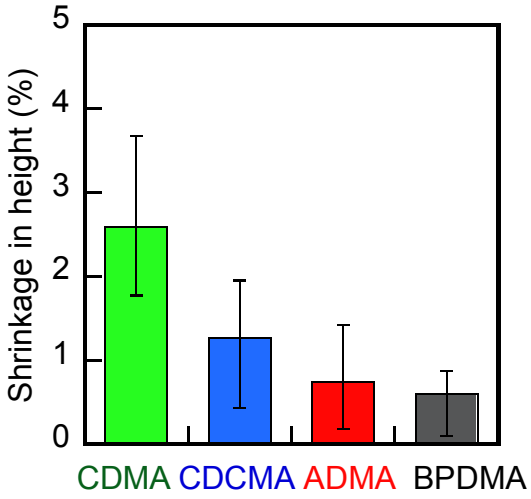

Figure 4-9. Effect of monomer structure on shrinkage in height of patterns. Applied pressure: 0.8 MPa. Line width of the mold: 20 μm. Line depth of the mold: 1 μm.

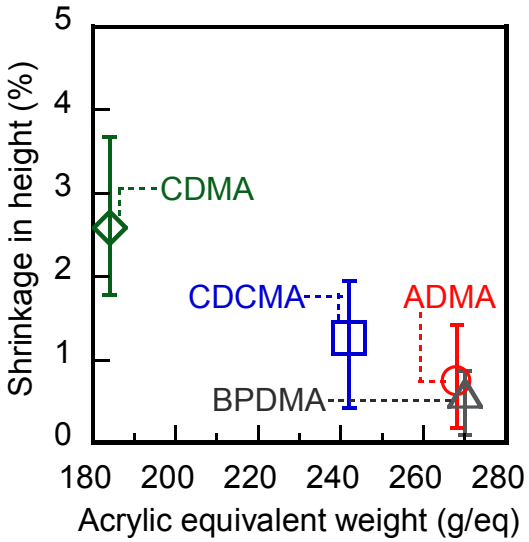

Figure 4-10. Effect of acrylic equivalent value of monomers on shrinkage of patterns. Applied pressure: 0.8 MPa. Line width of the mold: 20 μm. Line depth of the mold: 1 μm.

4-3-3-2. Kinetic chain length of UV cured resins

Four types of reworkable monomers were UV cured by photo-DSC and the kinetic chain lengths of cured resins were analyzed by SEC. When reworkable monomers containing DMPA were irradiated with 365-nm light under nitrogen atmosphere, efficient curing was observed. Figure 4-11 shows the conversion of methacrylate units of ADMA, CDMA, CDCMA, and BPDMA on irradiation. The effective polymerization occurred and the conversion was observed to be 50 - 60 % at the exposure dose of 600 mJ/cm^2. The inconsistency of the conversion for the reworkable monomers cured by UV-NIL and photo-DSC may be due to the difference of the calculation method. The kinetic chain length of reworkable monomers cured by photo-DSC was summarized in Table 4-1, where the number average molecular weight (*Mn*) was evaluated for the fractions of the polymers higher than 3000 in SEC profile. The kinetic chain length of CDCMA was not able to determine because degradation product of cured CDCMA did not afford poly(methacrylic acid), but afforded poly(hydroxyethyl methacrylate). In this experiment, the conversion of C=C bonds was almost the same (50 – 61 %). The kinetic chain length of reworkable monomers was in the range of 280 – 390. The core structure of reworkable monomers did not significantly affect the kinetic chain length of cured resins. Therefore, it was found that the acrylic equivalent value determined the degree of shrinkage of UV imprinted patterns when compared with different monomers.

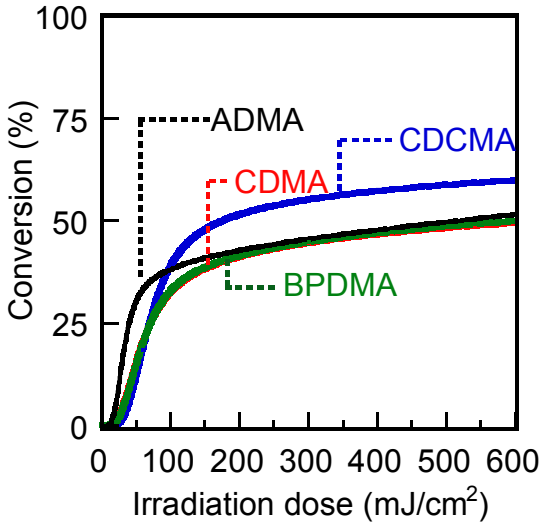

Figure 4-11. Effect of irradiation dose at 365 nm on conversion of reworkable monomers containing 1 wt% DMPA. Curing condition: exposed at 365 nm at 20 °C under nitrogen. Light intensity at 365 nm: 2.0 mW/cm^2.

Table 4-1. UV polymerization conditions and molecular weights of PMMA obtained from the cured reworkable resins[a].

Monomer	Irradiation dose at 365 nm (mJ/cm^2)[b]	Conversion (%)[c]	*Mn*[d]	Chain length	*Mw*/*Mn*[d]
ADMA	600	52	28,000	280	2.6
CDMA	600	61	35,000	350	2.4
BPDMA	600	50	39,000	390	2.8

a) All samples contained 1 wt% DMPA. b) Light intensity at 365 nm: 2.0 mW/cm^2.
c) Determined by photo-DSC. d) Determined by SEC.

4-3-4. Effect of UV imprinting conditions

4-3-4-1. Shrinkage of UV imprinted patterns

The effect of UV curing conditions on shrinkage of UV imprinted patterns was studied in detail using ADMA. Figure 4-12 shows the effect of light intensity at 365 nm on the shrinkage of UV imprinted patterns. Although the light intensity was changed from 3.7 to 13.3 mW/cm^2, the irradiation dose was adjusted to be 200 mJ/cm^2. The conversion of methacrylate units of ADMA was 70 %. It was found that degree of the shrinkage decreased as the light intensity at 365 nm increased. Figure 4-13 shows the effect of photoradical initiator concentration in the system on the shrinkage of UV imprinted patterns. Irradiation was carried out at 365 nm with the light intensity of 4 mW/cm^2. The conversion of methacrylate units of ADMA was adjusted to be 70 %. Degree of the shrinkage decreased with increasing DMPA concentration.

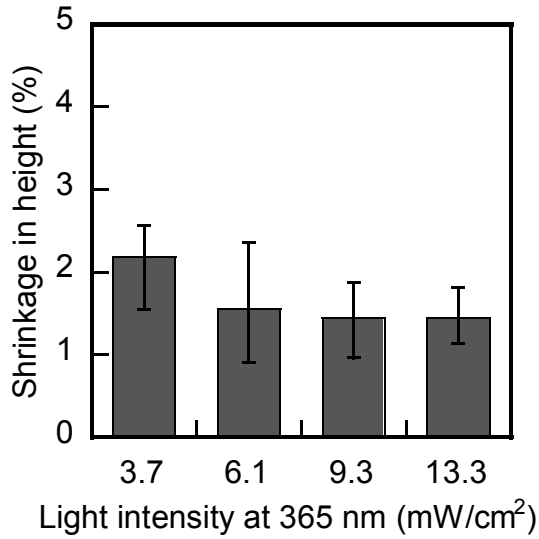

Figure 4-12. Effect of light intensity at 365 nm on shrinkage in height of imprinted patterns of ADMA. Applied pressure: 0.8 MPa. Line width: 20 μm. Line depth of mold: 1 μm.

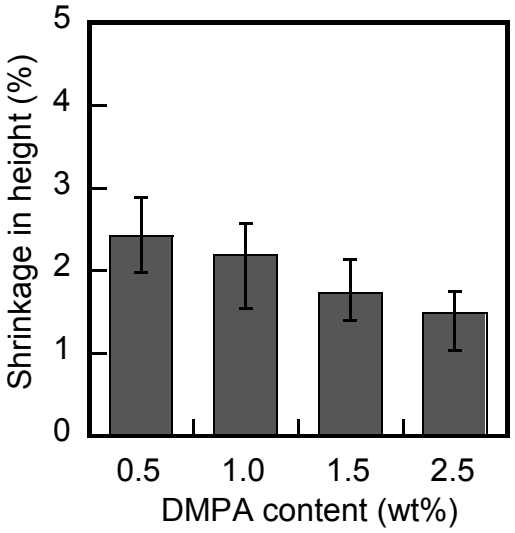

Figure 4-13. Effect of DMPA content on shrinkage in height of imprinted patterns of ADMA. Applied pressure: 0.8 MPa. Conversion of methacrylate unit of ADMA: 70 %. Line width: 20 μm. Line depth of mold: 1 μm.

4-3-4-2. Kinetic chain length of UV imprinted patterns

The shrinkage of the present monomers by UV curing was mainly determined by the acrylic equivalent value. The monomers with higher acrylic equivalent number showed lower shrinkage by UV curing. Furthermore, the shrinkage of ADMA was dependent on the UV curing conditions. To clarify the reason for the finding, kinetic chain length of the UV imprinted resins was investigated. Shrinkage by the curing of methacrylate monomers is caused by the decrease in free volume of the system. Van der Waals radius between monomers is estimated to be 0.3 - 0.6 nm. On the other hand, the distance of C-C and C=C bonds are 0.15 and 0.13 nm, respectively. Thus, if the conversion of monomers is the same, the cured resin with larger number of terminal is expected to show lower shrinkage. The number of terminal can be estimated by evaluating the kinetic chain length of the UV cured resin at a given conversion of monomers.

Figure 4-14 shows SEC traces of the PMMA obtained from UV imprinted films of ADMA with different intensities of irradiation light for curing. In this experiment, all samples were cured with a dose of 600 mJ/cm^2, but the light intensity was different from each other. The conversion of the monomers was 75 - 76 %. The chain length for the cured resins obtained by higher intensity of light (5.5 mW/cm^2) was lower, compared with the resins cured with lower intensities of light (0.5 – 2.0 mW/cm^2). The effect of several parameters on the kinetic chain length of the UV imprinted ADMA is summarized in Table 4-2. The kinetic chain length decreased with increasing the concentration of the photoradical initiator DMPA. This is the common phenomenon as that observed for the effect of concentration of photoradical initiator on kinetic chain length of UV cured resins.[11] At higher concentration (2.5 wt%) of DMPA, higher molecular weight PMMA coexisted with lower molecular weight PMMA, causing a larger value of polydispersity index (*Mw*/*Mn*). The effect of applied pressure on the kinetic chain length for the UV imprinting of ADMA was also investigated. Although the

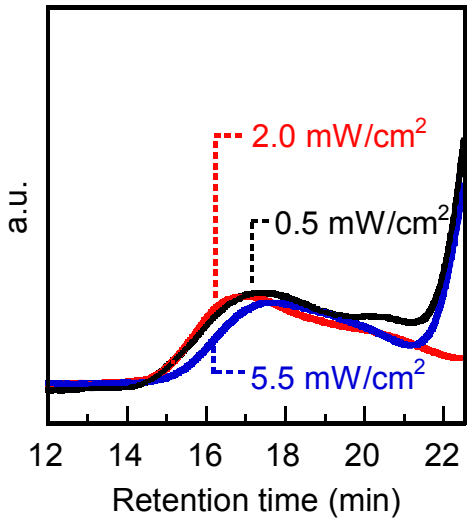

Figure 4-14. Effect of irradiation intensity on SEC profiles of PMMA obtained from the UV cured films of ADMA / DMPA (1 wt%) / DITF (1 wt%). Irradiation dose for curing at 365 nm: 600 mJ/cm^2. Degradation conditions: Irradiated at 254 nm with 200 mJ/cm^2 and baked at 100 ^{o}C for 10 min.

Table 4-2. UV curing conditions and molecular weights of PMMA obtained from cured ADMA[a].

DMPA (wt%)	Light intensity at 365 nm (mW/cm^2)	Monomer conversion (%)[b]	Applied pressure (MPa)	*Mn*[c]	Chain length	*Mw*/*Mn*[c]
1.0	0.5	75	0.8	43,000	430	2.9
1.0	2.0	75	0.8	43,000	430	3.3
1.0	5.5	76	0.8	37,000	370	2.5
0.5	2.0	75	0.8	46,000	460	3.2
1.0	2.0	78	0.8	43,000	430	3.3
1.5	2.0	81	0.8	26,000	260	3.3
2.5	2.0	81	0.8	6,000	60	6.8
1.0	2.0	75	0.8	43,000	430	3.3
1.0	2.0	75	1.6	40,000	400	2.8
1.0	2.0	74	2.5	37,000	370	3.5

a) All samples contained 1 wt% DITF. b) Determined by FT-IR spectroscopy.
c) Determined by SEC.

conversion of C=C bonds was almost the same (74 – 75 %), the kinetic chain length decreased with increasing applied pressure due to the restricted diffusion of ADMA during the UV curing reaction. In order to study the effect of mobility of UV imprinting formulation on kinetic chain length, ADMA / AMA blended system was also investigated. AMA was used as a monofunctional reworkable monomer having high mobility compared to ADMA. Effect of ADMA / AMA blending ratio on kinetic chain length was summarized in Table 4-3. The kinetic chain length increased with increase of AMA added due to the enhanced mobility of monomers.

Figure 4-15 shows effect of ADMA / AMA ratio on the shrinkage of UV imprinted patterns. The shrinkage increased with AMA content. The shrinkage for ADMA / AMA (5 / 5, molar ratio) was almost 5 % which is larger than the expected value from the data shown in Figure 4-10. The acrylic equivalent values of ADMA and AMA are 268 and 336, respectively. As shown in Table 4-3, the kinetic chain length of the cured ADMA / AMA (5 / 5, molar ratio) was larger than that of the cured ADMA. Thus, the reduced number of the terminal of the cured resin suggests the increased shrinkage of ADMA / AMA (5 / 5, molar ratio).

Generally, addition of chain transfer reagent to the UV curing system decrease the kinetic chain length, i. e., increase the number of chain terminal. Figure 4-16 shows the effect of 1-dodecanethiol added as a chain transfer reagent on the shrinkage of UV imprinted patterns of ADMA. Degree of shrinkage decreased with increasing 1-dodecanethiol content. In this experiment, conversions of C=C bonds of ADMA containing 0, 5, and 10 wt% of 1-dodecanethiol were 76, 90, and 90 %, respectively. Generally, shrinkage increases with the conversion of monomers. However, as shown in Figure 4-16, the shrinkage decreased with the amount of 1-dodecanethiol added. This finding suggests that the shrinkage can be reduced by decreasing the kinetic chain length of the cured resin.

Table 4-3. UV curing conditions and molecular weights of PMMA obtained from cured resins[a].

Formulation	Conversion (%)[c]	*Mn*[d]	Chain length	*Mw*/*Mn*[d]
ADMA	78	39,000	390	3.2
ADMA/AMA=8/2[b]	81	43,000	430	2.6
ADMA/AMA=7/3[b]	87	43,000	430	2.6
ADMA/AMA=5/5[b]	88	53,000	530	2.6

a) All samples contained 1 wt% DMPA and 1 wt% DITF. Irradiation dose for curing at 365 nm: 600 mJ/cm^2. b) Molar ratio. c) Determined by FT-IR spectroscopy. d) Determined by SEC.

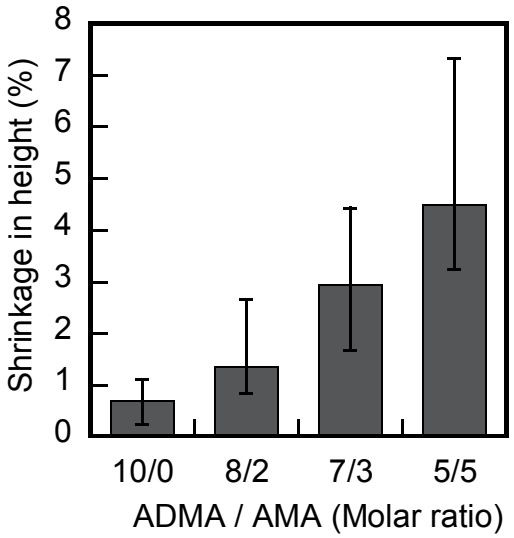

Figure 4-15. Effect of ADMA / AMA blend ratio on shrinkage in height of imprinted patterns of ADMA / AMA containing 1 wt% DMPA and 1 wt% DITF. Light intensity at 365 nm: 2.1 mW/cm^2. Conversion of methacrylate unit of ADMA / AMA = 75 %. Line width: 20 μm. Line depth of mold: 1 μm.

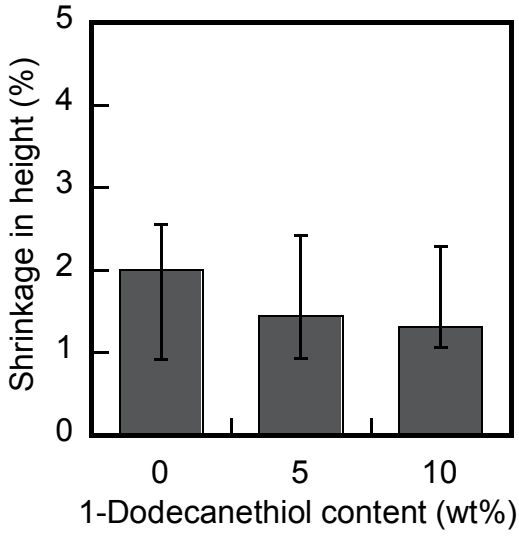

Figure 4-16. Effect of 1-dodecanethiol content on shrinkage in height of imprinted patterns of ADMA. Applied pressure: 0.8 MPa. Light intensity at 365 nm: 2.0 mW/cm^2. Irradiation dose at 365 nm: 600 mJ/cm^2. Conversion of methacrylate unit of ADMA: (0 wt% 1-dodecanethiol) 76 % and (5 wt% and 10 wt% 1-dodecanethiol) 90 %. Line width of mold: 20 μm. Line depth of mold: 1 μm.

4-4. Conclusion

Difunctional methacrylates having hemiacetal ester linkages in a molecule were synthesized. These monomers were cured on UV irradiation and the cured resin was successfully degraded at mild conditions. By applying these monomers to UV imprint lithography, fine line / space patterns with the line widths from 600 nm to 100 μm were obtained in good form. Application of reworkable resins to UV-NIL can prevent the fouling of the master mold. The effect of monomer structure on shrinkage of UV imprinted patterns was studied. It was exhibited that degree of shrinkage decreased with increasing the bulkiness of core structure of the monomer. The effect of UV imprint conditions on shrinkage of UV imprinted patterns was investigated from the aspect of kinetic chain length. The kinetic chain length of UV imprinted patterns was investigated by analyzing the degraded products of UV cured resins. The poly (methacrylic acid) obtained as degraded product was successfully methylated with diazomethane for SEC measurements. It was found that degree of shrinkage of UV imprinted patterns decreased with increasing acrylic equivalent value of the monomers and decreasing the kinetic chain length of the cured resin.

References

1. S. Y. Chou, P. R. Krauss, P. J. Renstrom, *Appl. Phys. Lett.*, 67, 3114 (1995).
2. S. Y. Chou, P. R. Krauss, P. J. Renstrom, *J. Vac. Sci. Technol.*, B14, 4129 (1996).
3. B. D. Gates, Q. Xu, M. Stewart, D. Ryan, C. G. Willson, G. M. Whitesides, *Chem. Rev.*, 105, 1171 (2005).
4. D. J. Resnick, S. V. Sreenivasan, C. G. Willson, *Mater. Today*, 8, 34 (2005).
5. H. Schift, *J. Vac. Sci. Technol.*, B26, 458 (2008).
6. A. del Campo, E. Arzt, *Chem. Rev.*, 108, 911 (2008).
7. W. K. Neo, M. B. Chan-park, *Macromol. Rapid Commun.,* 26, 1008 (2005).
8. P. E. M. Allen, G. P. Simon, D. R. Williams, E. H. Williams, *Macromolecules*, 22, 3555 (1989).
9. K. S. Anseth, C. Decker, C. N. Bowman, *Macromolecules*, 28, 4040 (1995).
10. E. Andrzejewska, M. Andrzejewski, *J. Polym. Sci.: Part A: Polym. Chem.*, 36, 665 (1998).
11. E. Andrzejewska, *Prog. Polym. Sci.*, 26, 605 (2001).
12. M. Shirai, K. Mitsukura, H. Okamura, *Chem. Mater.*, 20, 1971 (2008).
13. E. Ruckenstein, H. Zhang, *Polym. Bull.*, 47, 113 (2001).
14. K. S. Anseth, C. M. Wang, C. N. Bowman, *Macromolecules*, 27, 650 (1994).
15. J. Wei, F. Liu, *Macromolecules*, 42, 5486 (2009).
16. H. Zhang, E. Ruckenstein, *Macromolecules*, 31, 7575 (1998).
17. E. Ruckenstein, H. Zhang, *Macromolecules*, 31, 9127 (1998).

Chapter 5

Preparation of replicated resin mold for UV nanoimprint using reworkable resin

5-1. Introduction

Nanosized pattern fabrication becomes important in various fields such as sensors, optical devices, and microelectronics.[1-5] UV nanoimprint lithography (UV-NIL) is one of the most promising technologies for nanofabrication. UV-NIL utilizes UV light to cure a photoresist which was pressed with the patterned master mold to obtain patterned structures. Although the principles of UV-NIL are simple, there are some problems to be solved for this technique to be used for industrial applications.[2,5] Especially, the fouling of master mold during UV-NIL process is a serious problem because the mold is an expensive component.[6] Since, in particular, UV-NIL uses UV curable resins, it is almost impossible to remove the cured resins adhered to the surface of the master mold unless reworkable resin is used instead of conventional UV curing resin as described in Chapter 4. Therefore, development of the inexpensive mold composed of polymeric materials is desired.

This chapter describes the fabrication of resin replica of quartz master mold for UV-NIL. Scheme 5-1 shows how to fabricate the replicated resin mold. Firstly, UV imprinted patterns (primary patterns) of reworkable resin is obtained by using quartz master mold. Secondly, conventional UV-NIL is carried out using the primary patterns as a mold. To remove the primary patterns from the UV imprinted product, photo-induced and thermal degradation is carried out. Reworkable resin was applied to fabricate the replicated resin mold and UV-NIL using the replicated resin mold was studied.

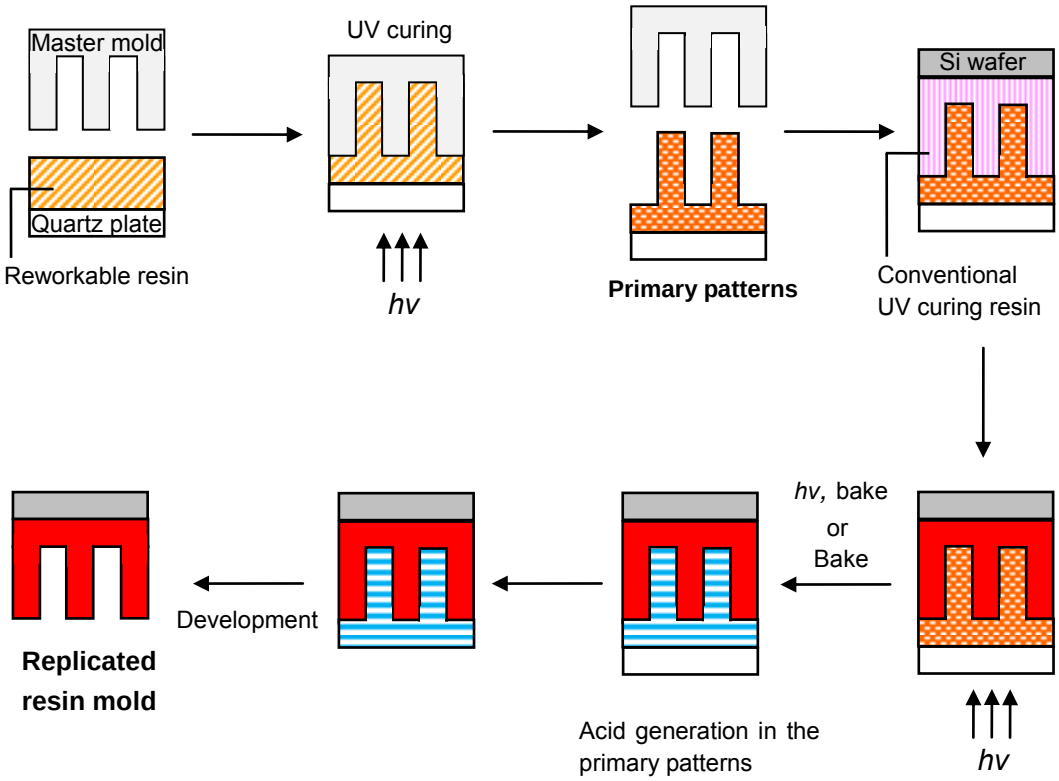

Scheme 5-1. Schematic diagram of fabrication of replicated resin mold.

5-2. Experimental

5-2-1. Materials

Hexamethyldisilazane and 3-methacryloxypropyltrimethoxysilane (γ-MPS) were used as received. DPHA and PTA were supplied from Shin-Nakamura Chemical Co., Ltd and used as conventional UV curing materials. Other solvents and reagents were purchased and used as received. The chemical structures of DPHA and PTA are shown in Scheme 5-2.

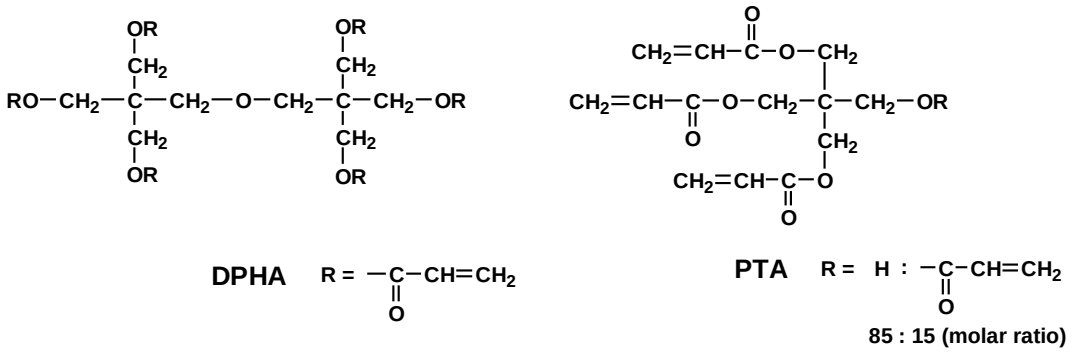

Scheme 5-2. Structures of conventional UV curing materials used.

5-2-2. Synthesis of thermoacid generator cyclohexyl-*p*-toluenesulfonate (***CHTS***)

A round-bottomed flask (100 mL) was charged with cyclohexanol (2.6 g, 26.0 mmol) and pyridine (31 mL), followed by the addition of *p*-toluenesulfonyl chloride (5.0 g, 26.2 mmol) under ice cooling to form a solution. The solution was stirred for 5 h as it was warmed gradually to room temperature. After completion of the reaction, the reaction mixture was poured into iced 4N H_2SO_4aq and stirred thoroughly. Following extraction with chloroform, the organic layer was washed with water and saturated brine and dried on anhydrous magnesium sulfate. After filtration, the solvent was evaporated to give colorless clear oil. This product was purified by column chromatography (eluent: chloroform), giving a white solid in a yield of

2.8 g (42 %). mp: 43.1 – 43.5 ^{o}C. T_d: 136 ^{o}C. ^{1}H NMR (300 MHz, $CDCl_3$; δ, ppm): 7.73, 7.26 (4H, d, aromatic), 4.43 (1H, m, C*H*), 2.38 (3H, s, CH_3), 1.77-1.12 (10H, br, -(CH_2)-). MS (EI): *m/z* 254 (M^+, 1.6), 82 (M^+-172, 100).

5-2-3. UV curing of reworkable monomer and degradation of cured resins

A sample for the UV curing was a mixture of ADMA, a photoradical initiator DMPA, and a photoacid generator DITF. Before use, the surface of quartz plate and Si plate was treated with OPTOOL DSX and hexamethyldisilazane, respectively. The UV curing process consisted of four steps: 1) dropping the sample solution on Si plate, 2) placing the quartz plate and pressing the resin, 3) irradiating at 365 nm through quartz plate to cure the resin, and 4) releasing the quartz plate to obtain the UV cured films of ADMA. The insoluble fraction was determined by comparing the film thickness before and after dissolution in methanol.

The UV cured films were irradiated at 254 nm and followed by baking at given temperatures to decompose the network structures formed. After the film was immersed in methanol for 10 min, the remaining film thickness was determined by comparing the thickness before and after dissolution in methanol.

5-2-4. Fabrication of replicated resin mold

The replicated resin mold was prepared according to Scheme 5-3. For the patterns formation on quartz plate (2.5 x 2.5 cm), the surface of quartz plate was treated with hexamethyldisilazane before use. Samples for the primary patterns formation using UV imprinting process were the mixture of the reworkable monomer ADMA, a photoradical initiator DMPA, and a photoacid generator DITF. The sample was put on quartz plate and a quartz mold was placed on the sample. To improve the release property, the surface of quartz mold (2.5 x 2.5 cm, 20 μm line patterns with an aspect ratio of 1/20) was treated with OPTOOL

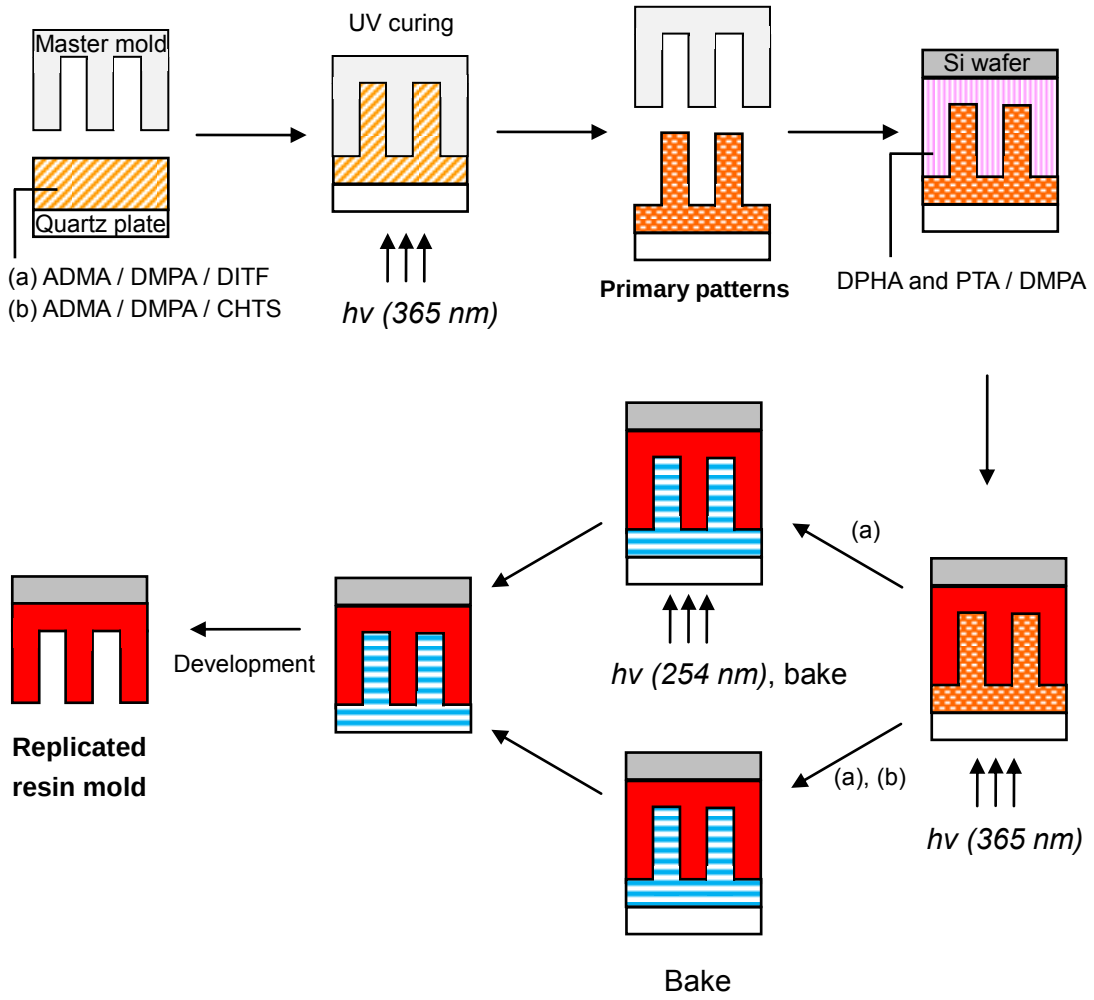

Scheme 5-3. Schematic diagram of UV imprinting and subsequent fabrication of replicated resin mold.

DSX before use. The depth of line patterns of quartz mold was about 1 μm. The sample was pressed at 0.8 MPa and irradiated at 365 nm under vacuum (~120 mmHg). The quartz mold was removed to obtain the UV cured films of the reworkable monomer on quartz plate. Degree of shrinkage in height of UV imprinted patterns was defined as $100 \times (h_1-h_2) /h_1$, where h_1 is the depth of line patterns of the mold and h_2 is the height of imprinted line patterns.

UV imprinting using the primary patterns as a mold was conducted. The sample for the secondary pattern formation was DPHA or DPHA / PTA blended system containing 1 wt% DMPA and was put on Si wafer which was previously treated with γ-MPS. The UV imprinting process was done at 1.2 MPa and irradiated at 365 nm with 600 mJ/cm^2. Then the samples were irradiated at 254 nm with 500 mJ/cm^2 in air and followed by baking at 100 ^{o}C for 15 min to degrade the primary patterns. The quartz plate was easily released because the cured resin on quartz plate was decomposed on irradiation at 254 nm and the adhesion force between the resin and quartz surface was considerably reduced. After washing the decomposed primary patterns with methanol, the replicated resin mold was performed on Si wafer.

It is possible to remove the primary patterns composed of UV cured ADMA / DMPA / DITF or UV cured ADMA / DMPA / CHTS by simple baking. The DPHA or DPHA / PTA mixed sample was put on Si wafer which was treated with γ-MPS and the primary patterns was placed on the sample. The UV imprinting process was conducted at 1.2 MPa and irradiated at 365 nm with 600 mJ/cm^2. Then the samples were baked at 140 ^{o}C for 15 min in air to degrade the primary patterns. In this process thermally generated acid from DITF or CHTS worked as a catalyst for the degradation of the primary patterns.

5-2-5. UV imprinting with replicated resin mold

The replicated resin mold and quartz plate was treated with OPTOOL DSX and γ-MPS, respectively. PTA containing 1 wt% DMPA was put on quartz plate and the replicated resin mold was placed on the sample. The sample was pressed at 0.8 MPa and irradiated at 365 nm under vacuum (~120 mmHg). The resin mold was removed to obtain the UV cured films of PTA on quartz plate.

5-3. Results and Discussion

5-3-1. UV curing and degradation of cured ADMA

When ADMA containing DMPA and DITF was irradiated at room temperature using 365-nm light under reduced pressure, efficient curing was observed. DMPA was used as a photoradical initiator which can generate radical species on irradiation at 365 nm. Figure 5-1 shows insoluble fraction and conversion of C=C bonds for ADMA containing DMPA and DITF on irradiation. Insoluble fraction and conversion of methacrylate units increased with irradiation dose and reached a constant value at the exposure dose of about 50 mJ/cm^2. The complete insolubilization was observed at the exposure dose of 50 mJ/cm^2. The conversion of methacrylate group of ADMA was 78 % at the exposure dose of 200 mJ/cm^2.

Although the UV cured ADMA resin was insoluble in methanol, it became soluble in methanol after exposure to 254-nm light. Triflic acid generated from DITF induced acid-catalyzed hydrolysis of the hemiacetal ester units of the cured resin. Figure 5-2 exhibits the dissolution of the cured ADMA (a) and the decomposed fraction of hemiacetal ester linkages of the cured ADMA (b) when baked at various temperatures after irradiation at 254 nm. About 50 % of the cured ADMA resin became soluble after irradiation at 254 nm at room temperature. Complete dissolution of the cured films was accomplished after baking at 40 ^{o}C for 10 min.

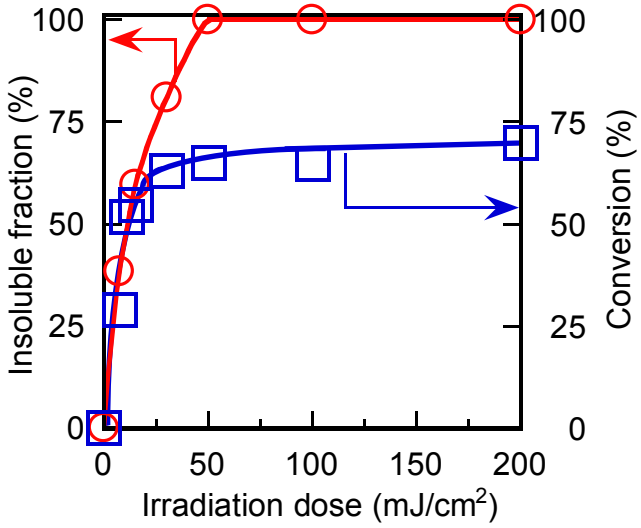

Figure 5-1. Effect of irradiation dose at 365 nm on insolubilization (○) and conversion (□) of ADMA containing 1 wt% DMPA and 1 wt% DITF. Applied pressure: 0.8 MPa. Dissolution: in methanol for 10 min. Irradiation condition: room temperature under reduced pressure (~120 mmHg). Film thickness: 1.0 μm.

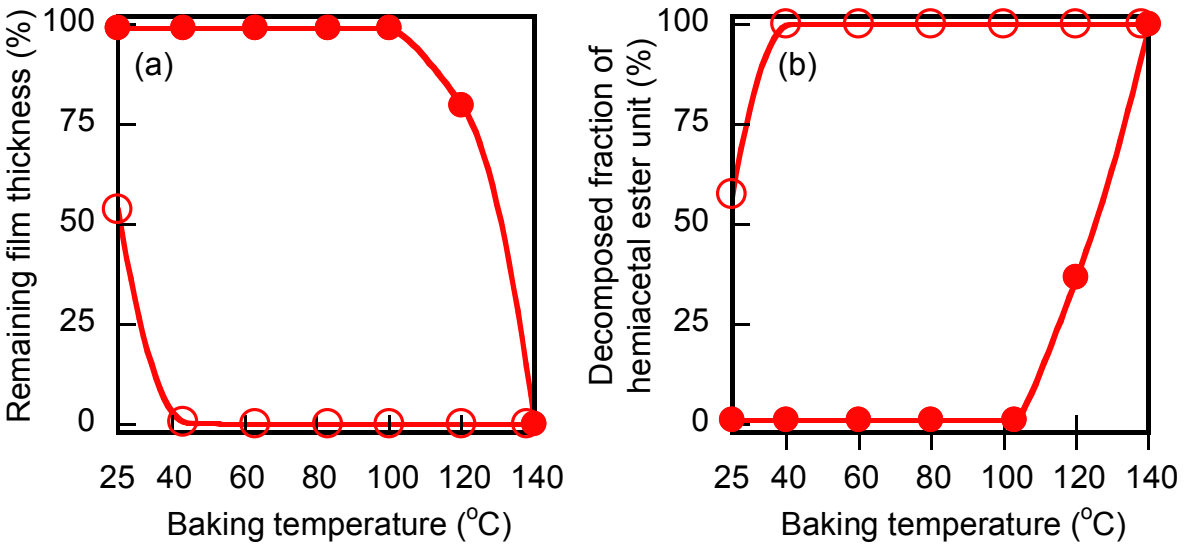

Figure 5-2. Effect of baking temperature on dissolution (a) and decomposed fraction of hemiacetal ester unit (b) of UV cured ADMA containing 1 wt% DMPA and 3 wt% DITF. Applied pressure: 0.8 MPa. Irradiation dose for curing at 365 nm: 200 mJ/cm^2. Open symbol: exposed at 254 nm with 200 mJ/cm^2. Solid symbol: unexposed at 254 nm. Dissolution: in methanol for 10 min. Baking time: 10 min. Film thickness: 1.0 μm.

The cleavage of the hemiacetal ester units was confirmed by the FT-IR spectroscopy. The peak at 1134 cm^{-1} due to -O-C-O- bonds completely disappeared when exposed to 254-nm light and followed by baking at 40 ^{o}C. The decomposed films became soluble in methanol when complete degradation of the hemiacetal ester units was achieved. The acid catalyzed the decomposition reaction of hemiacetal ester linkages to generate poly(methacrylic acid) together with acetaldehyde and an alcohol derivative. After baking at 140 ^{o}C for 10 min without irradiation at 254 nm, complete dissolution of cured resin was observed. In this case, thermally generated acid from DITF worked as a catalyst for the degradation of UV cured ADMA.

Dissolution of UV cured resin by simple baking was also conducted. When reworkable monomer ADMA containing DMPA and CHTS was irradiated at 365 nm with 200 mJ/cm^2 under reduced pressure, complete insolubilization was observed. CHTS was used as a thermoacid generator which can generate *p*-toluenesulfonic acid on baking. Figure 5-3 shows the dissolution of the cured resins and the decomposed fraction of hemiacetal ester linkages of the resins when baked at given temperatures. Complete dissolution of the cured films was observed after baking at 130 – 150 ^{o}C for 10 min. The cleavage of the hemiacetal ester units was confirmed by the FT-IR spectroscopy and the complete degradation of hemiacetal ester units was observed after baking above 120 ^{o}C. The degradation behavior was in accord with the thermal decomposition temperature of CHTS (136 ^{o}C). Figure 5-4 shows the IR spectral changes of UV cured ADMA on baking at 140 ^{o}C for 10 min. The peak at 1134 cm^{-1} due to -O-C-O- bonds disappeared when exposed to 254-nm light and followed by baking. On the other hand, the peak due to ester carbonyl (1727 cm^{-1}) showed slightly shift to 1702 cm^{-1} and the peak ascribed to hydroxyl groups (2800 – 3600 cm^{-1}) appeared, which was due to the formation of carboxylic acid groups. Thermally generated acid induced the acid-catalyzed degradation reaction of the hemiacetal ester units.

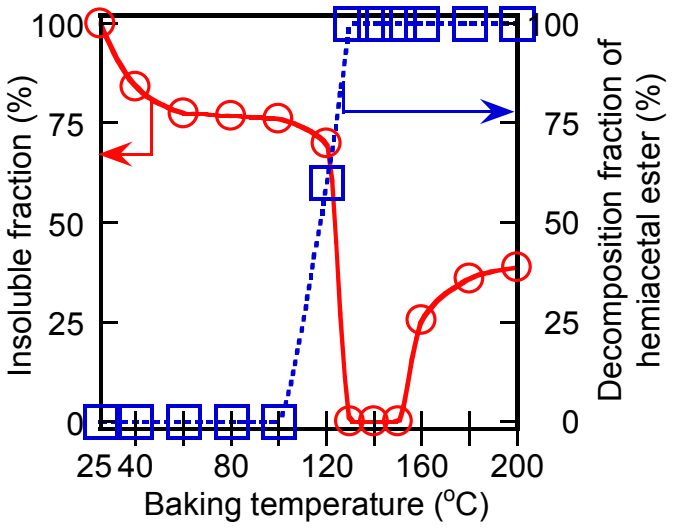

Figure 5-3. Effect of baking temperature on dissolution (○) and decomposed fraction of hemiacetal ester unit (□) of UV cured ADMA containing 1 wt% DMPA and 5 wt% CHTS. Applied pressure: 0.8 MPa. Irradiation dose for curing at 365 nm: 200 mJ/cm^2. Dissolution: in methanol for 10 min. Baking time: 10 min. Film thickness: 2.0 μm.

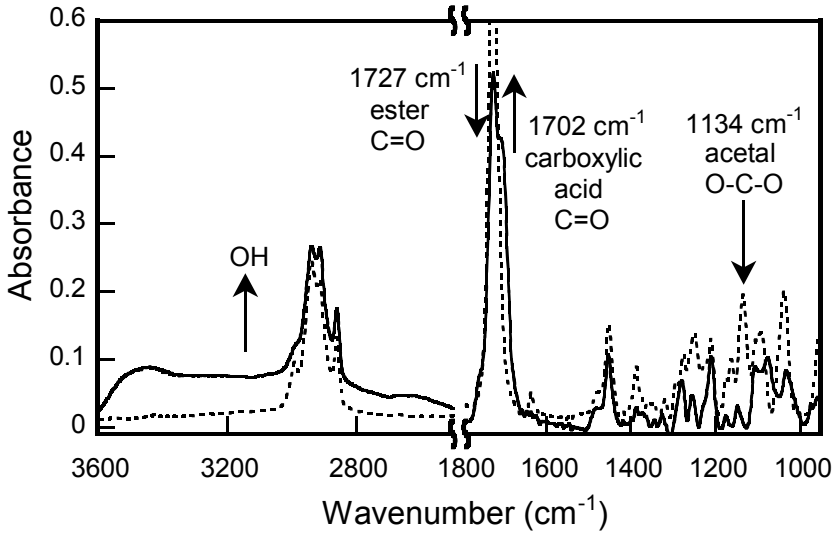

Figure 5-4. IR spectral changes of UV imprinted film of ADMA containing 1 wt% DMPA and 5 wt% CHTS on baking. Irradiation dose for curing at 365 nm: 200 mJ/cm^2. Applied pressure: 0.8 MPa. Dotted line: before baking. Solid line: after baking at 140 °C for 10 min. Film thickness: 2.0 μm.

5-3-2. Preparation of replicated resin mold

Firstly, preparation of replicated resin mold by using primary patterns consisted of ADMA / DMPA / CHTS was conducted. Primary patterns of ADMA / 1 wt% DMPA / 15 wt% CHTS were obtained by conventional UV-NIL (irradiation dose at 365 nm: 600 mJ/cm^2). Figure 5-5 shows the microscope photographs of master mold (20 μm line width), primary patterns of ADMA on quartz plate, replicated mold composed of DPHA on Si wafer, and replicated resin mold after development in methanol / 3 N HClaq = 1 / 9 (v/v). Figure 5-6 shows the SEM photographs of replicated resin mold after development. Primary patterns of ADMA were obtained in good form. On the other hand, replicated resin mold consisted of DPHA was not sufficiently formed. This might be due to the high loading of CHTS, i. e., precipitation of CHTS. After development, replicated resin mold was obtained in good form. Figure 5-7 shows the cross section profiles of master mold (20 μm line width), primary patterns of ADMA on quartz plate, replicated mold composed of DPHA on Si wafer, and replicated resin mold after development in methanol / 3 N HClaq = 1 / 9 (v/v) for 4 h. The edges and side wall of grooves and protrusions were not depicted precisely because the radius of stylus for surfcorder was 2 μm. However, it could analyze the depth / height of grooves / protrusions correctly. The height of the primary patterns was 0.96 μm and the shrinkage of the primary patterns of ADMA was ~1 % in height compared to master mold (0.97 μm). On the other hand, the depth of patterns for replicated resin mold was 0.63 μm and the degree of shrinkage was 35 %. It was confirmed by a separate experiment that the degree of shrinkage of DPHA was ~2 % in the same UV imprinting condition. This means that the shallow grooves of replicated mold were not only derived from the shrinking of DPHA but also insufficient degradation of primary patterns. The residual primary patterns were removed by development in acidic media and afforded finely replicated resin mold. The depth of replicated resin mold after development was 0.93 μm. Therefore, it was revealed that poor acidity of acids mainly induced insufficient degradation of

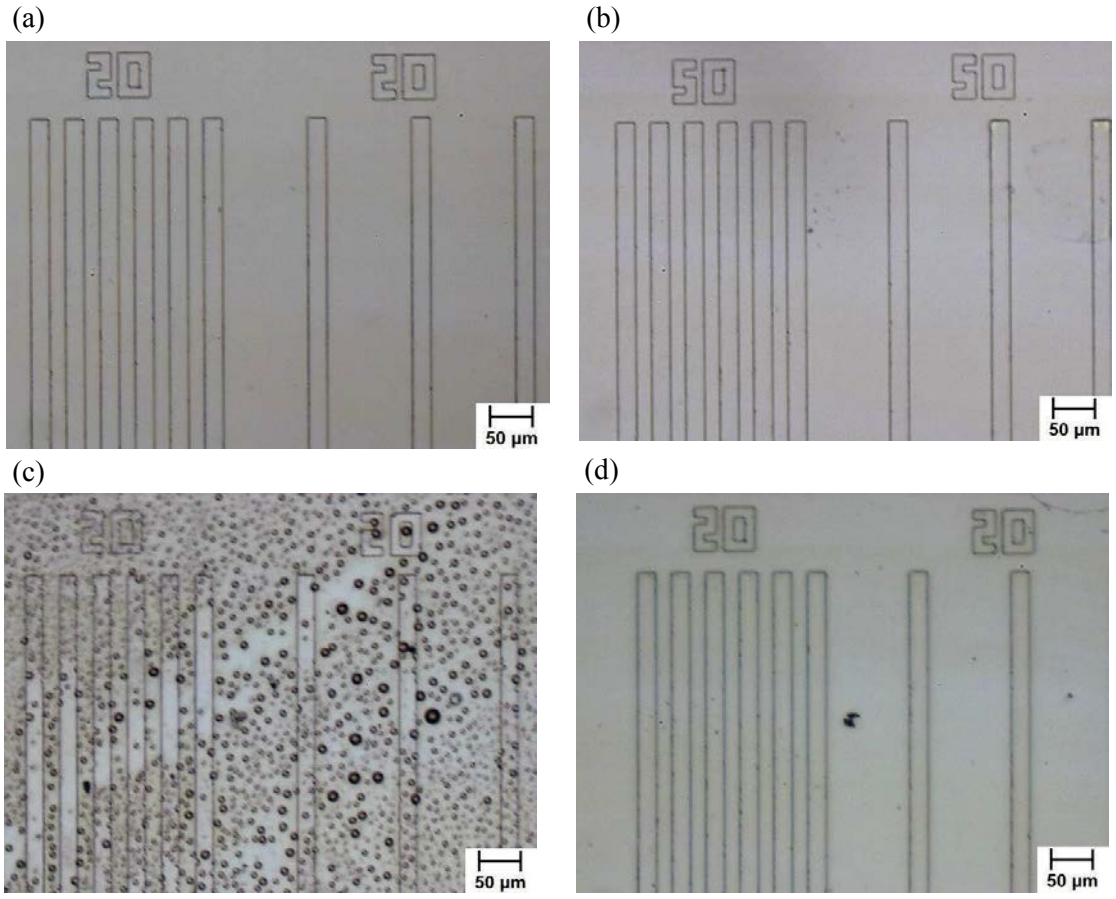

Figure 5-5. Optical micrographs of (a) quartz master mold, (b) primary patterns of ADMA on quartz plate, (c) replicated DPHA mold on Si substrate, and (d) replicated DPHA mold on Si substrate after development in methanol / 3 N HClaq = 1 / 9 (v/v).

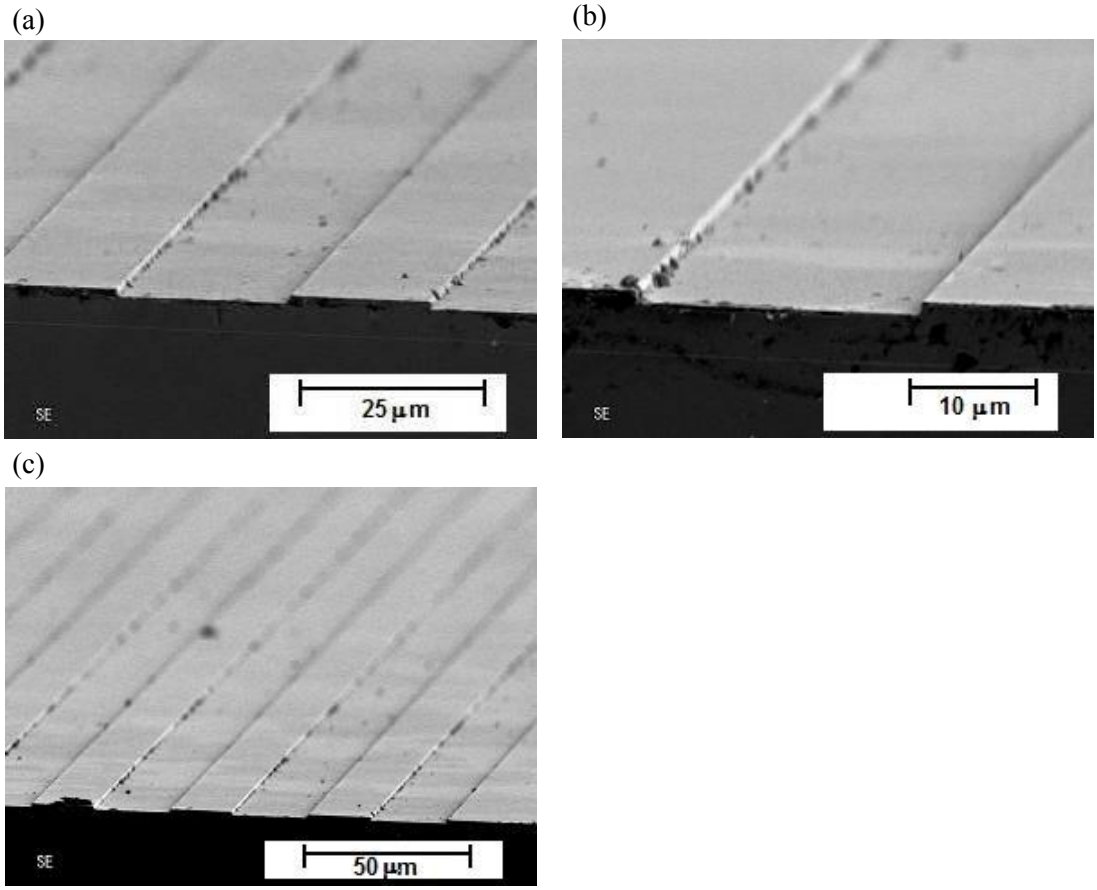

Figure 5-6. SEM photographs of replicated DPHA mold on Si substrate after development in methanol / 3 N HClaq = 1 / 9 (v/v). Line width: 20 μm.

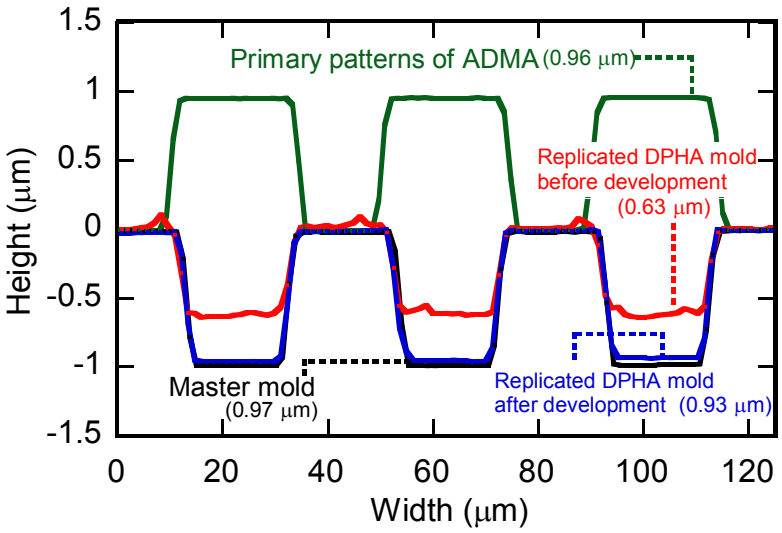

Figure 5-7. Cross section profiles of quartz master mold, primary patterns of ADMA, replicated DPHA mold on Si substrate before development in methanol / 3 N HClaq = 1 / 9 (v/v), and replicated DPHA mold on Si substrate after development in methanol / 3 N HClaq = 1 / 9 (v/v).

primary patterns.

Simple baking was also conducted to decompose the primary patterns composed of ADMA / DMPA / DITF. These processes have an advantage when a reworkable resin with aromatic units was used. In this experiment, a mixture of DPHA and PTA (DPHA / PTA = 2 / 3, molar ratio) was used for the preparation of replicated resin mold. The amount of hydroxyl groups of the sample was adjusted to the optimum condition for the reaction with OPTOOL DSX. If PTA was used for replication of master mold, the replicated PTA mold showed poor release property even after treatment with OPTOOL DSX because of residual unreacted hydroxyl groups. Figure 5-8 shows the microscope photographs of master mold (20 μm line width), primary patterns of ADMA on quartz plate, and replicated DPHA / PTA mold. The replicated mold was obtained in good form. Figure 5-9 shows the cross section profiles of master mold (20 μm line width), primary patterns of ADMA on quartz plate, and replicated DPHA / PTA mold. The depth of patterns and the degree of shrinkage for replicated mold were 0.72 μm and 26 %, respectively. The depth of resin mold was also insufficient compared to that of quartz master mold.

Preparation of replicated resin mold by photo-induced degradation of primary patterns consisted of ADMA / DMPA / DITF was conducted. After UV-NIL with primary patterns of ADMA / DMPA / DITF as a mold, the sample was irradiated at 254 nm with 500 mJ/cm^2 in air and followed by baking at 100 ^{o}C for 15 min to degrade the primary patterns. Figure 5-10 shows the microscope photographs of master mold (20 μm line width), primary patterns of ADMA on quartz plate, and replicated DPHA / PTA mold on Si wafer. Primary patterns and replicated mold were obtained in good form. Figure 5-11 shows the cross section profiles of master mold (20 μm line width), primary patterns of ADMA on quartz plate, and replicated DPHA / PTA mold on Si wafer. The height of the primary patterns was 0.96 μm and the shrinkage of the primary patterns of ADMA was ~1 % in height compared to master mold (0.97

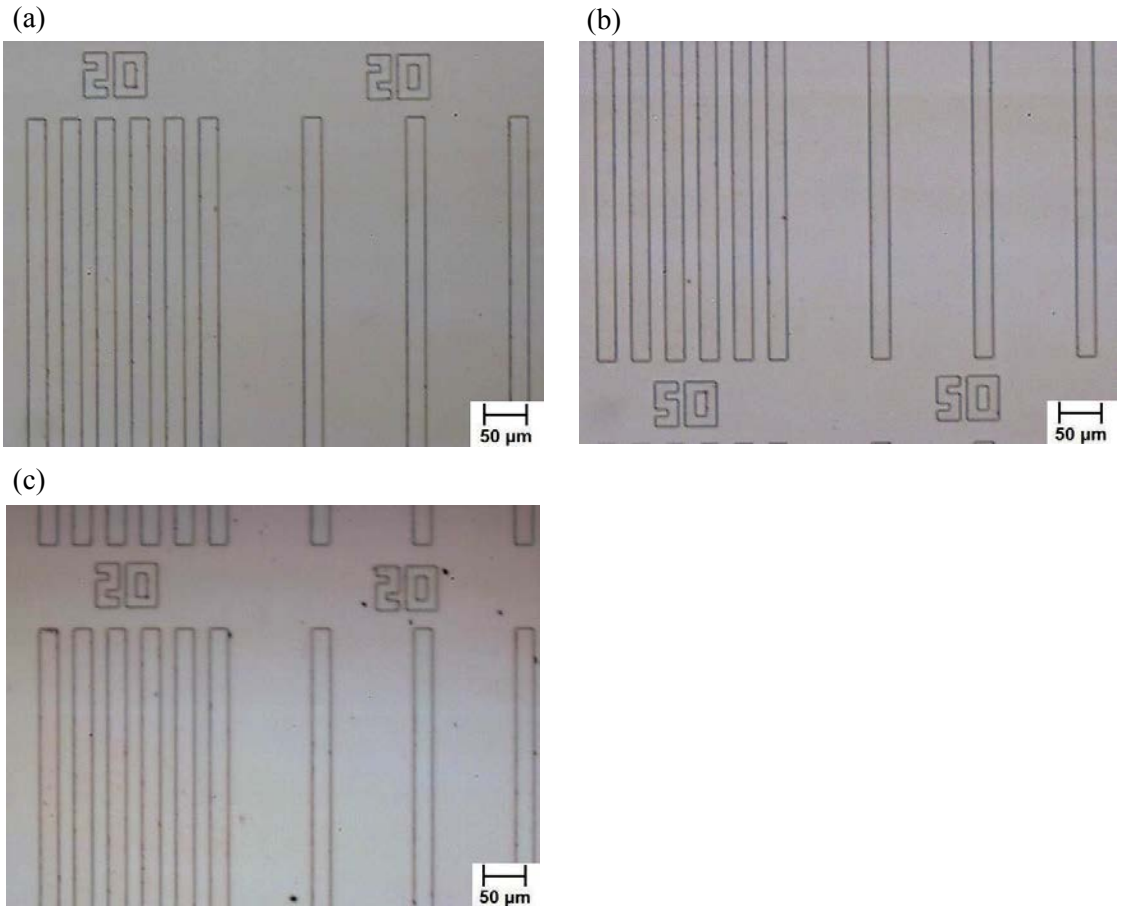

Figure 5-8. Microscope photographs for (a) quartz master mold, b) primary patterns of ADMA on quartz plate, and (c) replicated DPHA/PTA mold on Si substrate.

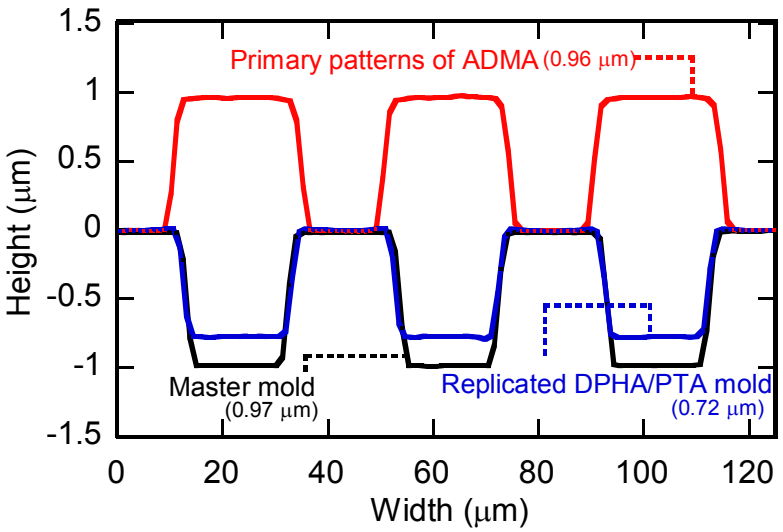

Figure 5-9. Cross section profiles of quartz master mold, primary patterns of ADMA, and replicated DPHA / PTA mold.

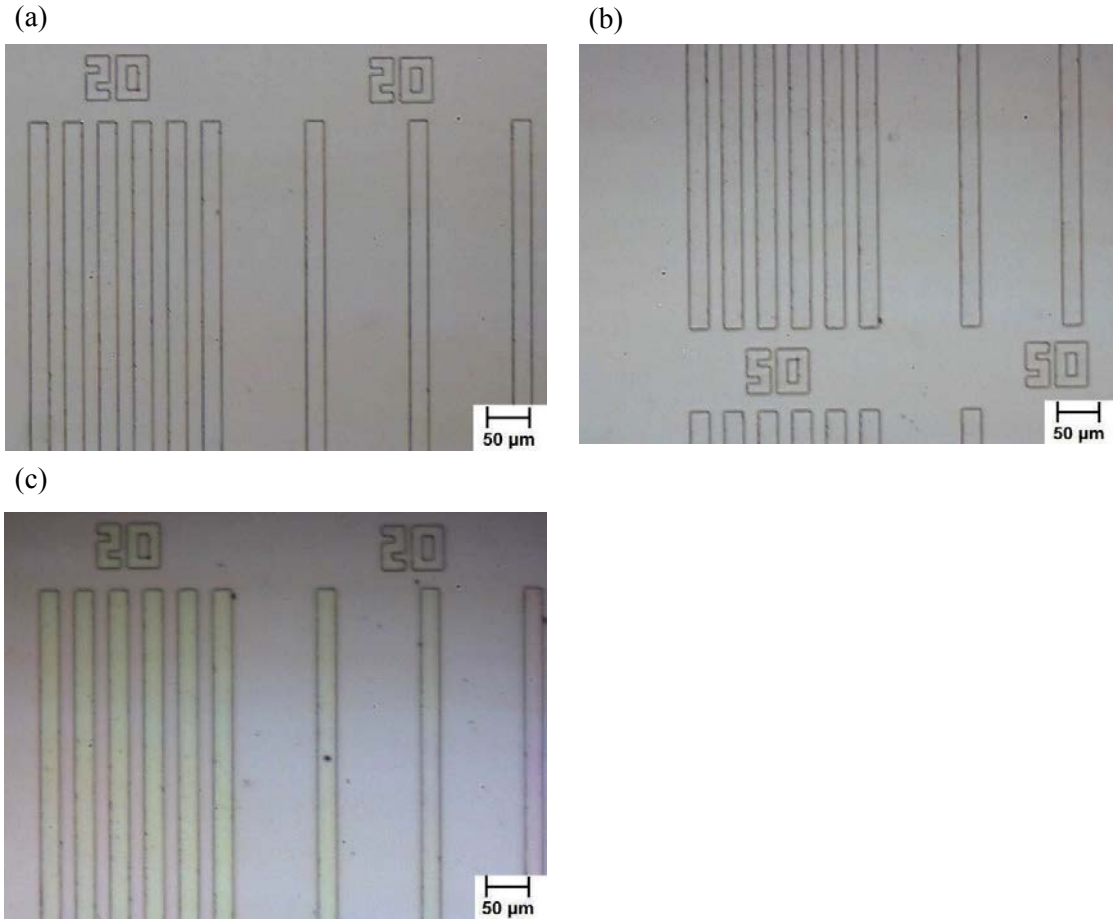

Figure 5-10. Microscope photographs for (a) quartz master mold, b) primary patterns of ADMA on quartz plate, and (c) replicated DPHA/PTA mold on Si substrate.

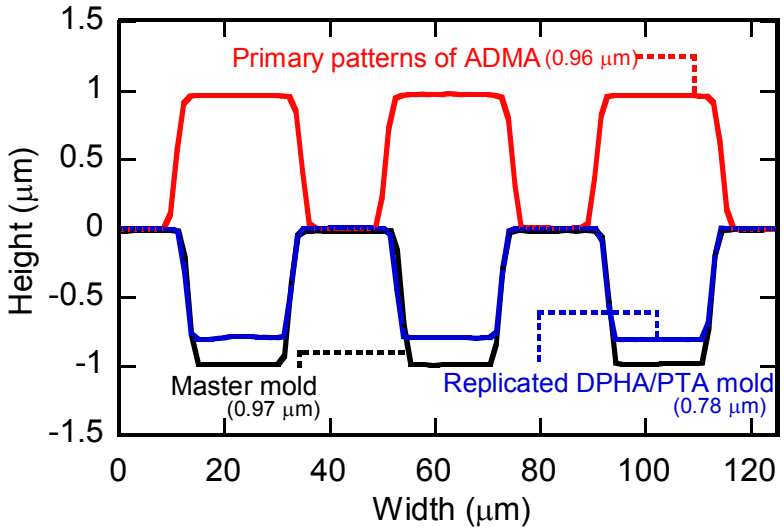

Figure 5-11. Cross section profiles of quartz master mold, primary patterns of ADMA, and replicated DPHA / PTA mold.

μm). On the other hand, the depth of patterns for replicated mold was 0.78 μm and the degree of shrinkage was 20 %. It was confirmed by a separate experiment that the degree of shrinkage of DPHA / PTA (2 / 3, molar ratio) was ~3 % in the same UV imprinting condition. This means that the shallow grooves of replicated mold were not only derived from the shrinking of DPHA / PTA but also other side reaction at interface between primary patterns and replicated mold. To clarify this problem, water contact angle of the resins was investigated. Generally, water contact angle of the UV imprinted DPHA / PTA was 66^{o}. However, the contact angle of secondary film of DPHA / PTA obtained by replica preparation method was 36^{o}. This means that the surface of secondary film of DPHA / PTA was covered by partially crosslinked poly(methacrylic acid). Unpolymerized ADMA on the surface of the primary resin might be copolymerized with DPHA / PTA on second irradiation at 365 nm and acid catalyzed hydrolysis of the primary resin afforded partially crosslinked poly(methacrylic acid) layer on the replicated DPHA / PTA mold. Thus, the side reaction might be significant in the fabrication of replicated resin mold by simple baking compared to photo-induced fabrication method because of higher baking temperature. It is suggested that to obtain good replicated mold, cationically polymerizable monomers are preferable instead of the radically polymerizable monomer such as ADMA.

5-3-3. UV imprinting with replicated resin mold

The replicated resin mold composed of UV cured DPHA / PTA has hydroxyl groups which can react with release reagent. Hence, the replicated resin mold obtained by photo-induced degradation of reworkable resin was treated with OPTOOL DSX to improve the release property before use. PTA containing 1 wt% DMPA was put on quartz plate and a replicated resin mold was placed on the sample. The sample was pressed at 1.2 MPa and irradiated at 365 nm with 600 mJ/cm^2 through quartz plate under vacuum (~120 mmHg). The replicated

resin mold was removed to obtain the UV imprinted patterns of PTA. Figure 5-12 shows the microscope photographs of master mold (20 μm line width), UV imprinted patterns of PTA obtained by using master mold, replicated resin mold consisted of DPHA / PTA, and UV imprinted patterns of PTA obtained by using replicated resin mold. The feature of replicated resin mold was in accord with that of the master mold and the feature of PTA patterns obtained by using replicated mold was identical with that of PTA patterns obtained by using master mold. Replicated resin mold with grooves of varying widths from 1 μm to 100 μm was fabricated. Figure 5-13 shows the cross section profiles of master mold (20 μm line width), UV imprinted patterns of PTA obtained by using master mold, replicated resin mold consisted of DPHA / PTA, and UV imprinted patterns of PTA obtained by using replicated resin mold. The PTA patterns obtained by using replicated mold showed remarkably well-replicated inverse structure of the corresponding replicated resin mold. The width of PTA patterns was nicely consistent with that of the patterns obtained by using original master mold. The height and degree of shrinkage of protrusions for PTA patterns obtained by using replicated resin mold were 0.75 μm and about 4 %, respectively. On the other hand, the height and degree of shrinkage of protrusions for PTA patterns obtained by using master mold were 0.95 μm and about 3 %, respectively. These differences were affected by the difference between the height of master mold and that of replicated resin mold. Additionally, it was confirmed by separate experiments that replicated resin mold obtained by utilizing thermal decomposition of primary patterns of ADMA afforded the same results in UV imprinting of PTA resin. Multiple patterns duplicated were obtained using the replicated resin mold.

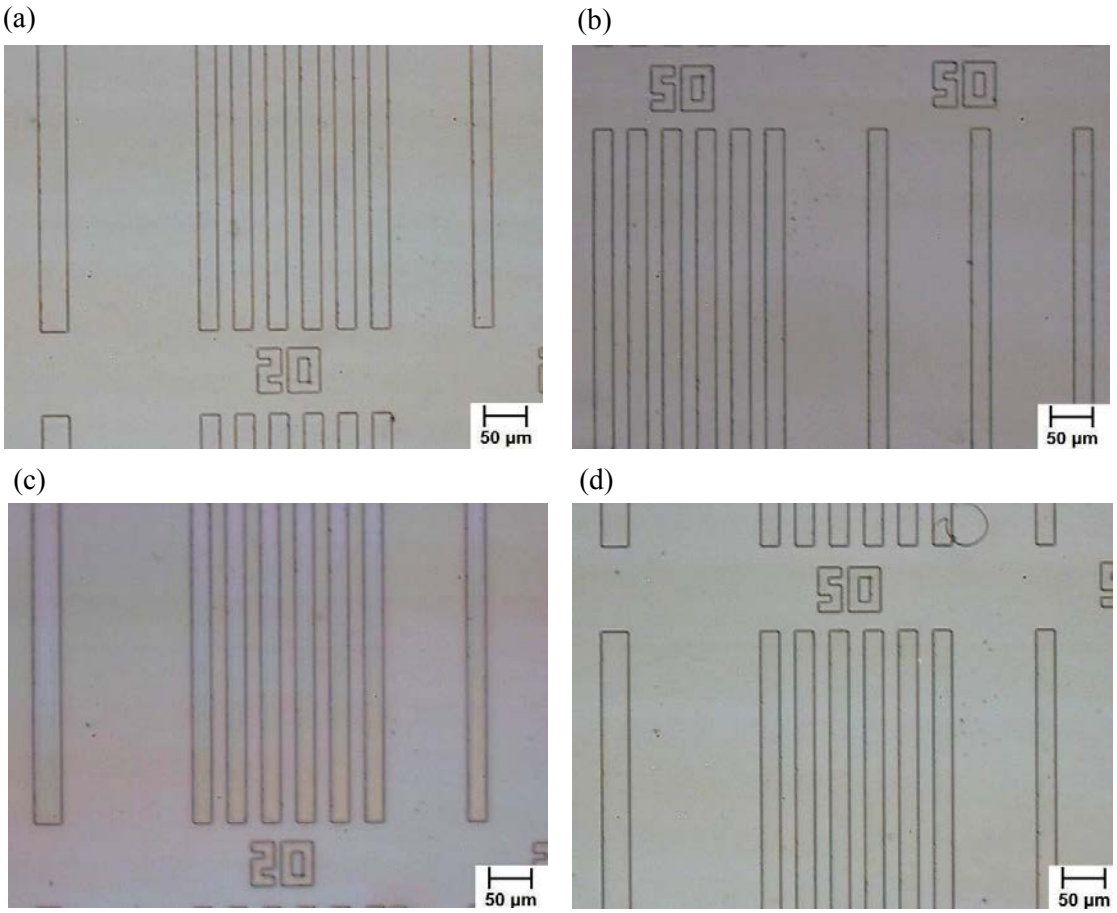

Figure 5-12. Microscope photographs of (a) quartz master mold, b) UV imprinted patterns of PTA obtained by using master mold, (c) replicated DPHA / PTA mold, and (d) UV imprinted patterns of PTA obtained by using replicated DPHA / PTA mold.

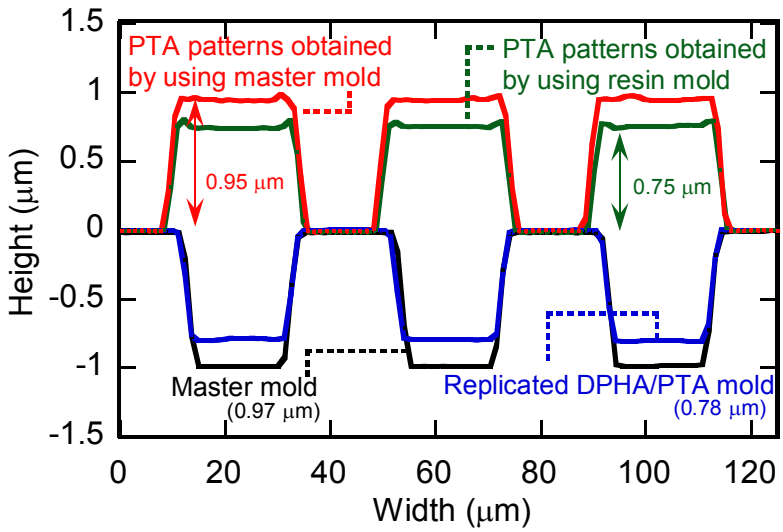

Figure 5-13. Cross section profiles of quartz master mold, primary patterns of PTA obtained by using master mold, replicated DPHA / PTA mold, and UV imprinted patterns of PTA obtained by using replicated DPHA / PTA mold.

5-4. Conclusion

UV imprinting of the reworkable monomer ADMA and photo-induced or thermal degradation of the UV cured ADMA were studied. The UV cured ADMA resin was degraded by exposure at 254 nm and/or baking. The ADMA was applied to make a replicated resin mold for UV imprint lithography. A mixture of ADMA, DMPA, and DITF was used as a resist for UV imprint lithography and primary patterns were obtained. Conventional UV-NIL was carried out using the primary patterns of ADMA as a mold. By degrading the primary patterns of ADMA, the replicated resin mold with grooves of varying widths from 1 μm to 100 μm was fabricated. UV-NIL using the replicated resin mold was accomplished.

References

1. D. S. Ginger, H. Zhang, C. A. Mirkin, *Angew. Chem. Int. Ed.*, 43, 30 (2004).
2. B. D. Gates, Q. Xu, M. Stewart, D. Ryan, C. G. Willson, G. M. Whitesides, *Chem. Rev.*, 105, 1171 (2005).
3. D. Bratton, D. Yang, J. Dai, C. K. Ober, *Polym. Adv. Technol.*, 17, 94 (2006).
4. B. Wu, A. Kumar, *J. Vac. Sci. Technol.*, B25, 1743 (2007).
5. H. Schift, *J. Vac. Sci. Technol.*, B26, 458 (2008).
6. F. A. Houle, E. Guyer, D. C. Miller, R. Dauskardt, *J. Vac. Sci. Technol.*, B25, 1179 (2007).

Chapter 6 Conclusions

Cured resins are widely used in various applications, e. g., coatings, printing inks, adhesives, photoresists, and solder masks. Recently, from the view point of environmental aspects, thermosets with reworkable property have been developed. Although the study on reworkable thermosets has increased gradually, works on UV curable resin with reworkable property are still not enough.

In this thesis, UV curable resins with reworkable property were described. In Chapter 1, the development of thermally cured resins with reworkable property, the roll of UV curable resins, and promising applications of UV curable resins were reviewed.

In Chapter 2, synthesis of novel difunctional (meth)acrylates bearing tertiary ester linkages was described. Photo-curing and thermal degradation, thermal curing and thermal degradation, and thermal curing and photoinduced degradation of the reworkable di(meth)acrylates were studied. The difunctional (meth)acrylates containing AIBN or AIBN and PAG were cured by baking and became insoluble in methanol. The cured di(meth)acrylates were dissolved in solvents after thermolysis of the tertiary ester linkages and complete dissolution was observed for the cured mTMBDMA. The dissolution behavior was strongly affected by the type of PAGs added to mTMBDMA. The temperature for the photo-induced degradation of the cured materials can be settled by choosing PAGs. The difunctional (meth)acrylates containing a photoradical initiator were cured on irradiation. The cured di(meth)acrylates were dissolved in solvents after thermolysis and complete dissolution was observed for the cured mTMBDMA. The dissolution behavior was strongly affected by the structures of the reworkable monomers.

A mechanism for the photo- or thermally curing and photoinduced thermal degradation was studied using FTIR, ^{1}H NMR, TGA, MS, and SEC analyses. Tertiary ester linkages were subject to breakdown into carboxylic acid and alkene by simple thermal treatment.

Chapter 6

In Chapter 3, synthesis of oligo(hemiacetal ester)s having methacrylate units and tertiary ester units in the side chains, their UV curing property, and degradation property of UV cured oligo(hemiacetal ester)s were described. Two types of oligo(hemiacetal ester)s were synthesized and the terminal carboxyl moieties of oligomers were methylated by diazomethane, which enhanced the thermal stability of the oligomers.

The oligo(hemiacetal ester)s containing a photoradical initiator and a PAG became insoluble in solvents after irradiation at 365 nm under nitrogen. Photo-induced insolubilization behavior was not influenced by the difference of main-chain structure of the oligomers. The UV cured oligomers became soluble in acetone after acids were generated in the system. Although insolubilization behavior was not influenced by main-chain structure, the solubilization behavior of UV cured resins was significantly affected by the oligomer structure. It was confirmed that de-crosslinking occurred by the cleavage of hemiacetal ester linkages and tertiary ester linkages.

In Chapter 4, synthesis of difunctional methacrylates having hemiacetal ester moiety in a molecule was mentioned. These monomers were cured on UV irradiation. Especially, the reworkable monomer with adamantyl core structure was highly curable on irradiation. The cured reworkable resins were successfully degraded at mild conditions. The dissolution behavior was dependent on the hydrophilicity of the core structures of reworkable monomers.

By applying these monomers to UV nanoimprint lithography (UV-NIL), fine line / space patterns with the widths from 600 nm to 100 μm were obtained in good form. Application of reworkable resins to UV-NIL could prevent the fouling of the master mold for UV-NIL. The effect of monomer structure on shrinkage of UV imprinted patterns was studied. Degree of shrinkage decreased with increasing the bulkiness of core structure of the monomer. The effect of UV imprint conditions on shrinkage was investigated from the aspect of kinetic chain length by utilizing the degradable property of the reworkable resins. The kinetic chain length

of UV imprinted patterns was investigated by analyzing the degraded products of UV cured resins. Degree of shrinkage of UV imprinted patterns decreased with increasing acrylic equivalent value of the monomers and decreasing the kinetic chain length of the cured resin.

In Chapter 5, UV imprinting of a reworkable monomer was conducted and the acid-catalyzed degradation of the UV imprinted resin was studied in detail. The UV imprinted resin containing a PAG was degraded by exposure with 254-nm light and followed by baking. The UV imprinted resin containing a thermoacid generator was degraded by simple baking. The complete degradation was observed regardless of the structure of acid generators.

A reworkable monomer was applied to make a replicated resin mold for UV-NIL. A mixture of reworkable monomer, a photoradical initiator, and acid generator was used as a resist for UV-NIL. Primary patterns were obtained in good form by UV-NIL. Conventional UV-NIL was carried out using the primary patterns of reworkable resin as a mold. To remove the primary patterns from the UV imprinted product, acid-catalyzed degradation was carried out. By degrading the primary patterns, the replicated resin mold with grooves of varying widths from 1 μm to 100 μm was fabricated. UV-NIL using the replicated resin mold was accomplished. A novel application of UV curable resin with reworkable property was developed.

At present, polymer waste is a serious problem in modern society because production and application of plastics and petroleum-based polymeric materials have been increased. Although UV curable resins are widely used in various applications, study on reworkable UV curing resins is not enough. In order to construct sustainable human society, a good design of UV curable materials with recyclability is highly desired.

In this thesis, the development of UV curable resins with reworkable property and their promising applications were shown. The results obtained from this thesis are expected to be useful for further development of reworkable resins.

List of Publications

Chapter 2.

Degradable Network Polymers Based on Di(meth)acrylates.

D. Matsukawa, H. Okamura, M. Shirai,

Chem. Lett., **36**, 1290-1291 (2007).

Novel reworkable resins: thermo- and photo-curable di(meth)acrylates.

D. Matsukawa, H. Okamura, M. Shirai,

Polym. Int., **59**, 263-268 (2010).

Chapter 3.

Photocurable oligo(hemiacetal ester)s having methacrylate side chains.

D. Matsukawa, T. Mukai, H. Okamura, M. Shirai,

Eur. Polym. J., **45**, 2087-2095 (2009).

Chapter 4.

Analysis of Chain Propagation in UV Curing Using Reworkable Resin.

D. Matsukawa, H. Okamura, M. Shirai,

J. Photopolym. Sci. Technol., **23**, 125-128 (2010).

Reworkable Dimethacrylates with Low Shrinkage and Their Application to UV Nanoimprint Lithography.

D. Matsukawa, H. Okamura, M. Shirai,

J. Mater. Chem., submitted.

Chapter 5.

A UV curable resin with reworkable properties: application to imprint lithography.

D. Matsukawa, H. Wakayama, K. Mitsukura, H. Okamura, Y. Hirai, M. Shirai,

J. Mater. Chem., **19**, 4085-4087 (2009).

Novel resist for replica preparation of mold for imprint lithography.

D. Matsukawa, H. Wakayama, K. Mitsukura, H. Okamura, Y. Hirai, M. Shirai,

Proc. SPIE, **7273**, 72730T-1-72730T-10 (2009).

Preparation of Replicated Resin Mold for UV Nanoimprint Using Reworkable Dimethacrylate.

D. Matsukawa, H. Okamura, M. Shirai,

J. Photopolym. Sci. Technol., **23**, 781-787 (2010).

Acknowledgments

The author would like to express his sincere gratitude to Professor Masamitsu Shirai of Department of Applied Chemistry, Osaka Prefecture University for his many helps in the preparation of this thesis and many useful comments and suggestions for its improvement.

The author would also like to acknowledge Professor Hiroyuki Nakazumi, and Professor Kenji Kono of Department of Applied Chemistry, Osaka Prefecture University for their useful advice and reviewing this thesis.

The author is also deeply grateful to Dr. Kanji Suyama, the Lecturer of Department of Applied Chemistry, Osaka Prefecture University for his instructive guidance and fruitful discussions for this work.

The author is also deeply grateful to Dr. Haruyuki Okamura, the Research Associate of Department of Applied Chemistry, Osaka Prefecture University for his kind advice and suggestions for this work.

The author would like to express his sincere appreciation to all of members in Shirai laboratory, Osaka Prefecture University for useful suggestions, their helps and collaborations through this work.

Finally, the author would like to express his gratitude to his family, Mr. Katsuhiro Matsukawa, Mrs. Mariko Matsukawa, Mr. Yuji Matsukawa, and Mrs. Atsumi Matsukawa for their kind understanding, encouragement and support through this work.

February, 2011

Daisaku Matsukawa